THE EFFECTS OF CDK4/6 INHIBITORS ON DORMANT FOLLICLES AND STEROIDOGENESIS IN HUMAN OVARY

by

Sevgi Yusufoğlu

A Dissertation Submitted to the
Graduate School of Health Sciences in Partial
Fulfillment of the Requirements for the Degree
of

Doctor of Philosophy

in

Reproductive Medicine

KOÇ ÜNİVERSİTESİ

September 24, 2025

THE EFFECTS OF CDK4/6 INHIBITORS ON DORMANT FOLLICLES AND STEROIDOGENESIS IN THE HUMAN OVARY

Koc University

Graduate School of Health Sciences

This is to certify that I have examined this copy of a doctoral dissertation by

Sevgi Yusufoğlu

and have found that it is complete and satisfactory in all respects,
and that any and all revisions required by the final
examining committee have been made.

Committee Members:

_____
Prof. Dr. Özgür Öktem (Advisor)

_____
Prof. Dr. Kayhan Yakın

_____
Assoc. Prof. Zelal Adıgüzel

_____
Prof. Dr. Volkan Turan

_____
Prof. Dr. Fazilet Kübra Boynukalın

Date: _____

ABSTRACT

THE EFFECTS OF CDK4/6 INHIBITORS ON DORMANT FOLLICLES AND STEROIDOGENESIS IN THE HUMAN OVARY

Sevgi Yusufoğlu

Doctor of Philosophy in (Reproductive Medicine) September 24, 2025

CDK4/6 inhibitors, including palbociclib and ribociclib, are established therapies for hormone receptor–positive breast cancer, yet their potential effects on ovarian physiology remain largely unexplored. The human ovary contains a finite pool of dormant follicles and relies on granulosa cell function for coordinated endocrine activity, raising the question of whether pharmacologic CDK4/6 inhibition could alter ovarian function.

This study investigated the effects of CDK4/6 inhibition in human ovarian models using a multilayered approach that incorporated proliferative non-luteinized granulosa cell lines (HGrC1, COV434), primary luteinized granulosa cells (HLGCs), and ovarian cortical explants. CDK4/6 inhibitors consistently enforced G1 arrest by preventing Rb phosphorylation and activating the pRb–E2F1–p21 cascade, confirming a cytostatic rather than cytotoxic mechanism. In HLGCs, modest dose and inhibitor-specific reductions in CYP19A1 and 3β-HSD expression were detected, but estradiol and progesterone secretion remained stable. In ovarian explants, estradiol and AMH secretion were preserved for up to 72 hours with steroidogenic enzyme expression remaining stable in the short term. Apoptotic activation was not observed with palbociclib, whereas ribociclib produced a compound-specific reduction in total PARP without loss of viability.

Taken together, these findings provide the first integrated preclinical evidence in human ovarian models that CDK4/6 inhibition may not acutely compromise endocrine function or reserve markers. While ovarian steroidogenesis appears resilient to short-term pharmacologic CDK4/6 inhibition, further long-term and in vivo studies are required to clarify the consequences of longer exposure on ovarian function.

OZETCE

CDK4/6 İnhibitörlerinin İnsan Overinde Dormant Foliküller ve Steroidogenez Üzerine Etkileri

Sevgi Yusufoğlu
Üreme Tıbbı, Doktora Programı
24 Eylül 2025

CDK4/6 inhibitörleri, palbosiklib ve ribosiklib dahil olmak üzere, hormon reseptörü–pozitif meme kanserinde yerleşik tedavi seçenekleri arasına girmiştir. Ancak, bu ajanların over fizyolojisi üzerindeki olası etkileri büyük ölçüde belirsizliğini korumaktadır. İnsan overi, üreme ve endokrin fonksiyon için kritik olan sınırlı bir dormant folikül rezervine sahip olup, granüloza hücrelerinin koordineli endokrin aktivitesine bağımlıdır. Bu durum, farmakolojik CDK4/6 inhibisyonunun over fonksiyonunu değiştirip değiştirmeyeceği sorusunu gündeme getirmektedir.

Bu tezde CDK4/6 inhibisyonunun insan over fonksiyonu üzerindeki etkileri, proliferatif non-luteinize granüloza hücre hatları (HGrC1, COV434), primer luteinize granüloza hücreleri (HLGC) ve over korteks eksplantlarını içeren çok katmanlı bir yaklaşımla araştırılmıştır. CDK4/6 inhibitörleri, Rb fosforilasyonunu engelleyerek ve pRb–E2F1–p21 kaskadını aktive ederek G1 arrestini tutarlı biçimde indüklemiş, bunun sitostatik ancak sitotoksik olmayan bir mekanizma olduğunu ortaya koymuştur. HLGC'lerde CYP19A1 ve 3β-HSD ekspresyonunda doza ve inhibitöre özgü sınırlı azalmalar saptanmış, ancak östradiol ve progesteron sekresyonu korunmuştur. Over eksplantlarında 72 saate kadar östradiol ve AMH düzeyleri sabit kalmış, kısa süreli değerlendirmelerde ise steroidogenez enzimlerinde herhangi bir değişiklik saptanmamıştır. Apoptoz aktivasyonu palbosiklib ile görülmezken, ribosiklib total PARP düzeyinde inhibitöre özgü bir azalma yapmış, fakat canlılık kaybına yol açmamıştır.

Sonuç olarak, bu çalışma CDK4/6 inhibisyonunun insan over modellerinde endokrin fonksiyon ve rezerv belirteçlerini akut dönemde bozmadığına dair ilk preklinik kanıtı sunmaktadır. Overyan steroidogenezin kısa süreli farmakolojik CDK4/6 inhibisyonuna karşı dirençli olduğu görülmekle birlikte, daha uzun süreli ve in vivo çalışmaların potansiyel üreme risklerini aydınlatmak için gerekli olduğu vurgulanmaktadır.

ACKNOWLEDGMENTS

I would like to thank all these amazing people for their contributions to complete this thesis. I owe my deepest gratitude to my advisor, Prof. Dr. Özgür Öktem, for believing in my potential and his constant encouragement. His guidance and mentorship have been extraordinary, and I am honoured to be one of his students. I would like to thank Prof. Dr. Kayhan Yakın and Assoc. Prof. Dr. Zelal Adıgüzel, Prof. Dr. Volkan Turan, and Prof. Dr. Fazilet Kübra Boynukalın for being on my thesis committee and sparing their precious time for me.

I extend thanks to Koç University School of Medicine for their generous financial support and funding for the projects. I am truly grateful to my fellow PhD student, Hesam Ghafouri Kalajahi, for helping me conduct the experiments. I owe special thanks to Can Benlioğlu for helping me with the analysis of the results.

I am thankful to my lab mates, Iklim Savaş and Samaneh Pirmoradi; it was a nice experience working together with you.

It has been a privilege to share this journey with Ece Iltümür and Merve Gözel. I hold immense appreciation for never leaving me alone and strengthening me throughout this difficult journey. I feel fortunate that Shaghayegh Soleimani and Farinaz Nazmi were always there to motivate and encourage me during tough times.

Lastly, I would like to thank my family for their unconditional support, and special thank you to my husband, Alphan Çanga; none of this would have been possible without his patience and love.

TABLE OF CONTENTS

LIST OF FIGURES

ABBREVIATIONS

AKT / PKB - Protein Kinase B

AMH - Anti-Müllerian Hormone

ATP - Adenosine Triphosphate

BIRC - Baculoviral IAP Repeat-Containing

BMP - Bone Morphogenetic Protein

BSA - Bovine Serum Albumin

CAK - CDK-Activating Kinase

cAMP - Cyclic Adenosine Monophosphate

CCN - Cellular Communication Network

Ccnd2 - Cyclin D2 gene

CDK - Cyclin-Dependent Kinase

CDK4 - Cyclin-Dependent Kinase 4

CDK4/6 - Cyclin-Dependent Kinases 4 and 6

CDK4/6i - CDK4/6 inhibitors

CDK6 - Cyclin-Dependent Kinase 6

CDKi - Cyclin-Dependent Kinase inhibitor

CDKN1B / p27 - Cyclin-Dependent Kinase Inhibitor 1B

CHO - Chinese Hamster Ovary

CI - Cell Index

CKIs - Cyclin-Dependent Kinase Inhibitors

CO_2 - Carbon Dioxide

COV434 - Human granulosa tumor–derived cell line COV434

CYP11A1 - Cholesterol Side-Chain Cleavage Cytochrome P450

CYP17A1 - 17α-Hydroxylase/17,20-Lyase

CYP19A1 - Aromatase

D1 / D2 / D3 - Cyclin D1 / D2 / D3

DHEA - Dehydroepiandrosterone

DMEM/F12 - Dulbecco's Modified Eagle Medium / Ham's F-12

DPBS - Dulbecco's Phosphate-Buffered Saline

DPBS-T - DPBS with Tween-20

E-Plate - Electronic microtiter plate

E2 - Estradiol (17β-estradiol)

E2F - E2F Transcription Factor

ECL - Enhanced Chemiluminescence

ECLIA - Electrochemiluminescence Immunoassay

ECM - Extracellular Matrix

EGF - Epidermal Growth Factor

EGFR - Epidermal Growth Factor Receptor

ER - Estrogen Receptor

FBS - Fetal Bovine Serum

FGF / FGFs - Fibroblast Growth Factor(s)

FOXL2 - Forkhead Box L2

FOXM1 - Forkhead Box M1

FOXO3 (FOXO3A) - Forkhead Box O3

FSH - Follicle-Stimulating Hormone

FSHR - Follicle-Stimulating Hormone Receptor

GCs - Granulosa Cells

GDF-9 - Growth Differentiation Factor 9

GnRH - Gonadotropin-Releasing Hormone

GnRH-agonist - Gonadotropin-Releasing Hormone Agonist

hCG - Human Chorionic Gonadotropin

hLGCs - Human Luteinized Granulosa Cells

HER2 - Human Epidermal Growth Factor Receptor 2

HER2- - HER2-negative

HGrC1 - Immortalized human granulosa cell line HGrC1

HR+ - Hormone Receptor–positive

HSD3B (3β-HSD) - 3-beta-Hydroxysteroid Dehydrogenase

HSD3B2 - 3β-Hydroxysteroid Dehydrogenase Type II

IGF / IGFs - Insulin-like Growth Factor(s)

IVF - In Vitro Fertilization

LH - Luteinizing Hormone

LHCGR - Luteinizing Hormone/Choriogonadotropin Receptor

LHR - Luteinizing Hormone Receptor

LHX8 - LIM Homeobox 8

MAPK1/3 (ERK2/ERK1) - Mitogen-Activated Protein Kinase 1/3

MAT1 - CDK-Activating Kinase Assembly Factor (Menage à Trois 1)

MEK - Mitogen-Activated Protein Kinase Kinase

mTOR / mTORC1 - Mechanistic (Mammalian) Target of Rapamycin / mTOR Complex 1

Myc - MYC proto-oncogene

OPU - Oocyte Pick-Up

P4 - Progesterone

PFA - Primordial Follicle Activation

PFGCs - Pre-granulosa Cells

PI - Propidium Iodide

PI3K - Phosphatidylinositol 3-Kinase

PIP2 - Phosphatidylinositol 4,5-Bisphosphate

PIP3 - Phosphatidylinositol 3,4,5-Trisphosphate

POF - Premature Ovarian Failure

POI - Premature Ovarian Insufficiency

PROTAC - Proteolysis-Targeting Chimera

PTEN - Phosphatase and Tensin Homolog

Rb / pRb - Retinoblastoma protein / phosphorylated Rb

RNase A - Ribonuclease A

ROS - Reactive Oxygen Species

RPE1 - Retinal Pigment Epithelial-1 cell line

RPM - Revolutions Per Minute

RTCA - Real-Time Cell Analysis

SD - Standard Deviation

Ser - Serine (amino acid residue)

SIRT1 - Sirtuin 1

SMAD3 - Mothers Against Decapentaplegic Homolog 3

StAR - Steroidogenic Acute Regulatory protein

TBS-T - Tris-Buffered Saline with Tween-20

TCs - Theca Cells

TGF-β / TGFβ - Transforming Growth Factor Beta

TPD - Targeted Protein Degradation

TSC1 / TSC2 - Tuberous Sclerosis Complex 1 and 2

YAP - Yes-Associated Protein

α-helix - Alpha helix (protein secondary structure)

CHAPTER 1

LITERATURE REVIEW

1. Ovarian Structure and Follicular Development

1.1 Ovarian Structure and Cellular Components

The ovary is a complex and dynamic organ essential for female reproduction and hormone production. Its detailed structure and various cell types coordinate to control folliculogenesis, steroidogenesis, and ultimately, fertility outcomes (1). A complete understanding of these components and their interactions is essential, especially in the context of conditions, for instance, premature ovarian insufficiency (POI) (2,3).

Anatomically, the human ovary consists of two primary regions: the outer cortex and the inner medulla (4). Located on the outer edge of the ovary, the ovarian cortex harbours dormant primordial follicles. These follicles remain inactive, quiescent until they're specifically triggered and activated to develop into primary follicles (5). In contrast, the medulla consists of loose connective tissue that is rich in blood vessels, lymphatics, and nerve fibres. This area provides the metabolic and endocrine support essential for follicular development and the distribution of hormones throughout the reproductive system axis (4) (Figure 1). Ovarian follicles are the primary functional units of the ovary, comprising its tissue and housing the female germ cells that contribute to reproductive capacity (6). These structures contain the female gametes and undergo various developmental stages. Primordial follicles are the most common type, usually numbering between 500,000 and 1,000,000 at birth. Each primordial follicle comprises an immature oocyte arrested in the diplotene stage of meiosis I, encased by a single layer of flattened pre-granulosa cells (7). Many of these follicles remain inactive for extended periods, while a small, steady group periodically becomes active. This natural process underscores how the body carefully

regulates these tiny structures, maintaining a healthy balance (8,9). This dormancy is essential because primordial follicles are non-renewable; once they are activated, they cannot revert to a dormant state, impacting a woman's reproductive lifespan (10). Primordial follicle activation is regulated by a balance between local signals that stimulate growth and intrinsic inhibitory mechanisms. Growth factors derived from the oocyte, granulosa, and stromal or theca compartments, including KIT ligand, LIF, KGF, FGF-2, and oocyte-secreted members of the TGF-β superfamily, such as GDF-9 and BMPs, have been shown to promote oocyte growth and granulosa cell proliferation during the primordial to primary follicle transition. In contrast, intrinsic repressors, such as PTEN, FOXO3a, and TSC1, together with cell-cycle regulators including p27 and the granulosa cell transcription factor FOXL2, help maintain dormancy and safeguard the follicle pool. Follicular granulosa-derived AMH provides an additional somatic restraint on the recruitment of primordial follicles. The interplay of these opposing signals generates a recruitment pattern that preserves ovarian reserve throughout the reproductive lifespan (7) (Figure 2).

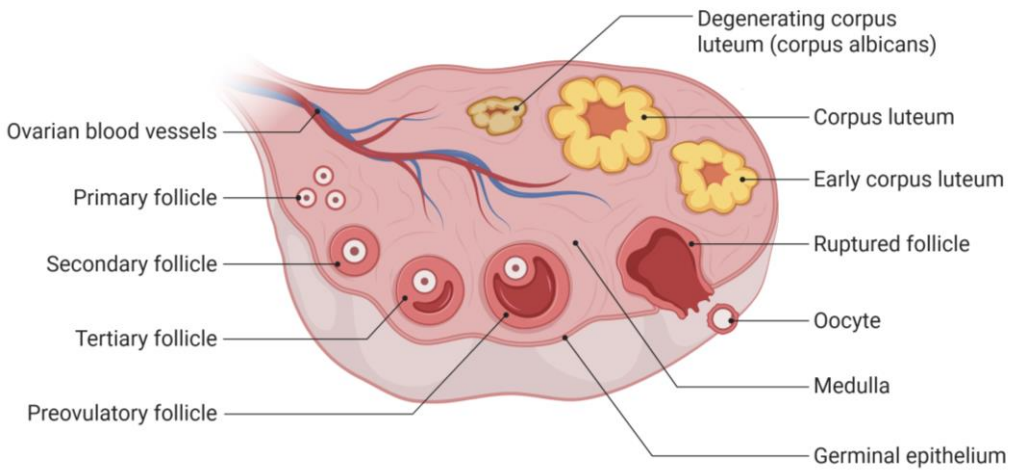

Figure 2: Structural organization of the human ovary. The cortex contains follicles at various stages of development, from primordial to preovulatory, while the medulla is enriched with blood vessels and stromal tissue. Post-ovulatory structures such as the corpus luteum and corpus albicans are also illustrated. Created with BioRender.com.

1.2 Initiation of Follicle Growth, In Other Terms, Activation of Primordial Follicles

Follicle activation, also known as initial recruitment, is a crucial step in folliculogenesis. During this process, the oocyte begins to enlarge, and the surrounding flattened pre-granulosa cells transform into cuboidal granulosa cells, marking the initiation of the next stage of proliferation (11,12). This process works independently of gonadotropin action (7). Activated follicles progress through primary, secondary, and antral stages, involving the proliferation and differentiation of two key somatic cell types. At the beginning of follicle development, the process is considered independent of gonadotropins. Later, the antral and preovulatory stages become dependent on gonadotropins (11,12) (Figure 2). Granulosa cells (GCs), which surround the oocyte directly, are vital for follicular development and play a key role in steroid hormone production. They generate estradiol by converting androgens from theca cells, a process enhanced by follicle-stimulating hormone (FSH) through aromatase activity (1). Their proper differentiation and adequate numbers are essential for follicle survival, as a lack of GCs or incorrect phenotyping can cause follicular atresia (13). Theca cells form a layer around the granulosa-oocyte structure as they develop after the secondary follicle stage (14,15). Theca layer consists of the theca interna, which is steroidogenic, and the theca externa, which provides structural support (16,17). Theca cells are the only cells that produce ovarian androgens such as testosterone and androstenedione, which they generate in response to luteinizing hormone (LH). These androgens serve as crucial precursors for estrogen synthesis by granulosa cells (16). After ovulation, theca cells undergo luteinization, supporting the development of the corpus luteum (18).

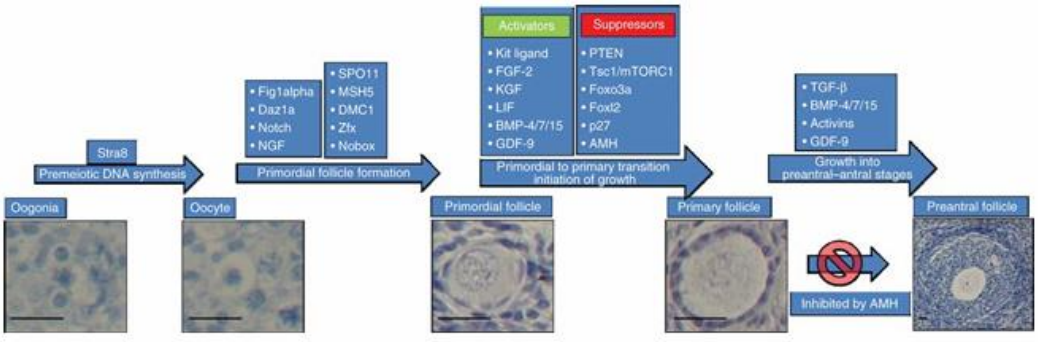

Figure 3: Schematic overview of early human folliculogenesis and its regulatory factors. During fetal development, oogonia enter meiosis between 8–13 weeks of gestation and differentiate into oocytes prior to the assembly of primordial follicles.

Primordial follicles first appear around 16 weeks, and they are established by six months after birth. Their subsequent growth into primary and preantral stages is modulated by a network of paracrine–autocrine signals, particularly members of the TGF-β superfamily. Stimulatory factors such as Kit ligand, FGF-2, KGF, LIF, BMPs, and GDF-9 promote follicle activation, whereas suppressors such as PTEN, Foxo3a, and AMH restrict recruitment. AMH serves as a critical inhibitory signal, while growth factors such as TGF-β, Activins, and BMPs facilitate progression toward the antral stage. Representative histological sections of each developmental stage are shown (7).

Ovary-specific stromal components include the ovarian surface epithelium, a flat-to-cuboidal layer that facilitates post-ovulatory repair (19) and the tunica albuginea underneath a thin, collagen-rich sheath that undergoes remodelling prior to ovulation (20). The extracellular matrix (ECM) provides structural and biochemical support (21). The basal lamina encircling each follicle separates the granulosa cells from the theca cells and regulates the diffusion of local growth factors (22).

Normal ovarian function, crucial for female fertility, depends on a precisely coordinated communication network among the oocyte, granulosa cells, and theca cells. This interplay is regulated by systemic reproductive hormones such as estradiol, follicle-stimulating hormone (FSH), luteinizing hormone (LH), and anti-Müllerian hormone (AMH), along with local growth factors including insulin-like growth factors (IGFs), fibroblast growth factors (FGFs), and the bone morphogenetic protein (BMP) system (1). Follicle activation and growth are mainly controlled by the oocyte PI3K/PTEN/Akt/Foxo3 pathway (23,24) and the pre-granulosa cell mTORC1 pathway, with further modulation from the Hippo and MAPK3/1 signalling cascades (25,26).

In conclusion, the ovarian structure is a finely balanced biological system, with components from dormant primordial follicles to supporting stromal cells and the extracellular matrix, each serving a specific, interconnected role (10). A more comprehensive understanding of these complex mechanisms is important for improving fertility treatments and safeguarding reproductive health.

1.3 Dormant (Primordial) Follicles and Their Activation

The process of initiating folliculogenesis by activating dormant primordial follicles is tightly regulated and essential for a woman's reproductive lifespan. Since the ovarian reserve is limited from birth, only a small number of follicles mature completely and ovulate. If this activation process becomes abnormal or accelerates, it may cause premature ovarian insufficiency (POI). Understanding the molecular signals involved in this transition is vital for creating strategies to preserve fertility (27,28).

1.3.1 Molecular Pathways Driving Follicle Activation

The activation process marks a significant transition, where the oocyte begins to grow, and its surrounding flattened pre-granulosa cells differentiate into cuboidal granulosa cells, starting to proliferate (28). This initial recruitment of primordial follicles differs from later stages because it is largely considered independent of gonadotropin regulation (9). Instead, it mainly depends on intrinsic signalling within the oocyte and pre-granulosa cells, as well as key factors in the ovarian microenvironment (29). Among the various contributing factors, two key signalling pathways, phosphatidylinositol 3-kinase (PI3K)/AKT and mammalian target of rapamycin (mTOR), have been thoroughly studied for their crucial roles in PFA (30). The PI3K/AKT pathway is vital for cell survival, growth, and migration in various tissues, and it plays a crucial role in regulating PFA within the mammalian ovary (31). Its activation involves PI3K transforming phosphatidylinositol 4,5-bisphosphate (PIP2) into phosphatidylinositol 3,4,5-trisphosphate (PIP3) (32). Subsequently, PIP3 recruits and activates AKT (also known as protein kinase B/PKB), which then phosphorylates downstream targets, particularly the forkhead transcription factor FOXO3 (24). FOXO3 plays a crucial role in follicular activation by remaining in the nucleus of dormant oocytes, where it suppresses the activation of follicles. When the PI3K pathway is activated, FOXO3 becomes phosphorylated and translocates from the nucleus to the cytoplasm, thereby lifting its inhibitory effect and triggering the activation of primordial follicles (24).

PTEN (phosphatase and tensin homolog deleted on chromosome 10) serves as a key negative regulator of the PI3K pathway by converting PIP3 back to PIP2, thereby helping to preserve follicular dormancy (33). Notably, deleting the Pten gene specifically in oocytes in mice causes overactivation and early exhaustion of the entire

primordial follicle pool, which directly results in premature ovarian failure (POF) (23). Although PTEN inhibition with agents like bpV(HOpic) has demonstrated potential in activating human primordial follicles in vitro, worries about DNA damage and reduced follicular survival require further research before it can be considered for routine clinical application (34,35).

The mTORC1 pathway is another essential initiator of PFA, mainly acting in pre-granulosa cells (30). This pathway is necessary for regulating cell growth and metabolism, particularly in promoting the biosynthesis of proteins and lipids. TSC1 and TSC2 (tuberous sclerosis complex 1 and 2) form a heterodimer complex that functions as a negative regulator of mTORC1 (36). The deletion of *Tsc1* or *Tsc2* in mouse oocytes can induce widespread activation and subsequent depletion of primordial follicles, thereby leading to premature ovarian failure (POF) (37). The activation of mTORC1 signalling within pre-granulosa cells (pfGCs) is vital for the start of primordial follicle activation (PFA). When mTORC1 is stimulated in pfGCs, it boosts the production of KIT ligand (KITL). This ligand then interacts with the KIT receptor on the oocyte surface, leading to the phosphorylation of KIT and the subsequent activation of PI3K signalling inside the oocyte. This cascade ultimately results in the relocation of FOXO3 and the successful initiation of PFA (30).

1.3.2 Regulatory Factors of Follicle Activation

Beyond the main pathways, an intricate and interconnected system of other elements and signalling processes carefully coordinates PFA regulation.

The p27 (Cyclin-Dependent Kinase Inhibitor 1B/CDKN1B) protein, an essential negative regulator of the cell cycle, is typically found in the nuclei of dormant mouse oocytes (38). In mice, a lack of p27 leads to early activation and depletion of the primordial follicle pool, notably contributing to POF (39).

Cyclin-dependent kinases (CDKs), particularly CDK6, play an essential role in cell cycle progression. They are especially important for the differentiation and proliferation of granulosa cells, which are essential for overall ovarian function (40). In human ovarian tissue, CDK6 is present in both primordial and primary follicles. It shows a decrease in transcription within oocytes but an upregulation in granulosa cells during the transition from primordial to primary follicles (41). Studies using mouse models have shown that inhibiting CDK6, with agents like BSJ-03-123 (BSJ), significantly elevates the proportion of primordial follicles while reducing the

proportion of primary follicles. This suggests that CDK6 has a suppressive effect on the activation of primordial follicles (PFA). Although blocking CDK6 primarily increases apoptosis in granulosa cells, it does not significantly affect reactive oxygen species (ROS) levels or the quality and meiotic development of oocytes. Additionally, no significant changes were observed in P-AKT or AKT levels after BSJ treatment (42). These findings highlight the crucial role of cell cycle control in the development of ovarian follicles and suggest a potential connection between CDK6 levels and the PI3K/AKT signalling pathway. While overexpressing CDK6 has been observed to enhance PI3K/AKT pathway activity in other cell types, further research is needed to understand the direct mechanisms involved in PFA (43).

Anti-Müllerian Hormone (AMH) functions as a primary regulator that prevents the activation of primordial follicles (44). Studies consistently indicate that Anti-Müllerian Hormone (AMH) plays a key role in regulating the start of primordial follicle development both in laboratory settings and within living organisms, functioning as an essential regulatory system to prevent the early exhaustion of the follicle reserve (28). AMH is commonly utilized in clinical settings as an indicator of ovarian reserve, representing the quantity of dormant primordial follicles (7).

1.3.3 Regulation of Ovarian Reserve

The activation of primordial follicles, which plays a vital role in shaping the duration of female fertility, is intricately controlled by numerous growth factors and transcription factors. Among the various growth factors, Bone Morphogenetic Proteins (BMPs), specifically BMP-4, BMP-7, BMP-15, and BMP-6, play a crucial role in promoting the transition from primordial to primary follicles and influencing granulosa cell differentiation. Additionally, Growth Differentiation Factor-9 (GDF-9) is crucial for the development of early primary follicles and overall follicular growth (7). Other factors, such as basic Fibroblast Growth Factor (bFGF) and Epidermal Growth Factor (EGF), also contribute to follicle activation, often interacting with pathways like PI3K (33). In contrast, Anti-Müllerian Hormone (AMH) functions as a crucial inhibitor, preserving the dormancy of primordial follicles and preventing their early depletion (44). Additionally, TGF-β may also contribute to dormancy by affecting mTOR signalling (45).

In the context of transcription factors, FOXO3A plays a crucial role in inhibiting primordial follicle activation in mice. When FOXO3A is missing, there is a

significant increase in follicle activation and early depletion. However, its exact function in humans is not yet fully understood (31). Additionally, FOXL2 (Forkhead box L2) plays a crucial role in the proper differentiation of pre-granulosa cells during activation, and its dysfunction is associated with early ovarian failure (46). Other factors, such as NOBOX and LIM homeobox 8 (LHX8), are also implicated in the regulation of early ovarian development and follicle activation, with LHX8 generally suppressing activation (47). Furthermore, p27 (Cyclin-dependent kinase inhibitor 1B) blocks early follicle activation by stopping the cell cycle (48). Recent research highlights the role of Sirtuin 1 (SIRT1) and Histone deacetylase 6 (HDAC6) in activation via pathways such as mTOR (49,50). and Cyclin-dependent kinase 6 (CDK6) is involved in regulating the transition from primordial to primary follicles, inducing granulosa cell apoptosis but not affecting oocyte quality.

The activation of dormant follicles is a complex and precisely coordinated process crucial for maintaining reproductive health throughout a woman's life. It involves a careful interplay of signals that either promote or inhibit this activation at the molecular, cellular, and tissue levels. Gaining insight into this process is crucial for understanding how external factors, such as CDK4/6 inhibitors, may potentially impact follicle health and long-term ovarian function. Currently, there is no comprehensive research that examines whether the pharmacological blocking of CDKs affects the balance between follicle rest and activation in humans (42).

1.4 The Role of Granulosa and Theca Cells in Folliculogenesis and Steroidogenesis

1.4.1 Steroidogenic Roles of Granulosa and Theca Cells

Ovarian steroid production is a carefully coordinated biochemical process mainly taking place in the secondary follicles, where granulosa cells (GCs) and theca cells (TCs) work together to convert cholesterol into key sex hormones, such as estrogens and progesterone (51). This regulation is most clearly explained by the two-cell, two-gonadotropin theory, which describes the sequential roles of two important pituitary hormones: follicle-stimulating hormone (FSH) and luteinising hormone (LH) (52,53).

The first and rate-limiting step in steroid hormone production involves transforming cholesterol into pregnenolone. This essential process is facilitated by the

cholesterol side-chain cleavage cytochrome enzyme (CYP11A), which is encoded by the CYP11A gene (54). The acute regulation of this process involves the steroidogenic acute regulatory protein (StAR), which facilitates the transport of cholesterol into the mitochondria, where P450scc is located (55). In human ovarian follicles, StAR expression gradually increases from the antral to the preovulatory phase, peaking around the time of ovulation in both mural granulosa and cumulus cells, indicating an increased capacity for steroid hormone production. CYP11A1 expression also increases markedly before ovulation, supporting the progressive acquisition of a steroidogenic phenotype by granulosa cells (56). Once pregnenolone is converted into either progesterone by 3β-HSD or androgen precursors, such as DHEA, by CYP17A1, it depends on the enzymatic environment. In the human ovary, estrogen is mainly produced from these androgen intermediates rather than from progesterone, indicating the predominant pathway for steroidogenesis (51,55).

The two-cell–two-gonadotropin model offers a concise explanation for how theca and granulosa cells share the responsibility for steroid biosynthesis. Theca cells (TCs), which consistently express luteinizing hormone receptor (LHR) and the enzyme CYP17A1, are mainly responsible for producing androgens in response to LH. When stimulated by LH, TCs synthesize androgens such as androstenedione and testosterone (16,57). While FSH receptors are generally found only on GCs, research in rats indicates that recombinant human FSH (rhFSH) can trigger ovarian CYP17 mRNA expression in thecal cells. Additionally, insulin, insulin-like growth factors (IGF)-1 and -2, and inhibin (a paracrine signal from GCs induced by FSH) promote androgen production in human theca cells (58,59). Granulosa cells (GCs) have follicle-stimulating hormone receptors (FSHR) but typically do not express CYP17A1. This specialization means GCs are unable to produce androgens on their own. Instead, they absorb androgens generated by theca cells (TCs) and, with FSH stimulation, convert these androgens into estrogens, primarily estradiol, via the enzyme aromatase (CYP19A1) (55,57) (Figure 3). The primary mechanism by which FSH and LH influence granulosa cells involves the adenylate cyclase–cAMP signalling pathway, which enhances the transcription of important enzymes involved in steroid production, including aromatase and P450scc (55).

During the transition from the early antral to preovulatory phase, follicle-stimulating hormone (FSH) significantly boosts the expression of aromatase (CYP19A1) in granulosa cells. This increase promotes the conversion of androgens

from theca cells into estrogens, creating an environment rich in estrogen, essential for the maturation of the dominant follicle (56). This two-cell, two-gonadotropin model provides the foundation for understanding how steroidogenesis is dynamically regulated during follicle maturation (60).

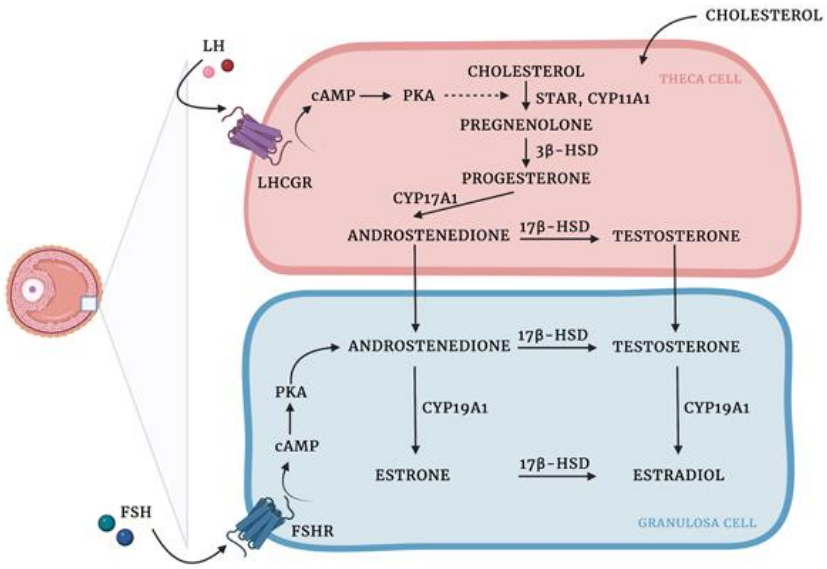

Figure 4: The two-cell, two-gonadotropin model of ovarian steroidogenesis. In theca cells, LH binds to its receptor (LHCGR) and activates the cAMP–PKA pathway, which enhances the activity of steroidogenic enzymes, including StAR and CYP11A1. This promotes the conversion of cholesterol to pregnenolone, which is subsequently converted to progesterone and androgen precursors via 3β-HSD and CYP17A1. Androgens, mainly androstenedione and testosterone, diffuse into the adjacent granulosa cells, which lack CYP17A1 but express follicle-stimulating hormone receptors (FSHR). Under FSH stimulation, granulosa cells activate the cAMP–PKA cascade, upregulate aromatase (CYP19A1), and convert theca-derived androgens into estrogens (estrone and estradiol). This intercellular cooperation provides the foundation for estrogen production, which is essential for follicular growth, ovulation, and reproductive function. This figure adapted from Jozkowiak et al., 2023.

1.4.2 Regulation of Steroid Production During Follicle Maturation

The production of progesterone varies significantly throughout the different phases of follicular development. In the early stages of follicle formation, granulosa

cells show minimal progesterone production, with low levels of 3-beta (β)-hydroxysteroid dehydrogenase (HSD) expression observed in these cells from preantral and small antral follicles. 3β-HSD is initially expressed in theca cells of small follicles but becomes strongly upregulated in granulosa cells during antral to preovulatory stages, paralleling increased progesterone production (56).

Research clearly indicates that FSH directly encourages the production and release of progesterone by human granulosa cells, without triggering luteinization. This process involves enhancing 3β-HSD gene expression and increasing its enzymatic activity. Unlike other steroidogenic enzymes, CYP17A1 exhibits minimal change in granulosa cells, which limits progesterone conversion into androgens and thereby contributes to its accumulation (56,61). FSH stimulates progesterone production in granulosa cells by upregulating 3β-HSD expression and activity, a mechanism also underlying elevated progesterone levels during IVF cycles (61).

As follicles develop, luteinizing hormone (LH) becomes increasingly important in the production of steroids. While LHCGR expression is low early on, it peaks before full follicle maturation, especially in granulosa cells of follicles over 10 mm (56). Activation of LH receptors in granulosa cells stimulates the transcription and synthesis of essential enzymes involved in steroid production, such as P450scc and aromatase (55). Progesterone levels rise when follicle diameters reach 11–12 mm, fluctuating during the follicular development phase. Elevated progesterone in the late follicular phase aids follicle maturation and prepares the body for ovulation (55–57).

Dominant follicle selection occurs within the cohort of antral follicles when individual follicles upregulate FSH and LH receptors and increase FSH-driven aromatase activity in granulosa cells. This allows follicles to produce more estradiol, thereby gaining a survival advantage, while less responsive follicles undergo atresia. At the same time, declining AMH levels reduce the inhibition of estrogen synthesis, switching from an activin-dominant to an inhibin-dominant environment, along with increased androgen production in the theca, which provides the substrate for aromatization. These hormonal and paracrine interactions secure the emergence of a single dominant follicle, establishing an estrogen-rich environment that's necessary for ovulation and fertility (7). Estrogen and progesterone production during the menstrual cycle relies on theca and granulosa cells working together. LH stimulates theca cells to produce androgens, which are then transformed into estrogens by granulosa cells in response to FSH. As the process continues, granulosa cells become increasingly

responsive to LH, leading to a surge in progesterone levels that is crucial for ovulation (55).

Given the crucial role of granulosa and theca cell proliferation in follicle growth and steroidogenesis, drugs such as CDK4/6 inhibitors that disrupt their growth or function can impact follicular development and hormonal balance. Understanding their physiology is crucial for evaluating the impact of targeted therapies on ovarian function.

2. The Role of CDKs in Ovarian Physiology

2.1 Overview Of the CDK Family and Cell Cycle Regulation

Cyclin-dependent kinases (CDKs) are conserved heterodimeric serine/threonine kinases in eukaryotes, activated by binding to cyclins. The human genome contains 20 CDKs, each with unique roles and regulation. They mainly regulate cellular signalling through the reversible phosphorylation of target proteins.

In eukaryotic cells, the cell cycle is a carefully controlled sequence of events that ensures proper cell division and prevents the transmission of DNA damage. This cycle is divided into four key phases: G1, S, G2, and M (62,63). Particular cyclin proteins control CDK activity by varying their levels in a precise manner (64).

The progression of the eukaryotic cell cycle depends on the step-by-step activation of CDK–cyclin complexes, each of which governs a specific phase of the cell cycle. During early G1, CDK4 and CDK6, associated with D-type cyclins (D1, D2, D3), respond to growth signals to initiate cell cycle entry and help cells pass the restriction point (65) (Figure 4). During the process of DNA replication, CDK2, when bound to cyclin E, triggers the transition from the G1 to the S phase (66). In the S phase, CDK2 pairs with cyclin A to facilitate accurate DNA synthesis and ensure replication fidelity (67). Progression into mitosis is regulated by CDK1, which first collaborates with cyclin A during late S and G2 phases, and subsequently with cyclin B at the G2/M boundary. This coordination controls chromatin condensation, nuclear envelope disassembly, and the formation of the spindle apparatus, all of which are essential for correct chromosome segregation (65).

The transition from G1 to S phase involves a key event in which the tumour suppressor protein Rb is phosphorylated. Rb normally inhibits E2F transcription factors, which are essential for the activation of genes needed for DNA synthesis. The

process begins with CDK4/6-cyclin D complexes attaching phosphate groups to Rb, causing it to release E2F and allowing the activation of S-phase genes. Later, cyclin E, associated with CDK2, further phosphorylates Rb, completely disabling its suppressive function and facilitating the cell's progression into the S phase (62).

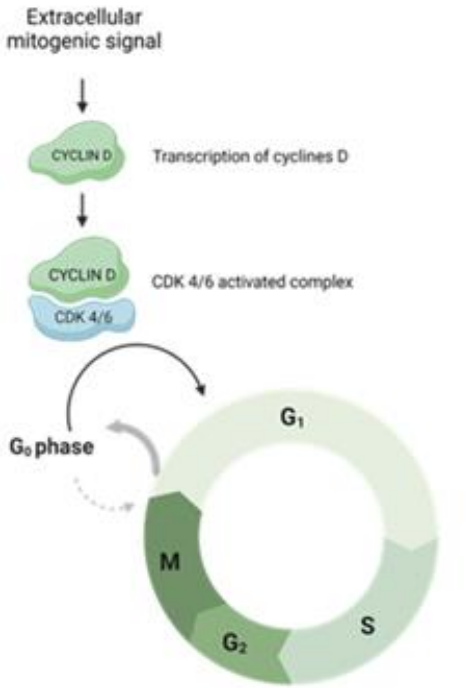

Figure 5: Schematic representation of CDK4/6 activation by mitogenic signals. Extracellular stimuli promote the transcription of D-type cyclins, which subsequently bind to CDK4/6 to form active complexes. These complexes facilitate G1 phase entry by enabling cells to exit quiescence (G0) and progress through the restriction point (40).

2.1.1 General Mechanisms of CDK Activation and Inhibition

The activity of CDK is strictly controlled via mechanisms that activate and inhibit it (64). Complete activation of cyclin-dependent kinases (CDKs) depends on their binding to cyclins and the phosphorylation of a specific threonine amino acid within the T-loop. This phosphorylation is carried out by the CDK-activating kinase complex, which consists of CDK7, cyclin H, and MAT1 (68). In contrast, Wee1 and Myt1 kinases inhibit CDKs through phosphorylation at Thr14 and Tyr15. This prevents their activity until Cdc25 phosphatases remove these phosphate groups,

which is critical for the correct timing of cell cycle progression within the ATP-binding domain (62).

Cyclin-dependent kinase inhibitors (CKIs) play a crucial role in regulating the activity of CDKs by serving as molecular brakes, thereby controlling cell cycle progression. The INK4 family, which includes p15, p16, p18, and p19, specifically targets CDK4 and CDK6 during the G1 phase. They form stable complexes with these kinases, hindering their association with cyclin D and preventing their activation. On the other hand, the Cip/Kip family, consisting of p21, p27, and p57, has a more extensive inhibitory function by interacting with both cyclins and CDKs, effectively blocking their enzymatic activity (69) (Figure 5). These inhibitory processes are closely linked to cell cycle control points, ensuring that the cell cycle stops if DNA damage occurs or replication is incomplete, until the issue is resolved, thereby protecting the genome's integrity (63).

The G1/S checkpoint halts the cell cycle upon detection of DNA damage, primarily through the activation of p53, which subsequently induces the production of p21. p21 inhibits CDK activity, providing the cell with an opportunity to repair its DNA. Conversely, the G2/M checkpoint ensures that cells do not advance to mitosis with damaged or incomplete DNA by maintaining CDK1 in an inactive state through phosphorylation and by suppressing Cdc25 via Chk1/Chk2 signalling (70). The spindle assembly checkpoint (SAC) prevents the onset of anaphase until all chromosomes are correctly bound to the spindle apparatus, controlling CDK1 activity during mitosis to ensure precise chromosome separation (71).

The regulation of the cell cycle by cyclin-dependent kinases (CDKs) is crucial for normal growth and development in living organisms. Since CDKs play a crucial role in regulating cell division, any disruption in their function can lead to severe health issues, including various types of cancer (70). In cancer, uncontrolled cell growth is commonly associated with genetic or epigenetic changes in the CDK-cyclin-CKI signalling pathways. This includes situations like the increased production of cyclins, such as cyclin D1, or the loss of function in CKIs, like p16INK4a (62). This insight has motivated the advancement of therapeutic approaches targeting CDKs, with selective CDK4/6 inhibitors showing encouraging clinical results by inducing G1 phase arrest in cancer cells (72). Cyclin-dependent kinases (CDKs) serve as key regulators of cell division in eukaryotic organisms, governed by mechanisms such as cyclin association, targeted phosphorylation, and specific inhibitory proteins. Their

precise regulation is essential for proper cell cycle progression and maintaining normal biological functions. Disruptions in CDK activity are commonly associated with cancer development, highlighting their importance as vital targets for therapeutic strategies.

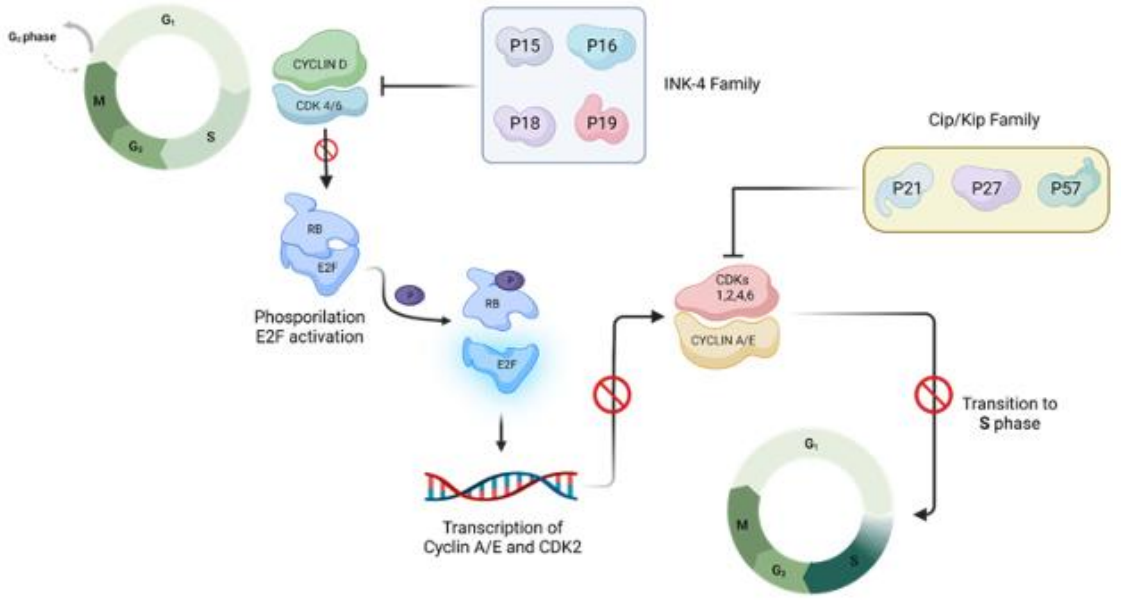

Figure 6: Regulation of CDK4/6 activity through activation and inhibition. Cyclin D–CDK4/6 complexes phosphorylate Rb, releasing E2F to drive transcription of S-phase genes. The INK4 family specifically inhibits CDK4/6, whereas Cip/Kip proteins broadly suppress CDK–cyclin activity, thereby maintaining strict control of G1/S progression (40).

2.1.2 CDK4/6 Pathway: Molecular Biology and Function

Cyclin-dependent kinases 4 and 6 (CDK4/6) play a crucial role in managing the eukaryotic cell cycle. They are primarily responsible for regulating the transition from the G1 phase to the S phase, a crucial step in cell growth and division. (73). In addition to their well-known primary functions, CDK4/6 also play roles in connecting cell cycle advancement with cellular growth processes. They can directly interact with tuberous sclerosis complex 2 (TSC2) and modify it by adding phosphate groups at specific sites, Ser1217 and Ser1452. This modification activates the mechanistic target of rapamycin complex 1 (mTORC1), a key regulator of cell growth (74). Inhibiting CDK4/6 with drugs rapidly decreases mTORC1 activity in various human and mouse

cell lines, including breast cancer cells. This decrease depends on the presence of TSC2 and occurs before any noticeable changes in retinoblastoma (RB) protein phosphorylation. These results suggest that CDK4/6 plays a dual role in promoting cell proliferation, not only by facilitating cell progression through the cell cycle via RB phosphorylation, but also by supporting cell growth by activating mTORC1. This coordination ensures cells reach an adequate size before they divide. (74).

The canonical mechanism of CDK4/6 functions is through its interaction with the RB–E2F pathway. (75). Upon mitogenic stimulation, D-type cyclins (D1, D2, D3) attach to and activate CDK4/6 enzymes. This process triggers a series of phosphorylation on the retinoblastoma protein (RB), specifically at various serine and threonine sites, including Ser807/811. (76,77). Phosphorylation causes RB to undergo conformational changes, which in turn release E2F transcription factors from the repression imposed by RB. This process facilitates the activation of genes essential for DNA replication, nucleotide production, and entry into the S phase of the cell cycle. (75,78).

Structural analyses have shown that cyclin D–CDK4/6 complexes bind to a distinctive C-terminal α-helix within RB (residues 895–915). This docking interface is unique and not seen in other cyclin–CDK complexes. (79). Disrupting this helix prevents RB from being phosphorylated by CDK4/6, leading to a blockade at the G1 phase and boosting RB's role in suppressing tumours. This particular structural feature could serve as a foundation for designing targeted therapies that specifically interfere with the CDK4/6–RB interaction, minimizing impact on other cyclin–CDK activities. (79).

The combined use of traditional and alternative methods underscores the vital function of CDK4/6 as central players in integrating signals that regulate cellular growth and metabolic processes. These kinases have emerged as significant therapeutic targets, particularly in hormone receptor-positive breast cancer, and their inhibition offers valuable insights into the tissue-specific regulation of the cell cycle. This understanding will help clarify their specific roles in follicular development and overall ovarian function, which will be addressed in the following section (80).

2.2 Expression of CDKs in Ovarian Tissue

The health of the ovary and female fertility rely on the precise and efficient progression of the cell cycle in granulosa cells. These somatic cells play a crucial role in guiding the development of follicles, the intricate process leading to ovulation, and the later formation of the corpus luteum (40). Usually, the granulosa cells found in primordial follicles remain in a quiescent G0 phase. The process of transitioning from a resting state to active cell division, known as primordial follicle activation, is a crucial early stage that drives the significant growth of preovulatory follicles (40,81). The transition from G0 to G1 and the subsequent progression into the cell cycle are primarily driven by the activation of particular cyclin-CDK complexes (40). D-type cyclins (D1, D2, and D3), when paired with CDK4 and CDK6, create complexes that initiate this process (82,83). When a mitogen signal from outside the cell activates it, these cyclin D-CDK4/6 complexes help the cell exit its resting state, enter the G1 phase, and then continue through the rest of the cell cycle. D-type cyclins are uniquely identified by their direct regulation through external mitogenic signals, setting them apart from other cyclin families (84). This positions them as essential linkers that facilitate the connection between external signals and the complex internal mechanisms governing the cell cycle (85). In ovarian biology, cyclin D2 has a specialized and vital role in the development and functioning of the gonads (86). Its expression is predominantly found in granulosa cells, and it is observed that its levels tend to rise notably when stimulated by various factors such as Follicle-Stimulating Hormone (FSH), estradiol, and insulin. The stimulating effect of FSH, for example, encourages the development and activation of the cyclin D2/CDK4 complex. This step is essential for starting DNA synthesis in granulosa cells (87,88). Meanwhile, Luteinizing Hormone (LH) has an opposing role; through MAPK1/3 activation, it can trigger cell cycle arrest by stimulating the body's natural CDK inhibitors, thus finely regulating the growth of granulosa cells (40). In primordial follicles, granulosa cell proliferation is suppressed to maintain dormancy. A study showed that this is mediated by TGFβ-activated SMAD3, which promotes *Ccnd2* while repressing *Myc*; here, Cyclin D2 forms inhibitory complexes with p27 (89). As follicles activate, SMAD3 levels decline, thereby elevating Myc repression. Supporting biochemical evidence suggests that Cyclin D–CDK4 phosphorylates SMAD3, thereby reducing its inhibitory activity and facilitating progression from the G1 to the S phase (90). These results suggest a feedback link between TGFβ–SMAD3 and Cyclin D–CDK4 in controlling granulosa cell proliferation timing (89,90).

CDK4 and CDK6 primarily facilitate the G1/S phase transition by adding phosphate groups to the retinoblastoma (Rb) protein, thereby inactivating it. (91,92). When phosphorylation occurs, E2F transcription factors dissociate from Rb. This change enables E2F to activate the transcription of genes that promote cell proliferation, such as those encoding cyclins E and A, as well as other proteins essential for DNA replication (91). In adult female mice, the absence of CDK4 (Cdk4^-/-) results in significant reproductive issues, such as ovaries smaller than those of wild-type mice, decreased ovulation rates, and total failure of embryo implantation caused by impaired luteal function, which is associated with low serum levels of progesterone and prolactin; fertility is fully restored by progesterone treatment (93). In contrast, CDK6-deficient (*Cdk6*^-/-) females generally develop normally and remain fertile, though around 30% are sterile with a reduced number of mature follicles (94). While Cdk4^-/- granulosa cells still proliferate in response to FSH, this proliferation is insufficient to sustain the luteal activity essential for reproduction, underscoring CDK4's unique role (93).

2.2.1 Oocyte Maturation and Disease Implications

CDK6 has been recognized as a significant and influential factor in the essential process of transitioning from primordial to primary follicles (42). Analysis of human ovarian transcriptomes shows that, during the transition from primordial to primary follicles, CDK6 expression declines in oocytes but shows a modest increase in surrounding granulosa cells. Experimental inhibition of CDK6 using a selective degrader revealed that lowering CDK6 levels reduces primordial follicle activation and promotes apoptosis in granulosa cells, while leaving oocyte maturation unaffected at the MII stage (42). Collectively, these findings suggest that CDK6 plays a key role in regulating granulosa cell survival and the initiation of follicle growth (42,95). In terms of meiotic progression, however, evidence suggests that CDK6 is not indispensable. Adhikari et al. (2012) examined the functional requirements of cyclin-dependent kinases during oocyte meiotic resumption in mice. Their findings showed that Cdk1 is both essential and sufficient for this process, as its oocyte-specific deletion causes permanent arrest at the germinal vesicle stage and complete infertility. In contrast, deletion of Cdk2 had no effect on oocyte maturation, MII arrest, or fertility. Previous studies referenced in their work further indicate that mice lacking Cdk3, Cdk4, or Cdk6 develop normally and display normal oocyte maturation,

suggesting that these kinases are not required for the meiotic maturation of oocytes (96).

As previously outlined, CDK activity in ovarian cells is modulated by cyclin availability, endogenous CDK inhibitors, and phosphatases, ensuring precise control over both mitotic and meiotic events (40). These interconnected regulatory mechanisms maintain granulosa cell proliferation, follicle development, and oocyte maturation, while their disruption is often linked to ovarian tumorigenesis (40,85). For example, mutations in the Rb gene and increased expression of cyclin D, sometimes associated with gene amplification in other studies, have been reported in ovarian cancer (85,97)Therapeutic strategies targeting CDKs, particularly CDK4/6, have shown promising outcomes in breast cancer and may inform treatment approaches for hormone receptor-positive gynaecologic cancers (85).

Recent evidence suggests that CDK4 and CDK6 play crucial roles in regulating granulosa cell proliferation, follicle development, and overall ovarian function. While these kinases are well known for controlling the G1-to-S phase transition in proliferative tissues, their specific distribution and functions in the ovary remain incompletely understood. Transcriptomic analysis of human ovarian follicles has revealed that CDK6 expression shifts between oocytes and granulosa cells during the primordial-to-primary transition. The selective pharmacological degradation of CDK6 significantly reduces follicle activation without impairing oocyte maturation (Ataei-Nazari et al., 2022). Given the increasing clinical use of CDK4/6 inhibitors in reproductive-age women, defining their roles in follicular activation, steroidogenesis, and ovarian reserve has become a priority, especially since current data on their potential gonadotoxic effects remains scarce.

Currently, there is no experimental evidence directly connecting CDK4/6 activity with the regulation of key steroidogenic enzymes in human ovarian tissue. (40). This significant gap highlights the critical need for focused investigations into how CDK4/6 modulation may impact ovarian reserve and hormone synthesis.

3. General overview of CDK inhibitors

Aberrant expression or dysregulation of CDK pathways, often leading to uncontrolled cell proliferation, is a hallmark of many types of cancer. Cyclin-dependent kinase inhibitors (CDKis) were developed as targeted therapies to block abnormal cell cycle progression by inhibiting specific CDK–cyclin complexes (73).

Beyond their central role in cell division, certain CDKs also participate in transcriptional regulation. For instance, CDK7 acts as a CDK-activating kinase (CAK) together with cyclin H and Mat1, while CDK8 and CDK9 regulate transcriptional programs, linking CDK biology to both cell cycle and gene expression control (98–100). This diverse role of CDKs means that inhibiting them can affect not only the process of cell division but also the gene expression programs that are crucial for the survival and growth of cancer cells. The development of CDK inhibitors (CDKIs) has been an ongoing process of improvement, motivated by the challenges faced with earlier versions. The initial wave of broad-spectrum CDK inhibitors, such as Flavopiridol (Alvocidib) and Roscovitine (Seliciclib), emerged in the late 1990s and early 2000s. (80). These substances were developed to target and block a range of cyclin-dependent kinases, such as CDK2, CDK4, CDK6, and CDK9, particularly in the case of Flavopiridol (101), and CDK1, CDK2, CDK5, CDK7, and CDK9 for Roscovitine. While the compounds demonstrated strong in vitro activity by inducing G1 and G2 cell cycle arrest and apoptosis, their clinical use was notably constrained by high toxicity and unsatisfactory efficacy (73). This broad-spectrum inhibition frequently led to off-target effects on normal, healthy cells, compromising the therapeutic window (77). Later studies showed that the toxicity observed with these initial inhibitors was likely due to their effect on CDKs responsible for transcription, specifically CDK7 and CDK9, which resulted in decreased RNA transcription. Aware of the drawbacks of broad-spectrum inhibition, researchers have begun to prioritize the creation of more targeted and specific CDK inhibitors (73).

A significant advancement was achieved with the second generation of CDKIs, especially the selective CDK4/6 inhibitors: Palbociclib, Ribociclib, and Abemaciclib (102). These drugs exert their therapeutic effect by competitively binding to the ATP-binding pocket of CDK4 and CDK6, thereby inhibiting their kinase activity (77) (Figure 6). This inhibition prevents the phosphorylation of the retinoblastoma protein (pRb), which in turn arrests cells in the G1 phase of the cell cycle and suppresses tumour progression. These selective CDK4/6 inhibitors have achieved remarkable clinical success, especially in estrogen receptor (ER)-positive, HER2-negative metastatic breast cancer, where they are now a cornerstone of treatment (103). Their toxicity profiles are generally manageable, but notable differences exist; for instance, Palbociclib and Ribociclib are often linked to neutropenia, whereas Abemaciclib may cause diarrhoea and fatigue (104). A recently

developed, short-acting CDK4/6 inhibitor called Trilaciclib has been approved for reducing myelosuppression caused by chemotherapy in patients with small-cell lung cancer. It achieves this by inducing a reversible G1 cell cycle arrest (105)**.** Expanding on standard kinase inhibition, Targeted Protein Degradation (TPD) strategies, such as Proteolysis Targeting Chimeras (PROTACs) and molecular glues, promote the specific breakdown of target proteins through the cell's natural ubiquitin-proteasome system (106). PROTACs are bifunctional chimeric molecules that connect target ligands to E3 ligases, facilitating protein degradation (107). Research into how cancer cells develop resistance to CDK4/6 inhibitors is continually evolving, with the goal of improving their effectiveness. The PI3K/AKT/mTOR pathway, being a key upstream regulator of cyclin D-CDK4/6 activity, is emerging as a promising target for combination treatment strategies (108). To overcome current limitations and emerging resistance, researchers are increasingly turning to combination therapies. These strategies involve using CDK inhibitors in combination with other treatments, such as chemotherapy, targeted drugs like MEK, PI3K, mTOR, or EGFR inhibitors, or immunotherapies (e.g., anti-PD-1 therapy). The aim is to create synergistic effects that facilitate more personalized and effective treatment options (73,103). While their role in cancer therapy is well established, the potential effects of CDK4/6 inhibitors on ovarian function, with a focus on dormant follicle activation and the control of steroidogenic pathways, are still largely unexplored.

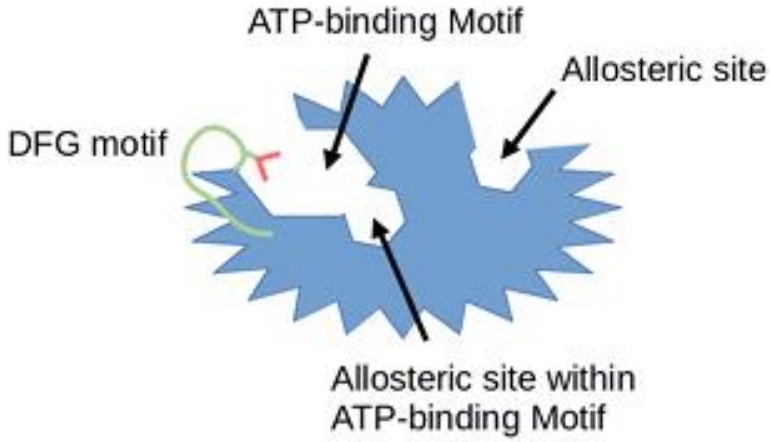

Figure 7: Structural organization of a typical CDK kinase domain. The diagram highlights key motifs relevant for inhibitor binding, including the ATP-binding cleft, the DFG motif, and potential allosteric sites that can be targeted by different classes of CDK inhibitors (80).

4. CDK4/6 Inhibitors: Palbociclib and Ribociclib

4.1 Palbociclib: Mechanism and Clinical Profile

CDK4/6 inhibitors, such as palbociclib and Ribociclib, both of which are approved agents by FDA (109), have revolutionized the treatment of hormone receptor-positive, HER2-negative advanced or metastatic breast cancer. These drugs are the most extensively studied and commonly utilized in clinical settings. They work by specifically blocking CDK4 and CDK6, halting the cell cycle at the G1 phase through the hypophosphorylation of the retinoblastoma (Rb) protein, which prevents tumour cell proliferation that depends on Rb (40,77,110).

Palbociclib is an orally available, reversible small-molecule inhibitor that effectively targets CDK4 and CDK6 (111). Palbociclib exhibits minimal or no inhibitory activity against other cyclin-dependent kinases, as well as a broad spectrum of tyrosine and serine/threonine kinases (112).

Palbociclib inhibits cyclin D–CDK4/6 complexes by competitively binding to the ATP-binding pocket, thereby blocking catalytic activity and preventing Rb hyperphosphorylation (112,113). This maintains Rb in an active, hypophosphorylated state that binds to E2F transcription factors and enforces G1 arrest (83,111). The sustained repression of E2F by active pRb, due to palbociclib's action, leads to the downregulation of E2F-targeted genes, which include the S-phase cyclins, cyclin A and cyclin E, and CDK2. This effectively blocks the progression into the S phase (114). The collective impact of these molecular interactions results in a strong G1 phase cell cycle arrest, thereby inhibiting tumour growth (77). Importantly, palbociclib's anti-tumour effects rely on the presence of an active Rb1 protein. Tumours lacking Rb1 activity due to inactivation or loss usually show resistance to palbociclib (115,116). Recent mechanistic studies demonstrated that palbociclib, beyond its catalytic inhibition of CDK4/6, induces a rapid, non-catalytic effect by

selectively dissociating p21 from cyclin D–CDK4 complexes within minutes, thereby releasing p21 to inhibit CDK2 activity; this effect is not observed with p27 or with CDK6 complexes and depends on unique sequences in the C-lobe of CDK4, indicating an allosteric selectivity mechanism (117).

Preclinical studies demonstrate palbociclib's broad anti-cancer activity across multiple tumour models. It reduces the expression of genes regulated by E2F (118), which are crucial for cell cycle progression, and inactivates the transcription factor FOXM1, a key regulator of tumour cell proliferation (118,119). Across various in vitro and xenograft models, palbociclib has demonstrated strong anti-tumour activity against different cancer types. These include estrogen receptor-positive (ER+) breast cancer, where it preferentially targets luminal ER+ cell lines (120), as well as colon cancer, glioblastoma (121), prostate carcinoma (122), sarcomas (123), pancreatic ductal adenocarcinoma (124), melanoma (125), non-small cell lung cancer (126), oesophageal adenocarcinoma, acute myeloid leukaemia, multiple myeloma (114), and Rb-positive germ cell tumours (127). Overall, these findings highlight the strong therapeutic potential of palbociclib, particularly in cancers that maintain functional retinoblastoma (RB) pathway signalling, enabling its mechanism of action to be fully utilized and achieve sustained cell-cycle arrest (77).

4.2 Ribociclib: Mechanism and Clinical Profile

Ribociclib has shown antitumor effects in both preclinical and clinical studies across various tumour types, including breast cancer, melanoma, and neuroblastoma. Although single-agent activity has been observed, Ribociclib also improves the effectiveness of combination treatments and helps delay the development of treatment resistance in both preclinical and clinical settings (110).

Ribociclib is another orally available, selective inhibitor targeting CDK4 and CDK6, with many mechanistic similarities to palbociclib (110,114). Similar to palbociclib, Ribociclib binds to the ATP binding site of CDK4 and CDK6, leading to their inactivation, and this direct inhibition blocks the kinase activity of these complexes, which is critical for their function in cell cycle progression (103).

Ribociclib and palbociclib share lipophilicity features; however, ribociclib exhibits higher kinase selectivity, which likely reduces off-target effects (110). Chemoproteomics analyses showed Ribociclib is considerably more selective for

CDK4 and CDK6 compared to palbociclib, which affects over twice as many kinases, including various off-target protein and lipid kinases. This higher selectivity of Ribociclib is believed to contribute to its unique pharmacological properties and potentially reduce off-target toxicities compared to less selective CDK4/6 inhibitors (128).

Preclinical data indicate that Ribociclib appears less toxic to bone marrow mononuclear cells compared to Palbociclib and Abemaciclib (129). It inhibits cell growth in ER-positive breast cancer cell lines, significantly slows the proliferation of neuroblastoma and liposarcoma cell lines, and induces G1 arrest and senescence in neuroblastoma models (114,130). In neuroblastoma mouse xenograft models, Ribociclib treatment decreased levels of phosphorylated Rb, Ki67, and overall cell proliferation, resulting in a notable delay in tumour growth (130,131). These effects indicate a clear decrease in RB1 phosphorylation and a predominantly cytostatic G1 arrest (131). Importantly, this mechanism depends on the presence of an active Rb protein (132). Similar to Palbociclib, Ribociclib not only catalytically inhibits CDK4/6 but also promotes the redistribution of p21, thereby effectively blocking the phosphorylation of pRb and the subsequent downstream events, which prevent the cell from progressing into S phase (103). The non-catalytic p21 dissociation described for palbociclib is also shared by ribociclib and abemaciclib. This suggests a common mechanism among current clinical CDK4/6 inhibitors. The release of p21 redirects it toward CDK2 complexes, providing an extra level of cell cycle control and potentially improving therapeutic effectiveness (117).

Overall, both drugs modulate the CDK4/6–Rb axis with overlapping yet distinct profiles, underscoring their central role in cancer therapy and guiding future combination strategies (77,110).

5. Effects of CDK4/6 Inhibitors on Ovarian Function

Chemotherapy is well known to cause ovarian damage through both structural and functional mechanisms, leading to follicular depletion via apoptotic cell death in both oocytes and surrounding somatic cells (133). Additionally, vascular injury has been reported (134), along with premature activation and subsequent atresia of primordial follicles, a phenomenon called burn-out (135). However, there is still a lack

of comprehensive data regarding the ovarian effects of newer anticancer treatments, such as targeted therapies. The use of cyclin-dependent kinase 4/6 (CDK4/6) inhibitors, including Palbociclib, Ribociclib, and Abemaciclib, has significantly transformed the treatment strategy for hormone receptor-positive (HR+), human epidermal growth factor receptor 2-negative advanced or metastatic breast cancer, typically in conjunction with endocrine therapy (136).

Although CDK4/6 plays vital roles in ovarian physiology, there is limited data on the gonadotoxic effects of external CDK4/6 inhibitors. These agents are being used more frequently in clinical settings, but making fully informed treatment choices for premenopausal patients concerned about premature ovarian failure (POI) and infertility remains difficult (40). At this stage, it is crucial to redirect attention from oncology-specific results to reproductive endpoints, especially regarding dormant follicle behaviour and steroidogenic potential.

Growing data are shedding light on the diverse biological roles of the CDK4/6 inhibitor palbociclib, including its influence on cell cycle regulation and potential tissue-protective effects in ovarian somatic cells. Experiments with Chinese hamster ovary (CHO) cells demonstrated that, without the endogenous CDK inhibitor p21, palbociclib boosts both the stability and activation of cyclin D3–CDK4/6 complexes. However, this effect disappears when p21 is co-expressed, indicating a competitive interaction between palbociclib and p21 for stabilizing these complexes (137). This mechanistic insight is particularly relevant for ovarian function, as the growth of granulosa cells during follicle development relies heavily on the proper activation of cyclin D–CDK4/6 complexes at the right time. Supporting these insights, recent research using immortalized human granulosa-lutein (hGL) cells has revealed a potential protective effect of palbociclib when cells are exposed to oxidative stress induced by chemerin. Chemerin, a pro-inflammatory adipokine associated with obesity and reproductive issues, is known to increase the production of reactive oxygen species (ROS), which can lead to cell death by initiating apoptosis. In this harmful process, palbociclib helps by lowering ROS levels inside the cells and reducing the expression of proteins that promote cell death, ultimately providing a protective, anti-apoptotic effect (138,139). These observations imply that palbociclib's effects on ovarian cells may go beyond its canonical role as a G1-phase cell cycle inhibitor. It might also influence stress-response pathways. Clinically, this dual functionality suggests that CDK4/6 inhibition may preserve granulosa cell integrity

and ovarian reserve in reproductive-age women receiving targeted therapy, without compromising anticancer efficacy. This approach could reduce the risk of premature ovarian failure without diminishing the drug's anticancer effectiveness (137–139). Conversely, research by Crozier et al. (2022) showed that prolonged exposure to CDK4/6 inhibitors, such as palbociclib and ribociclib, can induce replication stress and DNA damage in tumour cells, including the RB-proficient MCF7 breast cancer cell line and non-cancerous retinal pigment epithelial (RPE1) cells. This cellular stress activates the p53 pathway, resulting in cell cycle arrest and, in some cases, cellular senescence. Although these effects are intended to inhibit cancer cell growth, similar responses in healthy cells raise concerns about safety. Such mechanisms might also occur in ovarian granulosa and luteal cells, affecting ovarian reserve and fertility. This underscores the importance of determining whether similar responses also occur in ovarian somatic cells. While monitoring ovarian function and fertility preservation are important, evidence mainly comes from non-ovarian cell models, leaving a gap in understanding responses in human ovarian cells (140)**.**

There is limited clinical data specifically examining the effect of CDK4/6 inhibitors on ovarian function. Among available adjuvant studies, only the phase III Penelope-B trial assessed hormonal markers, reporting no significant changes in estradiol or FSH levels when combined with endocrine therapy following chemotherapy. Although these results suggest that systemic endocrine disruption might be minimal, they do not provide information on the behavior of dormant primordial follicles or steroidogenic function of the secondary follicles. Additionally, there is a lack of similar data for Abemaciclib and Ribociclib, underscoring a noticeable gap in understanding their specific effects on ovarian health and physiology (141,142).

Cyclins and their associated CDKs are crucial regulators of the cell cycle, and their dysregulation is a hallmark of cancer. Although CDK4/6 inhibitors have revolutionized breast cancer therapy, there is limited and debated information about their effects on healthy ovarian cells (40). Conflicting findings highlight the complexity of palbociclib’s effects: while some studies suggest protective actions in ovarian cells, others indicate potential risks, including replication stress and DNA damage. As the use of CDK4/6 inhibitors becomes more common in clinical use of CDK4/6 inhibitors, particularly in younger breast cancer patients with fertility concerns, there's an urgent need for focused research. Such studies are crucial to fully

understand any possible effects on the ovaries, which can inform better counselling and help women make well-informed decisions about their treatment options. Given the current uncertainties, further research is necessary to clarify the effects of CDK4/6 inhibitors on ovarian hormone production and reproductive health (40).

CHAPTER 2

MATERIAL & METHODS

2.1 Patients

Ovarian cortical tissue samples were obtained from reproductive-age women undergoing laparoscopic surgery at Koç University Hospital. Ovarian cortical tissue was collected from young female participants (mean age ± SD: 32.8 ± 4.7 years) (n = 4). Tissues embedded within excised cysts were dissected under sterile conditions and used for *ex vivo* culture. Additionally, human primary luteinized granulosa cells (hLGCs) were collected from 20 IVF patients at Koç University Hospital IVF Unit at the time of oocyte retrieval. Controlled ovarian stimulation was performed using a recombinant FSH–GnRH antagonist protocol. At the time of oocyte retrieval, with recombinant hCG (Ovitrelle) for normal responders and with leuprolide acetate (GnRH-agonist trigger) for hyper-responders, with oocyte pick-up occurring 36 h post-trigger.

All human samples are collected with informed consent and in compliance with institutional ethics regulations, approved by the Institutional Review Board (IRB No: 2024.243.IRB2.108).

2.2 Human Luteinized Granulosa Cells and Tissue Culture

2.2.1 Non-Mitotic Human Luteinized Granulosa Cell Isolation and Culture

Patients undergoing treatment at Koç University Hospital's infertility clinic for oocyte retrieval have the residual fluid from the washing process collected after oocyte selection during follicle aspiration. For the experiments, primary human luteinized granulosa cells (HLGCs) were used. These highly differentiated cells are post-mitotic, meaning they do not divide spontaneously or when exposed to mitogenic

agents, and they are characterized by their ability to secrete large amounts of progesterone and estradiol in culture (143). Human luteal granulosa cells (hLGCs) are extracted from the follicular fluid obtained from the washing procedure and purified from tissues and red blood cells. The following protocol was established in previous studies for the isolation of hLGCs (143,144). Initially, the follicular fluid undergoes centrifugation at 500 rpm for 5 minutes, followed by careful aspiration of the upper phase without disturbing the pellet. The pellet is then resuspended in ddH_2O and 10x phosphate-buffered saline (PBS) and centrifuged again at 500 rpm for 5 minutes. The upper phase is then removed. The number of washing steps is determined based on the presence of red blood cells in the follicular fluid. Following purification from red blood cells, hLGCs, recognizable as a white pellet, will be cultured in 6-well plates at a density of 5 × 10^5 cells/well in DMEM-F12 culture medium supplemented with 10% fetal bovine serum (FBS), 1% penicillin-streptomycin, and 1:1000 Amphotericin B at 37°C and 5% CO_2. After allowing cells to adhere, they were exposed to CDK4/6 inhibitors Palbociclib (PZ0383, Sigma Aldrich) or Ribociclib (S7440, Selleckchem) at concentrations ranging from 0.625 to 10 μM for up to 72 hours.

2.2.2 Ovarian Tissue Isolation and Culture

Following immediate transfer of ovarian tissue into collection tubes containing HEPES-buffered DMEM/F12 supplemented with 20% FBS, samples were minced into 0.5 × 0.5 cm pieces and cultured for 24 hours in 6-well plates (3 mL media/well) in DMEM/F12 medium containing 20% fetal bovine serum (FBS), 1% penicillin-streptomycin, and 1:1000 Amphotericin B. On the same day, in isolation, while taking the tissue pieces into a culture plate, they were exposed to CDK4/6 inhibitors (Palbociclib or Ribociclib) at concentrations of 0.625 and 10 μM for 24 hours directly.

2.3 HGrC1 and COV434 Cell Line Culture

The human granulosa cell lines HGrC1 and COV434, representing non-luteinized and tumour-derived granulosa cell models, respectively, were used to investigate granulosa cell-specific responses in vitro. The COV434 cell line (Sigma Co.), established from a human granulosa cell tumour, was utilized due to its key biological properties. The cells are known to produce 17β-estradiol in response to FSH and can undergo apoptosis; however, they are unable to luteinize and lack LH

receptors (145). The HGrC1 human granulosa cell line, which is immortalized, was graciously supplied by Dr. Akira Iwase (Nagoya University, Japan). This mitotic non-luteinized HGrC1 cell line models the characteristics of early-stage follicular cells by expressing key steroidogenic enzymes and gonadotropin receptors. Functionally, HGrC1 cells respond to FSH stimulation by increasing aromatase activity and estradiol production (146). Cells were counted and seeded at assay-specific densities into appropriate culture plates and maintained in DMEM/F12 with 10% FBS and 1% penicillin–streptomycin at 37 °C, 5% CO_2. These granulosa cells were cultured under identical conditions to serve as standardized models for evaluating the mitotic response to CDK inhibition at doses ranging from 0.625 to 10 μM for up to 72 hours.

2.4 Cell Cycle Synchronization and Flow Cytometry

Flow cytometry was used to evaluate the effects of CDKi on cell cycle progression. For synchronization at the G1/S boundary, cells were first serum-starved for 24 hours and then treated with 2 μg/mL aphidicolin in complete media for 18 hours to induce synchronization at the G1/S boundary. Following synchronization, aphidicolin was removed, and cells were allowed to progress through the cell cycle in complete media for 6 hours post-release, corresponding to the G2/M transition. Then, they were treated with only 2.5 μM of Palbociclib and Ribociclib at different incubation time points. Cells were collected at 6-, 8-, 10-, 12-, 14-, and 16-hour intervals post-synchronization. Trypsinized cells were washed with PBS, then fixed with FxCycle™ PI/RNase Staining Solution, vortexed, and incubated for 10 minutes at room temperature in the dark. DNA content and cell cycle distribution (G0/G1, S, G2/M) were analysed using a FACS Calibur system, and the results were processed with FlowJo software to assess the cytostatic effects of CDK4/6 inhibition, along with proper controls for cell cycle arrest.

2.5 MTT Cell Viability Assay

Cell viability was assessed with the MTT (3-(4,5-dimethylthiazol-2-yl)-2,5-diphenyltetrazolium bromide) assay, a colorimetric technique that measures mitochondrial dehydrogenase activity in cells. These enzymes reduce yellow tetrazolium salt to insoluble purple formazan crystals. After dissolving these crystals

with DMSO, the resulting colour intensity, directly proportional to the number of viable cells, was quantified by measuring absorbance at 570 nm (147).

MTT assay was used to assess the viability of granulosa cells following exposure to CDK4/6 inhibitors. Cells were seeded in 96-well plates and treated with the inhibitors for 24 and 48 hours. After incubation, 200 μL of MTT reagent (0.5 mg/mL) was added to each well and incubated at 37°C for 3–4 hours. The resulting formazan crystals were dissolved in DMSO, and absorbance was measured at 570 nm to quantify viable cells.

2.6 Real-Time Monitoring of the Proliferation of the Granulosa Cells with Impedance-based xCELLigence RTCA System Platform

Real-time monitoring of cell proliferation and viability was conducted using the xCELLigence Real-Time Cell Analyzer (RTCA) system, a label-free, impedance-based system. This instrument utilizes E-plates with interdigital gold microelectrodes to non-invasively measure changes in electrical impedance, which directly reflect cell attachment, spreading, and proliferation. The electronic readout is quantitatively expressed as a Cell Index (CI), enabling the generation of kinetic cell response profiles.

For the experiments, cells were cultured to their logarithmic growth phase before being treated with the specified compounds. Following treatment, CI values were recorded at 30-minute intervals over a total period of up to 140 hours. To enable comparison between different treatment groups, the results were expressed as a Normalized Cell Index, which was calculated by dividing the CI at each time point by the CI value recorded immediately prior to the addition of the compounds (148).

Added complete medium to each well of the E-Plate and let it equilibrate at room temperature for 15 minutes. Subsequently, baseline impedance was measured. Granulosa cells were seeded into 16-well E-plates at a density of 5,000-7,000 cells per well for HGrC1 and 10,000-15,000 cells per well for COV434 cells in 200 μL of medium, then allowed to adhere at 37°C with 5% CO2. Impedance will be monitored every 30 minutes. Once the cells reached logarithmic growth approximately 20 hours after plating, they were treated with CDK4/6 inhibitors at different concentrations (0.625–20 μM). The impedance-derived Cell Index (CI) was normalized to a reference point just before drug addition, setting CI = 1. For quantitative comparison between treatment groups, the area under the curve (AUC) of normalized CI values over the

first 72 hours was calculated, providing a summary metric of overall proliferative activity. Data was collected continuously for up to 120 hours using RTCA Software 1.2. This approach enabled dynamic assessment of the cytostatic effects of the inhibitors on cell viability and proliferation kinetics.

2.7 Western Blotting

To investigate the effect of CDK inhibitors, Western blot analysis was performed. This analysis aimed to assess the expression levels of various proteins, including StAR, 3β-HSD, and CYP19A1, as well as the levels of CDK4, CDK6, E2F, p21, Rb, and p-Rb, and PARP. After cell harvesting, proteins were lysed in a Radio Immunoprecipitation Assay lysis buffer mixture with phosphatase inhibitor and protease inhibitor cocktail (Sigma, MA, USA), and after incubating on ice for 20 minutes, the samples were spun in a centrifuge at 16,000xg, 20 minutes at 4°C to collect the supernatants, which contain the total cell extract. Total protein levels were measured using the bicinchoninic acid assay with a standard curve of 0–2 mg/mL BSA; at 562 nm absorbance was recorded on a microplate reader (model). Samples were analysed in duplicate, and concentrations were calculated from the standard curve. Then, same quantity of protein from each sample will be mixed with 4x Laemmli sample buffer with 2-mercaptoethanol and separated via SDS-polyacrylamide gel electrophoresis. The proteins were subsequently transferred to a polyvinylidene difluoride membrane. Then, non-specific binding sites were blocked with non-fat dry milk in Tris-buffered saline-Tween 20 (TBS-T) at room temperature for one hour. Subsequently, 1:1000 diluted primary antibodies were incubated with the membrane overnight at 4°C. The next day, the membrane was incubated using goat anti-mouse IgG (H+L) and goat anti-rabbit IgG (H+L) horseradish peroxidase conjugated secondary antibodies at a dilution of 1:2000. Protein levels were quantified using Clarity™ Western Enhanced chemiluminescence Substrate, and chemiluminescence was detected using the ChemiDoc MP Imaging System (BioRad, USA).

2.8 Immunofluorescence Staining

The cells, fixed with 4% paraformaldehyde for 20 minutes at room temperature for immunofluorescence staining, were then permeabilized by Triton X-

100 solution diluted in 1X DPBS for 15 minutes. Then, cover slips were washed in 0.1% Tween-20 in DPBS (DPBS-T). Afterwards, they were immersed in a blocking solution (SuperBlock, ThermoFisher) for 20 minutes. Following the blocking step, cells were left to incubate overnight at 4°C. with phospho-Rb, Rb, StAR, 3β-HSD, and PARP antibodies at a 1:100 dilution. After DPBS-Tween washing, fluorochrome-conjugated secondary antibodies (Alexa Fluor 488 and 594) were incubated for 1 hour at 37°C, followed by additional DPBS-Tween washing. A mounting medium containing DAPI stain was added to the microscope slide to cover the coverslip, and imaging was performed using a confocal microscope (DMI8, Leica) using appropriate channels.

2.9 Hormone Measurement

Levels of estradiol (E2), progesterone (P4), and Anti-mullerian hormone (AMH) in the culture media were measured using electrochemiluminescence immunoassay (ECLIA) with Elecsys and Cobas analysers from Roche Diagnostics, USA. The detection thresholds and coefficients of variation (CV%) were 5.00 pg/mL with 1.4% CV for E2 and 0.030 ng/mL with 1.2% CV for P4. AMH levels were quantified using a MIS/AMH ELISA kit (Diagnostic Systems Laboratories, USA), with a detection sensitivity of 0.006 ng/mL and intra-assay variability ranging from 2.4% to 4.6%, depending on the concentration.

2.10 Statistical Analysis

Levels of steroidogenic enzymes, hormone concentrations, and signal intensities observed in immunoblotting and confocal imaging were considered continuous variables and presented as mean ± SEM from at least three independent experiments unless otherwise stated. Parametric data comparisons used ANOVA/Tukey's test, whereas non-parametric data were analysed with Kruskal–Wallis/Dunn post hoc tests. Flow cytometry–based cell-cycle phase proportions were analysed as compositional data after centred log-ratio (CLR) transformation and modelled via linear regression with treatment and time as covariates (Python 3.12; statsmodels); in parallel, dead-cell percentages were analysed on the raw scale using linear regression with robust standard errors. The sample size required for statistical

significance and reliable interpretation was calculated based on immunoblot assay results.

CHAPTER 3

RESULTS

3.1 Effects of CDK4/6 inhibition on granulosa cell viability and proliferation

3.1.1 Effects of Palbociclib and Ribociclib on HGrC1 Viability

To assess how inhibiting CDK4/6 affects granulosa cells viability, HGrC1 cells were treated with increasing concentrations of Ribociclib and Palbociclib (0.63–10 µM) and analysed after 24 h and 48 h using the MTT assay. After 24 hours, both inhibitors showed minimal effects, with relative absorbance values remaining close to control levels and no significant reductions across different doses (Figure 7A, 7B). A significant reduction was detected only at the highest concentration of ribociclib (10 µM; $p < 0.0001$) after 24 h (Figure 7A). By 48 h, however, both drugs induced a slight, time- and dose-dependent decrease in viability. Ribociclib produced a moderate reduction in viability, whereas palbociclib showed a more pronounced effect at equivalent concentrations. All reductions at 48 h were statistically significant compared with controls ($p < 0.0001$; Figure 7C, 7D).

These findings indicate that Palbociclib and Ribociclib suppress HGrC1 metabolic activity in a dose and time dependent manner, with Palbociclib exerting slightly stronger effects.

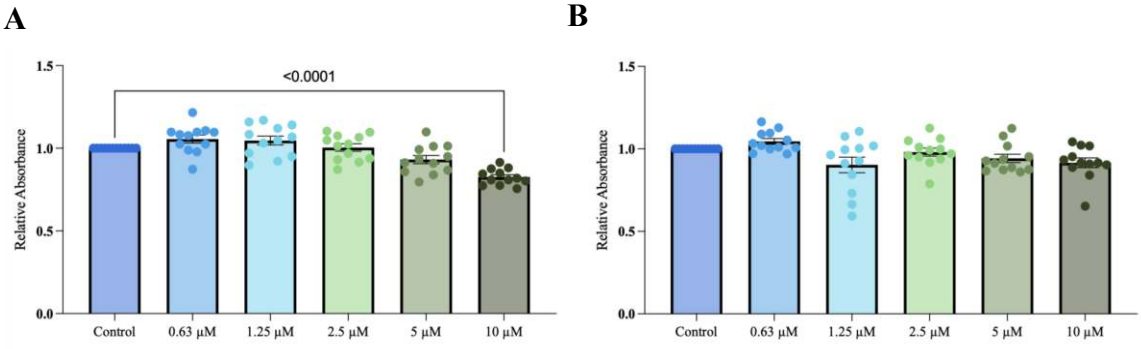

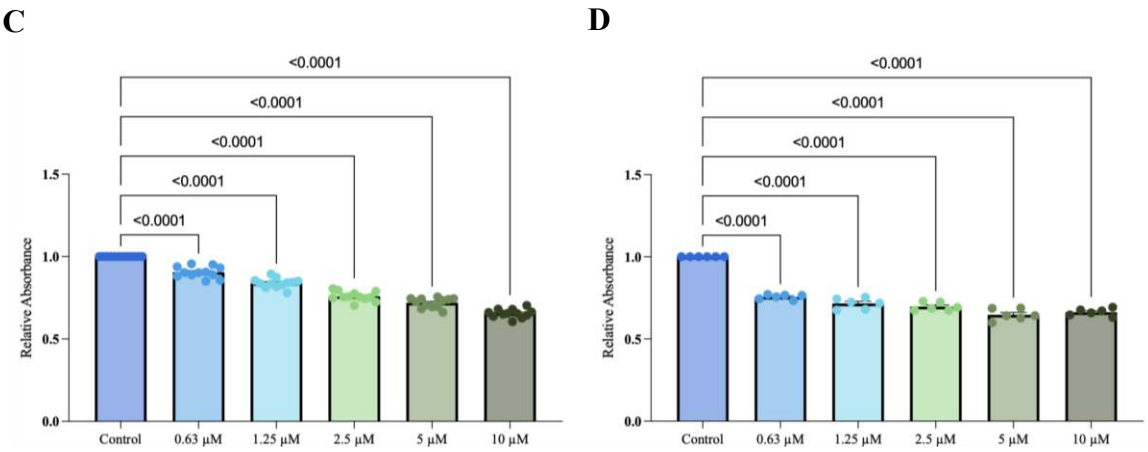

Figure 8: Palbociclib and ribociclib effects on viability of HGrC1 cells in a time- and dose-dependent manner. (A) Ribociclib treatment for 24 h maintained metabolic activity across most concentrations, with a reduction evident only at the highest dose (10 µM). (B) Palbociclib exposure for 24 h did not significantly alter viability at any tested concentration. (C) Ribociclib treatment for 48 h induced a dose-dependent decrease in viability compared with control. (D) Palbociclib exposure for 48 h resulted in a robust, dose-dependent suppression of viability across all tested concentrations. Data are shown as mean ± SEM; significance values are indicated in the figure.

3.1.2 Viability of Primary Luteinized Granulosa Cells to CDK4/6 Inhibition

To assess the effect of CDK4/6 inhibition on primary luteinized granulosa cell viability, HLGCs were treated with increasing concentrations of Ribociclib and Palbociclib (0.63–10 µM) for 24 h (Figure 8A, 8B).

Unlike the proliferative HGrC1 model, HLGCs displayed no measurable decline in viability across the tested range. Relative absorbance values remained stable, fluctuating around control levels, and statistical analyses confirmed that there are no significant differences. This lack of response is consistent with the non-mitotic state of luteinized granulosa cells, which no longer rely on CDK4/6 activity for cell-cycle progression. The findings indicate that CDK4/6 inhibitors do not exert cytotoxic

effects in this terminally differentiated context, reinforcing the notion that their action is predominantly cytostatic in proliferative cells.

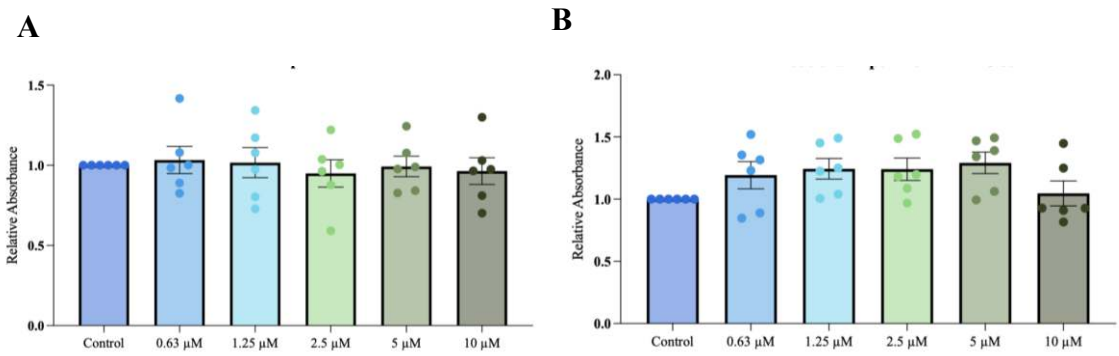

Figure 9: CDK4/6 inhibition did not impair the viability of non-mitotic luteinized granulosa cells (A) HLGCs treated with ribociclib (0.63–10 µM, 24 h). Relative absorbance values remained stable compared with controls, indicating no significant reduction in metabolic activity. (B) HLGCs treated with palbociclib (0.63–10 µM, 24 h). Similar to ribociclib, no significant changes were observed across concentrations (mean ± SEM).

3.1.3 Viability of COV434 Cells Under CDK4/6 Inhibition

The impact of CDK4/6 inhibition on metabolic activity was further assessed in the mitotic non-luteinizing malignant COV434 granulosa cell line using the MTT assay. After 24 h of palbociclib exposure, a significant reduction in cell viability was detected only at the highest concentration (10 µM; $p < 0.0001$), whereas lower doses (0.63–5 µM) did not differ from controls (Figure 9A). Prolonged exposure for 48 h revealed a similar pattern, with metabolic activity significantly decreased at 10 µM ($p < 0.01$), while no changes were observed at lower concentrations (Figure 9B).

To evaluate whether the observations with palbociclib were conserved across different CDK4/6 inhibitors, viability assays were repeated with ribociclib. After 24 hours, cell viability remained comparable to that of controls across all tested concentrations, with no significant changes (Figure 9C). In contrast, after 48 h of treatment, ribociclib induced a marked inhibitory effect, with significant reductions detected at 0.63, 1.25, 2.5, 5, and 10 µM compared with control cells (all $p < 0.0001$; Figure 9D). The inhibition was dose-dependent, reaching its maximum at 10 µM.

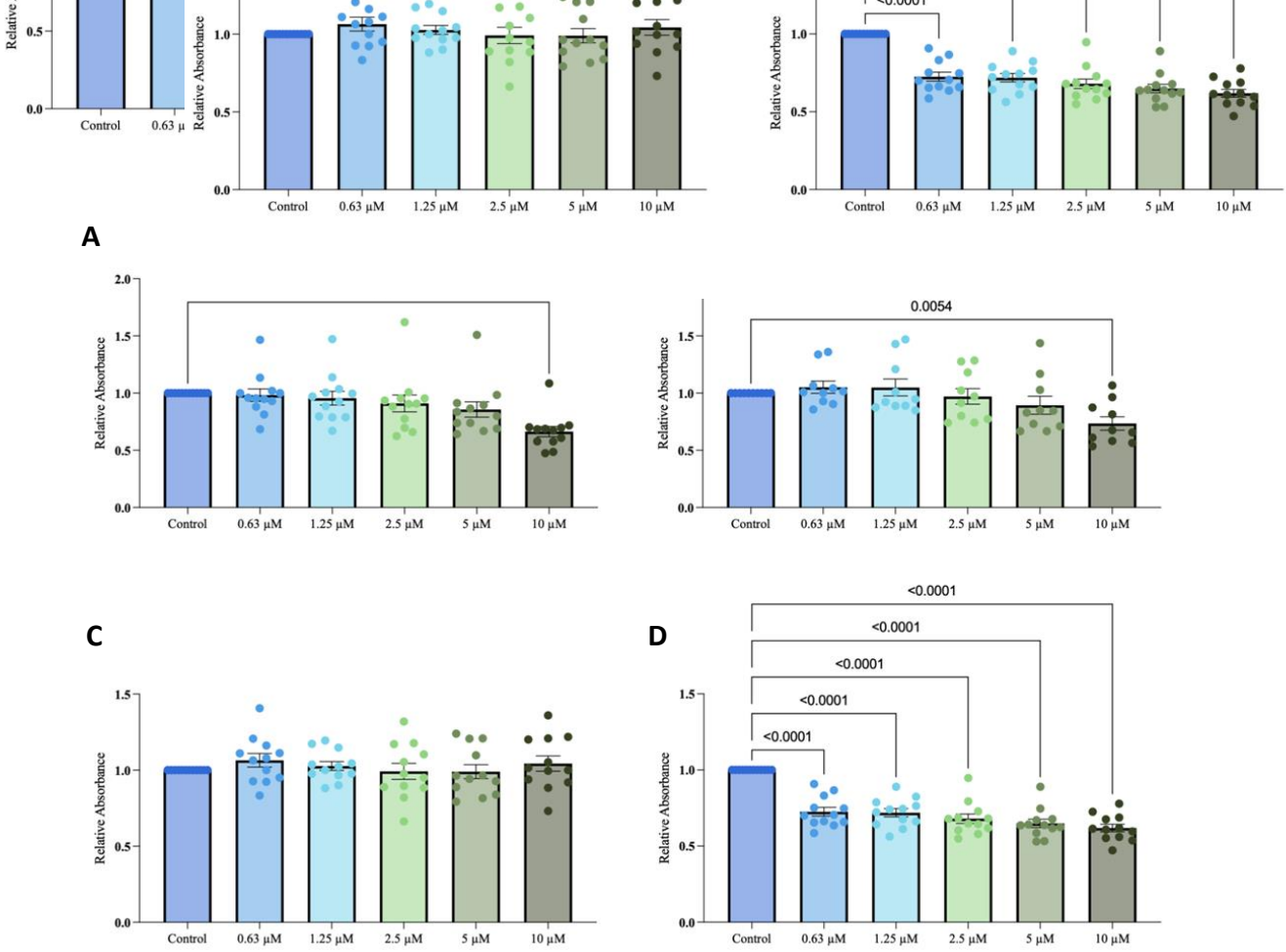

Figure 10: Viability of COV434 cells following palbociclib and ribociclib treatment. (A) MTT assay of COV434 cells after 24 h exposure to palbociclib (0.63, 1.25, 2.5, 5, and 10 µM). A significant reduction in metabolic activity was observed only at 10 µM. (B) Viability following 48 h palbociclib treatment under the same concentrations, showing decreased activity at 10 µM. (C) Ribociclib treatment for 24 h did not significantly alter cell viability across concentrations. (D) At 48 h, ribociclib induced a clear dose-dependent decrease, with significant reductions detected at 0.63–10 µM.

3.1.4 Real-time Effects of CDK4/6 Inhibition on Granulosa Cell Proliferation

To analyze the impact of CDKis on granulosa cell proliferation, the cells were monitored using the xCELLigence real-time cell analysis system. HGrC1 and COV434 cells were seeded in E-Plate 16 and treated 24 hours later with increasing concentrations of palbociclib or ribociclib (0.63–20 µM). Cell index values were recorded every 15 minutes for up to 120 h and normalized to the time of drug addition. For quantitative evaluation, the area under the curve (AUC) of normalized cell index values over the first 72 h was calculated.

In HGrC1 cells, palbociclib exposure induced a concentration and time-dependent reduction in proliferation (Figure 10). Low doses produced curves similar

to those of the controls, whereas higher concentrations of 2.5 µM progressively suppressed cell growth. At concentrations of 5–10 µM, the cell index plateaued within 48–72 hours, and proliferation was almost completely suppressed at 20 µM. This pattern was mirrored in the AUC values, which declined proportionally with increasing concentrations.

In COV434 cells, both inhibitors reduced proliferation in a dose-dependent manner. Palbociclib exerted a more immediate effect, with clear suppression observed from early time points, while ribociclib produced a gradual but consistent inhibition. At concentrations ≥10 µM, both agents markedly suppressed proliferation by 72–96 hours, with cell index curves stabilizing well below control levels (Figures 11A and 11B). AUC analysis confirmed these findings, showing steep declines across increasing concentrations for both inhibitors.

No xCELLigence experiments were conducted in primary luteinized granulosa cells due to their non-proliferative nature, consistent with MTT data showing no significant changes in viability upon CDK4/6 inhibition.

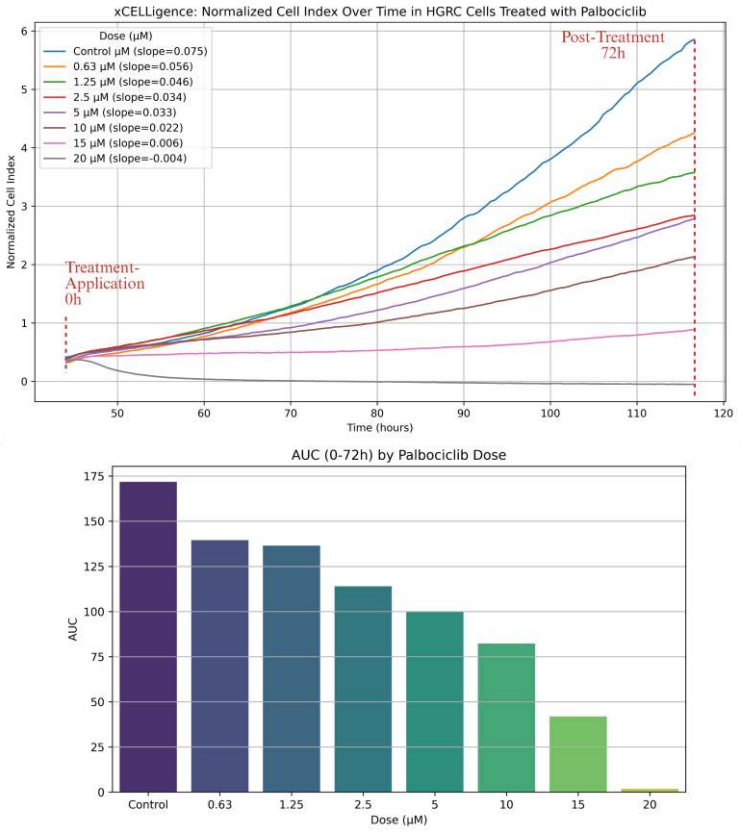

Figure 11: Real-time effects of CDK4/6 inhibition on granulosa cell proliferation measured by xCELLigence. HGrC1 cells were seeded into E-Plate 96 and exposed to

palbociclib (0.63–20 µM) after 24 h. Normalized cell index was recorded every 15 minutes over 72 h, revealing a clear dose-dependent suppression of proliferation. Area under the curve (AUC, 0–72 h) analysis confirmed progressive declines in proliferation with increasing drug concentrations (mean ± SEM).

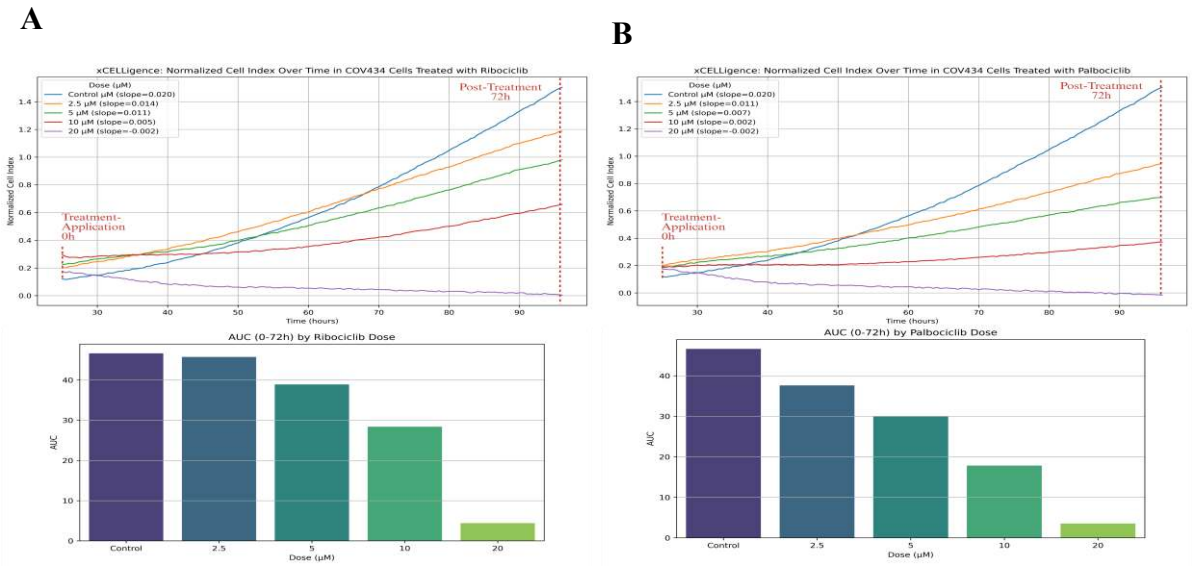

Figure 12: Real-time effects of CDK4/6 inhibition on proliferation of COV434 granulosa cells. (A) COV434 cells treated with ribociclib (2.5–20 µM) showed a gradual, dose-dependent inhibition of proliferation over 72 h. AUC (0–72 h) values supported the inhibitory profile observed in the real-time curves. (B) COV434 cells exposed to palbociclib (2.5–20 µM) exhibited stronger early suppression of proliferation compared to ribociclib, with AUC analysis confirming the concentration-dependent decline (mean ± SEM).

3.2 Effects of CDK4/6 Inhibition on Cell-Cycle Distribution

3.2.1 Time-dependent effects in HGrC1 cells

To ensure accurate evaluation of CDK4/6 inhibition at the G1–S transition, HGrC1 cells were first synchronized at the G1/S boundary using aphidicolin prior to drug exposure. Flow cytometry analysis was then performed following treatment with 2.5 µM Palbociclib and Ribociclib for 6–16 h. Flow cytometry analysis showed that exposing HGrC1 cells to either palbociclib or ribociclib resulted in a progressive, time-dependent change in cell-cycle progression. At early time points (6–8 h), both

inhibitors caused a modest increase in the G0/G1 population with a corresponding reduction in S-phase cells. This effect became more pronounced at later time points (12–16 h), where palbociclib-treated cells displayed the strongest accumulation in G0/G1 (Figures 12A and 12B), closely followed by ribociclib (Figures 13A and 13B). S-phase fractions declined accordingly, indicating an effective block at the G1–S transition. G2/M proportions remained largely stable across treatment, with only minor fluctuations.

To further assess whether the observed effects reflected cytostatic rather than cytotoxic outcomes, cell death was quantified in parallel. Dead-cell percentages generally remained low throughout the experiment, with palbociclib-treated cells staying at around 1–2% and ribociclib-treated cells showing a moderate rise at later time points, reaching up to 8%. Neither treatment induced a significant increase compared with controls, confirming that CDK4/6 inhibition primarily enforces a G1 arrest without triggering apoptosis under these conditions (Figure 14).

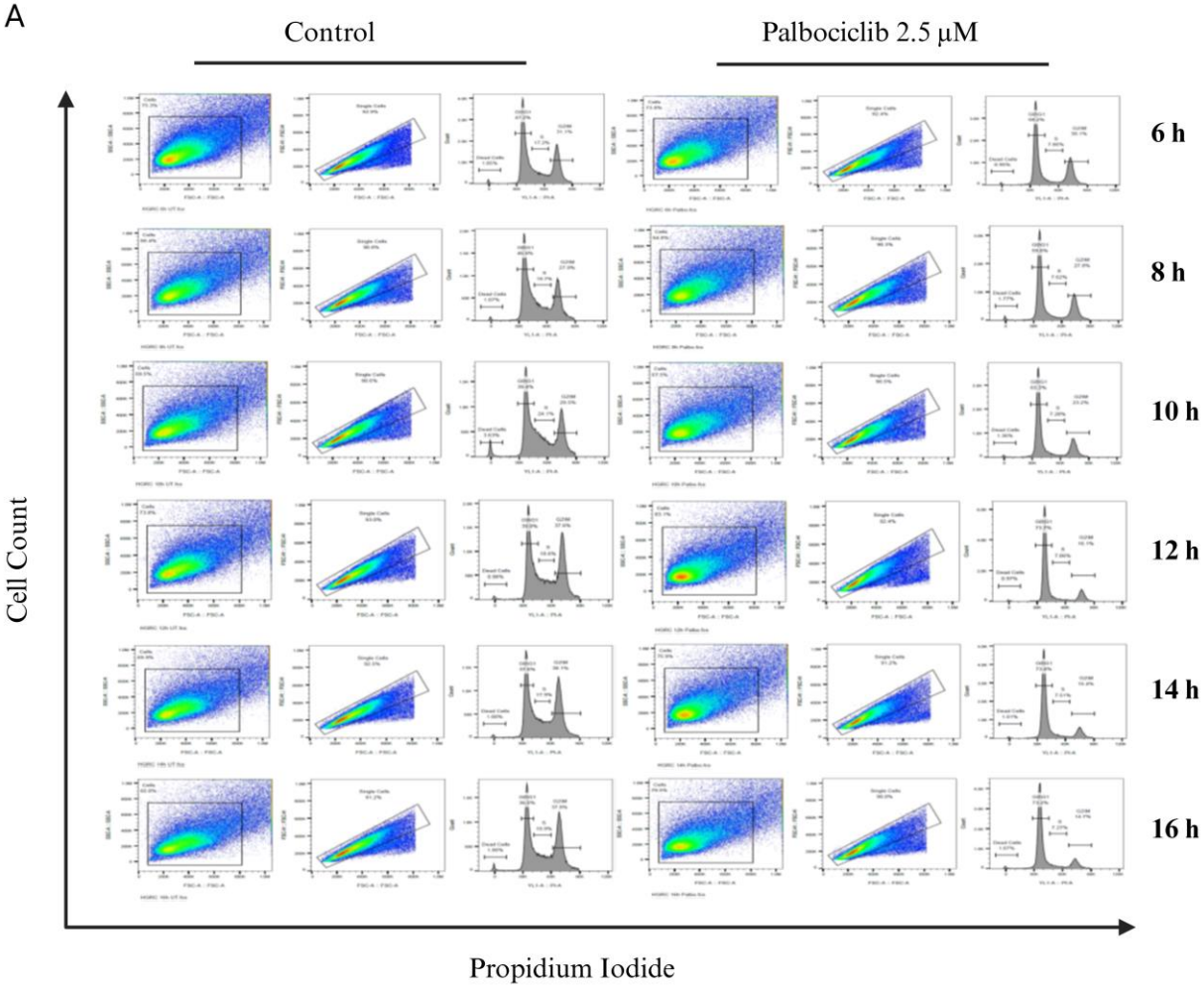

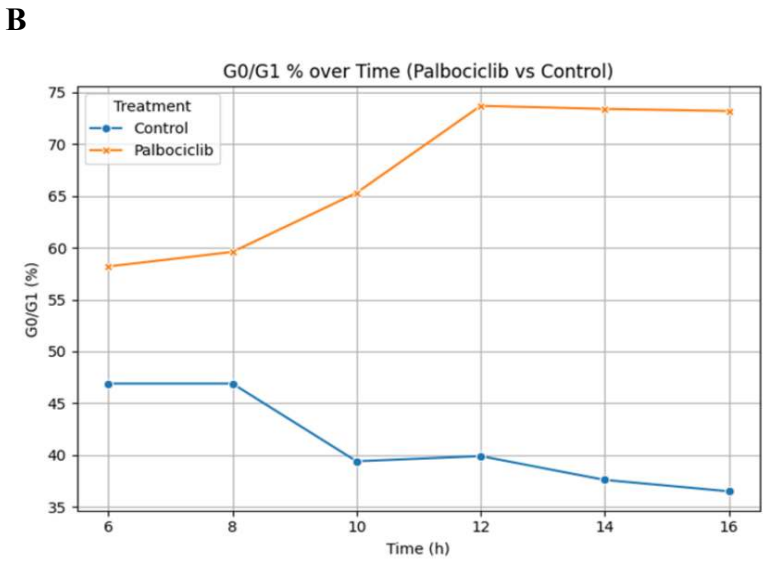

Figure 13: Time-dependent effects of palbociclib on cell-cycle distribution in HGrC1 cells. (A) Flow cytometry plots of HGrC1 cells treated with 2.5 µM palbociclib for 6–16 hours demonstrate a progressive accumulation in G0/G1 phase with a concomitant reduction in S-phase compared to controls. (B) Quantification confirmed a significant, time-dependent G0/G1 arrest ($p < 0.05$), whereas G2/M fractions showed only minor decreases at later time points.

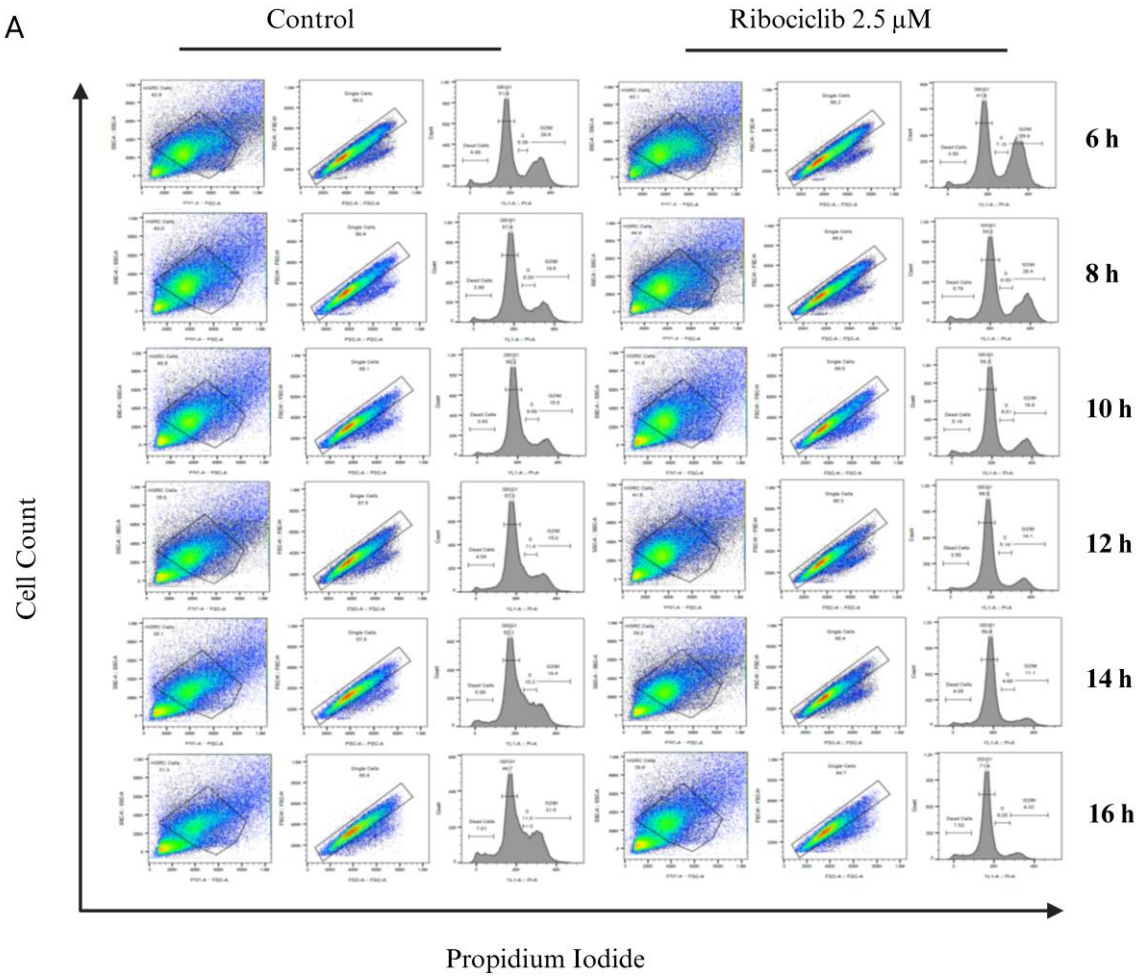

B

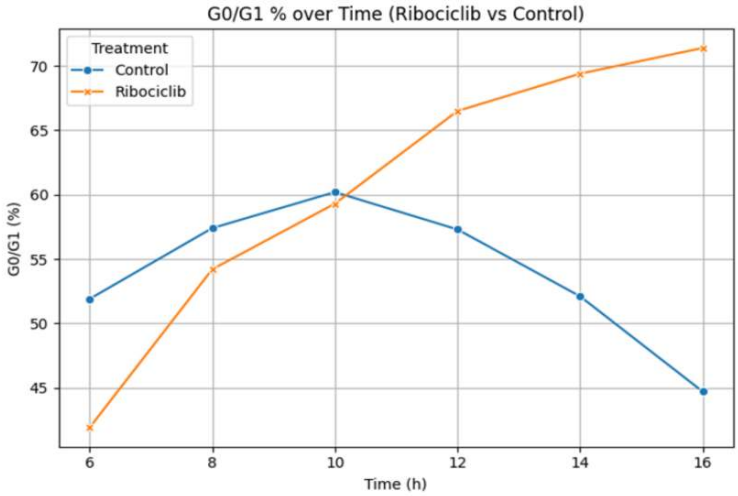

Figure 14: Time-dependent effects of Ribociclib on cell-cycle distribution in HGrC1 cells. (A) Flow cytometry plots of HGrC1 cells treated with 2.5 µM ribociclib for 6–16 hours show a progressive increase in G0/G1 fractions, accompanied by a corresponding reduction in the S-phase compared to controls. (B) Quantification confirmed a significant time-dependent G0/G1 arrest ($p < 0.05$), while G2/M fractions showed only minor late decreases without a consistent trend.

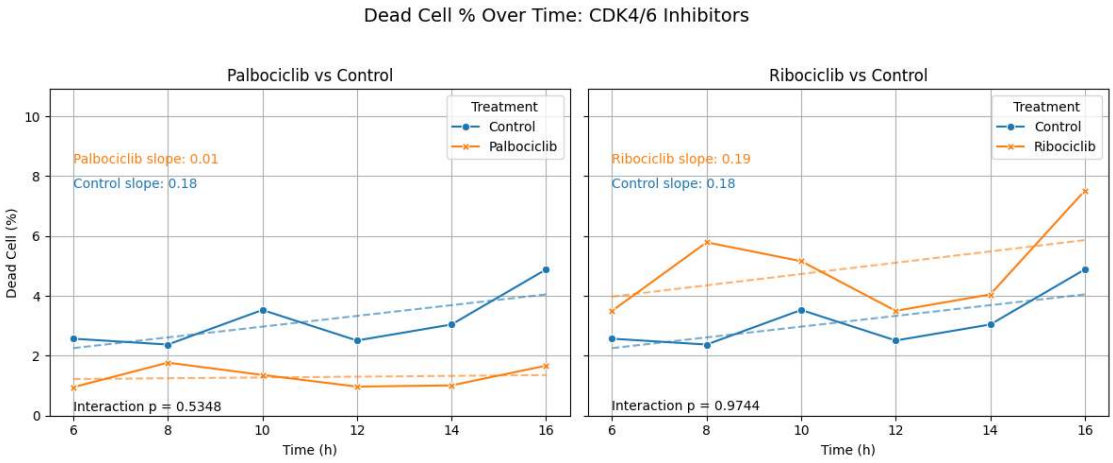

Figure 15: Effects of CDK4/6 inhibition on cell death in HGrC1 cells. HGrC1 cells synchronized with aphidicolin were treated with 2.5 µM palbociclib or ribociclib for 6–16 h. Dead-cell percentages were monitored by flow cytometry and remained consistently low across all time points (<8%). Neither palbociclib nor ribociclib induced a significant increase in cell death compared with controls ($p > 0.5$),

supporting that the observed effects of CDK4/6 inhibition were cytostatic rather than cytotoxic.

3.2.2 Dose-dependent effects of CDK4/6 inhibition by CDK inhibitors on cell cycle progression in HGrC1 Cells

Flow cytometric analysis revealed that treatment of HGrC1 cells with increasing concentrations of palbociclib or ribociclib, at doses ranging from 0.625 to 10 µM for 24 hours, resulted in a clear, dose-dependent alteration in cell-cycle distribution (Figure 15A). In untreated controls, the majority of cells were distributed across G0/G1, S, and G2/M phases with stable proportions and minimal cell death. Upon exposure to palbociclib, a progressive accumulation in the G0/G1 population was observed with increasing doses, accompanied by a corresponding reduction in S-phase entry. At intermediate to high concentrations from above 2.5 µM, this arrest became more pronounced, suggesting an effective block at the G1–S transition. Ribociclib produced a comparable pattern, though the shift appeared slightly more gradual across the dose range. In both treatment groups, the G2/M fractions showed no consistent trend, remaining relatively stable compared to the controls. Cell death fractions remained low, supporting the interpretation that the observed effects were primarily cytostatic rather than cytotoxic. HGrC1 cells maintained live cell rate above 90% following 24-h treatment with either palbociclib or ribociclib at all tested concentrations (Figure 15B).

A

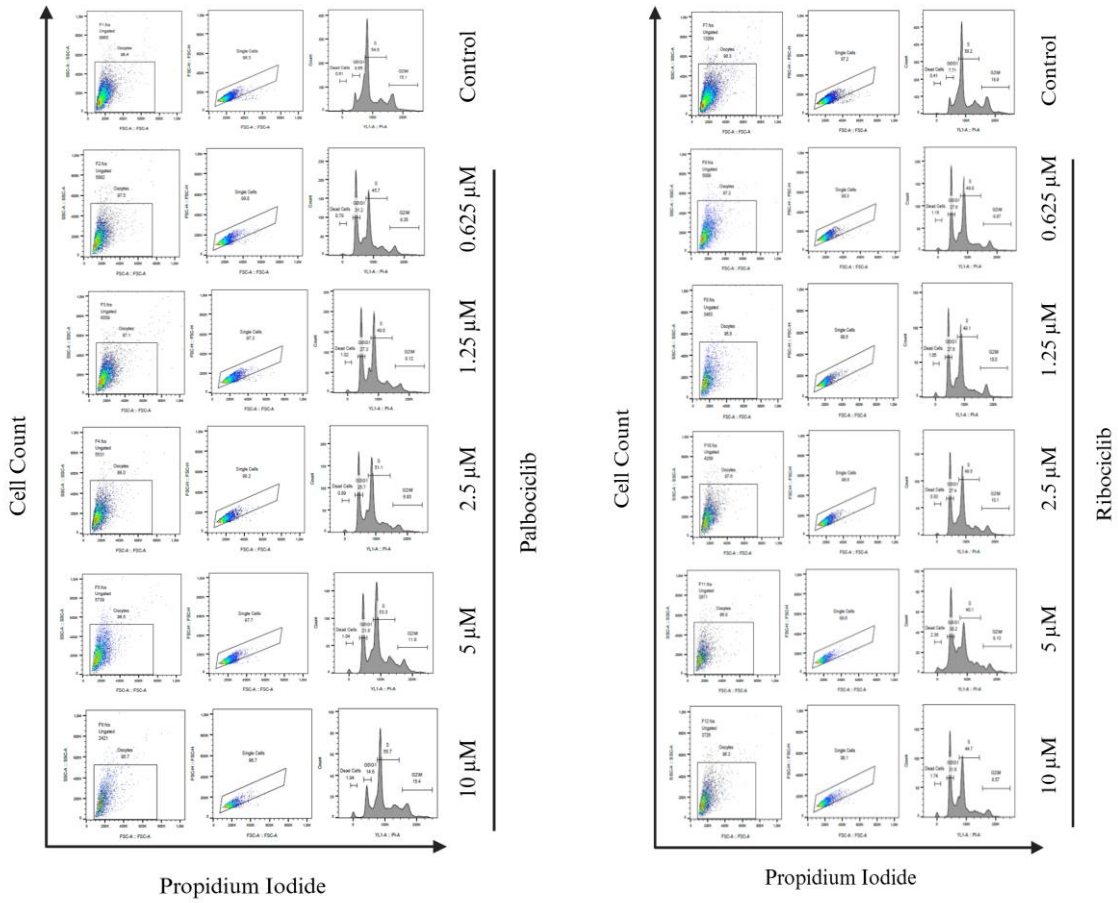

B

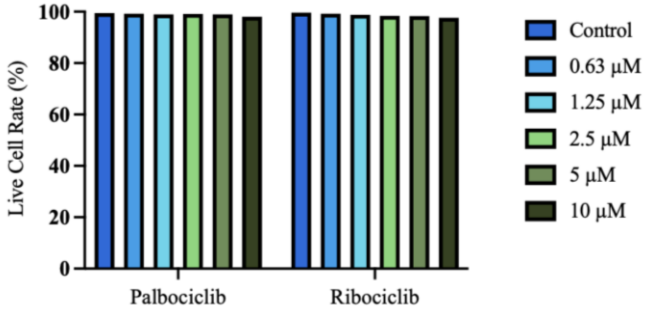

Figure 16: Dose-dependent effects of palbociclib and ribociclib on cell-cycle distribution in HGrC1 cells. (A) Flow cytometry plots show representative distributions following 24 h treatment with increasing concentrations (0.625–10 µM). Both inhibitors progressively increased the G0/G1 population with a corresponding reduction in S-phase, while G2/M remained largely unaffected. (B) Live cell rates of HGrC1 cells after 24-h exposure to palbociclib or ribociclib, with live-cell rates consistently above 90% across all conditions.

3.2.3 Dose-dependent effects of CDK4/6 inhibition by CDK inhibitors on cell cycle progression in COV434 Cells

COV434 cells treated with palbociclib (0.625–10 µM, 24 h) displayed a clear, dose-dependent increase in G0/G1 fractions. This shift was accompanied by a proportional reduction in the S-phase, while the proportions of G2/M remained broadly unchanged. Similar to HGrC1, higher concentrations produced the strongest arrest, supporting the cytostatic action of palbociclib. Cell death remained minimal, consistent with a cytostatic rather than cytotoxic response (Figure 16A).

Ribociclib treatment of COV434 cells produced a parallel trend (Figure 16A). Increasing doses led to a progressive enrichment of the G0/G1 phase with suppression of S-phase entry, while the G2/M fractions and cell death showed no substantial changes. The degree of arrest was again most apparent at higher concentrations, although the shift appeared slightly more gradual compared to palbociclib. Similarly to HGrC1 results, in COV434 cells, live cell rates remained above 90% across all palbociclib- and ribociclib-treated groups at 24 h (Figure 16B), further supporting the evidence that CDK4/6 inhibitors act in a cytostatic rather than cytotoxic manner in proliferative granulosa-derived tumour cells.

A

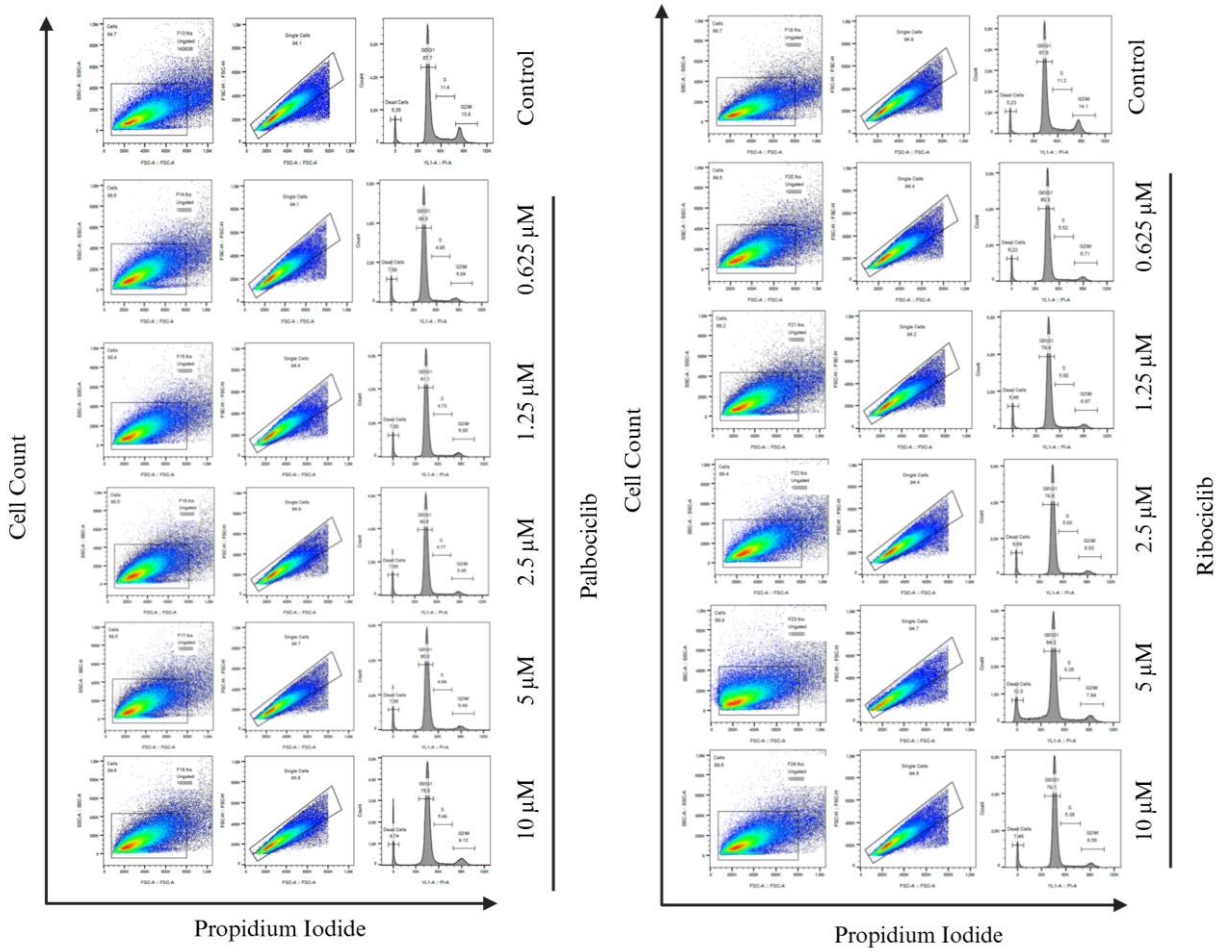

B

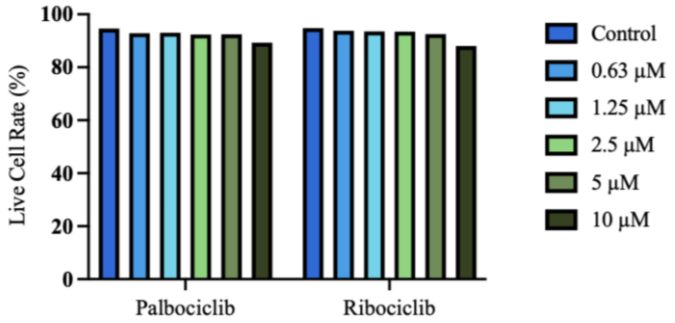

Figure 17: Dose-dependent effects of CDK4/6 inhibitors on cell-cycle distribution in COV434 cells. (A) Flow cytometry plots show representative distributions following 24 h treatment with palbociclib or ribociclib (0.625–10 µM). Both inhibitors induced a concentration-dependent accumulation in G0/G1 phase with reduced S-phase entry,

while G2/M and cell death fractions remained largely unaffected. (B) Live cell rate of COV434 cells after 24-h exposure to palbociclib or ribociclib across all doses.

3.3 Effects of CDK4/6 Inhibition in HGrC1 Cells

3.3.1 Time- and dose-dependent effects of CDK4/6 inhibitors (ribociclib and palbociclib) on Rb pathway and steroidogenic proteins in HGrC1 cells

At 24 h, phosphorylated Rb (pRb) levels were markedly reduced in a dose-dependent manner. A significant decrease was observed starting from 0.625 μM treatment ($p < 0.05$), and this effect became more pronounced at higher concentrations. In contrast, total Rb expression remained largely unchanged with no significant differences compared to control ($p > 0.05$). p21 protein expression showed a clear induction with ribociclib exposure, reaching significance at 1.25 μM and above ($p < 0.05$). E2F1 expression gradually decreased across doses, and the reduction was statistically significant compared with the control ($p < 0.05$) (Figure 17A).

At 48 h, ribociclib treatment continued to suppress pRb expression at all tested concentrations, with significant decreases evident from 1.25 μM onwards ($p < 0.01$). Total Rb expression remained stable ($p > 0.05$). CDK6 protein levels did not show significant variation across the dose range ($p > 0.05$) (Figure 17B).

At 72 h, a similar pattern was observed. Ribociclib significantly reduced pRb levels, with strong decreases detected at concentrations of 2.5 μM and higher ($p < 0.01$). Total Rb remained unchanged ($p > 0.05$), and CDK6 protein expression did not exhibit significant alterations ($p > 0.05$) (Figure 17C).

Together, these findings demonstrate that ribociclib consistently suppresses Rb phosphorylation in HGrC1 cells in a dose-dependent manner while maintaining stable total Rb and CDK6 expression. In parallel, ribociclib induces p21 and reduces E2F1 protein expression, both changes reaching statistical significance.

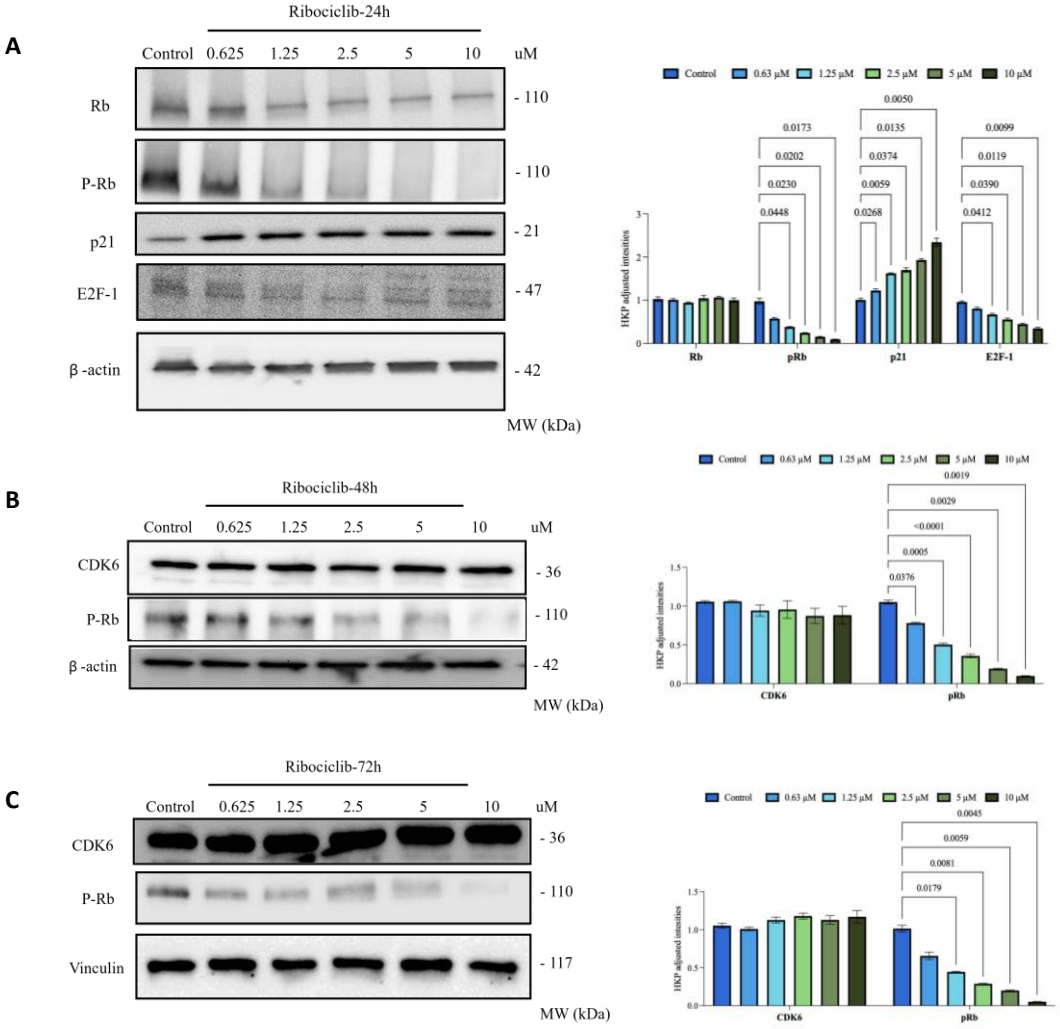

Figure 18: The protein levels of Rb pathway proteins in HGrC1 cells treated with ribociclib for 24–72 h. (A) At 24 h, ribociclib reduced pRb levels in a dose-dependent manner, induced p21 expression, and decreased E2F1, while total Rb remained unchanged. (B) At 48 h, pRb reduction persisted, with stable total Rb and no significant change in CDK6. (C) At 72 h, ribociclib further suppressed pRb, whereas total Rb and CDK6 remained stable.

Following the ribociclib experiments, the effects of palbociclib were examined in HGrC1 cells after 24 h exposure. As shown in Figure 18A, palbociclib treatment induced consistent alterations in Rb pathway proteins and related markers.

In Figure 18 panel A, a clear dose-dependent reduction in phosphorylated Rb (pRb) levels was observed, whereas total Rb expression remained largely stable ($p > 0.05$). E2F1 levels decreased significantly at higher concentrations ($p < 0.05$), while CYP19A1 did not exhibit notable changes.

In Figure 18, panel B demonstrates that palbociclib induced p21 expression in a concentration-dependent manner ($p < 0.05$), while PARP and StAR expression remained unchanged compared with control. CDK4 and CDK6 protein levels also did not show significant variation across doses ($p > 0.05$). Together, these findings indicate that palbociclib suppresses Rb phosphorylation and downregulates E2F1, while maintaining stable total Rb, PARP, StAR, and CYP19A1 levels in HGrC1 cells after 24 hours of treatment.

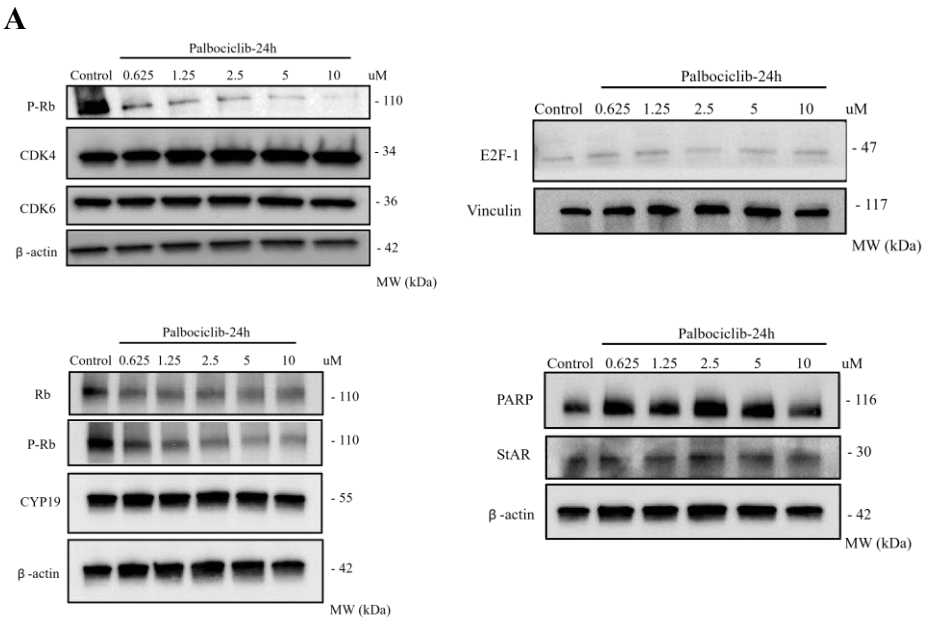

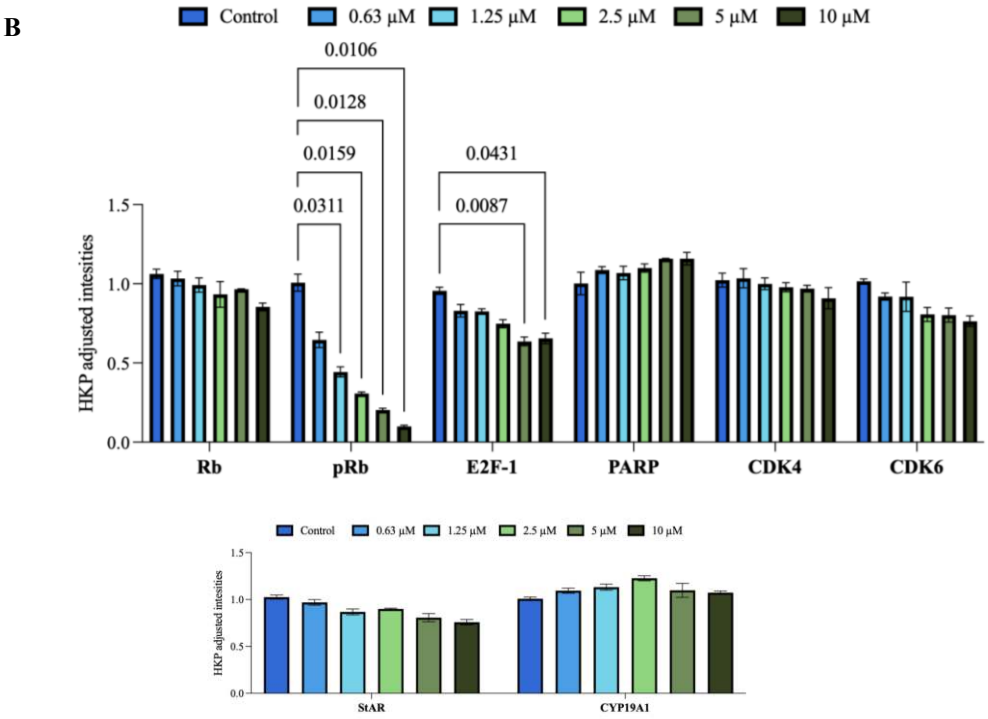

Figure 19: Dose-dependent changes in Rb pathway proteins and evaluation of steroidogenic markers in HGrC1 cells treated with palbociclib for 24 h. (A) The protein expressions show a dose-dependent decrease in phosphorylated Rb (pRb) and an increase in p21, with a reduction in E2F1 only at higher concentrations. The expression of total Rb, PARP, StAR, CYP19A1, CDK4, and CDK6 did not show significant changes. (B) Quantification of band intensities normalized to HKP (housekeeping protein; β-actin or vinculin.

Following the 24-h findings, the effects of palbociclib were further evaluated at 48 and 72 h in HGrC1 cells (Figure 19). Palbociclib treatment for 48 h led to a marked, dose-dependent decrease in phosphorylated Rb (pRb), which became statistically significant from 1.25 μM onwards ($p < 0.01$). In parallel, p21 expression was induced in a dose-dependent manner, with significant increases evident at concentrations of 2.5 μM and higher ($p < 0.05$). E2F1 levels decreased gradually, with significant reductions observed particularly at higher doses ($p < 0.05$). By contrast, total Rb, CDK4, and CDK6 expression remained largely stable ($p > 0.05$) (Figure 19A). Evaluation of CYP19A1 showed no significant alterations across the tested concentrations ($p > 0.05$) (Figure 19B).

At 72 h, suppression of pRb was further enhanced, with significant decreases observed at concentrations ≥2.5 μM ($p < 0.01$). In contrast, total Rb and CDK6 expression remained unchanged throughout treatment ($p > 0.05$) (Figure 19C).

Taken together, these results indicate that palbociclib consistently inhibits Rb phosphorylation in a time- and dose-dependent manner in HGrC1 cells, accompanied by induction of p21 and high-dose suppression of E2F1. In contrast, CYP19A1 levels, representing a key steroidogenic marker, were not significantly affected.

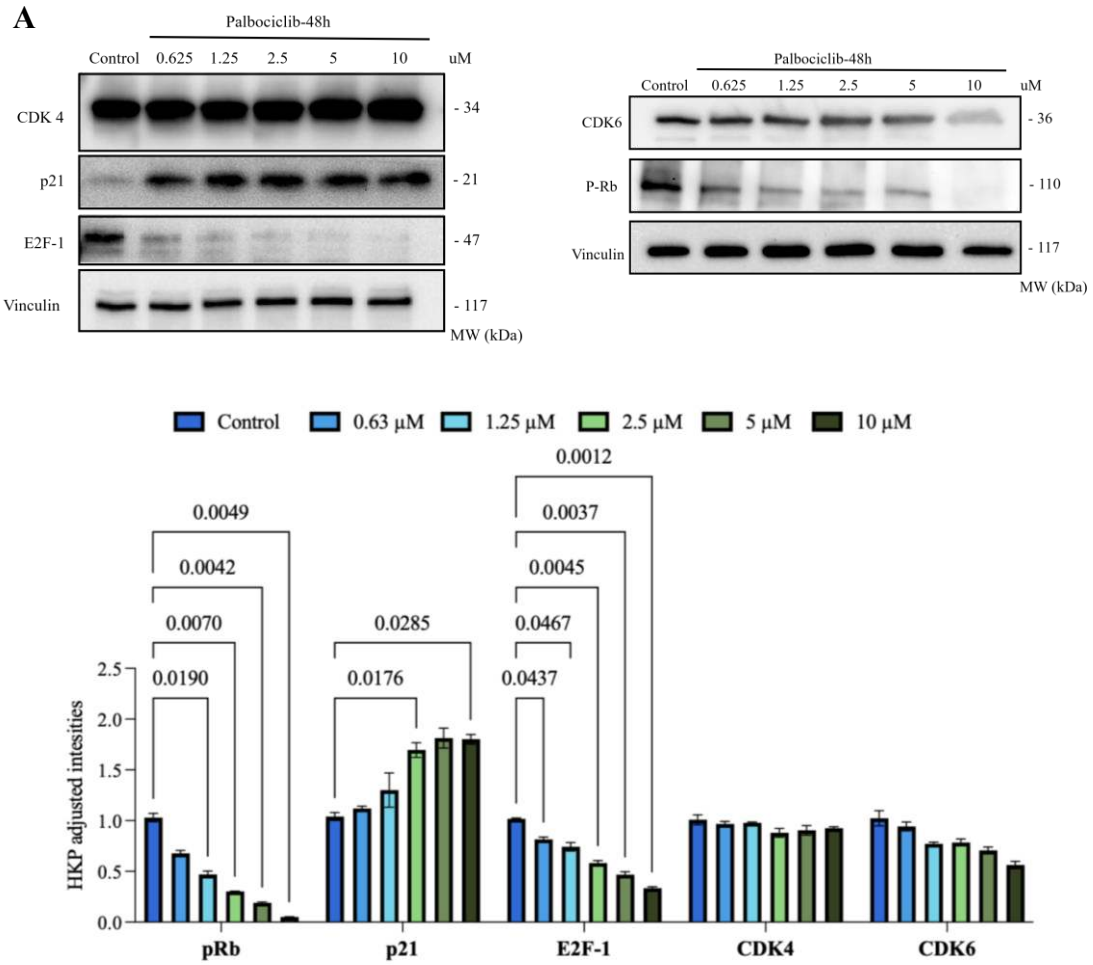
A
Palbociclib-48h
Control 0.625 1.25 2.5 5 10 uM
CDK 4
p21
E2F-1
Vinculin
- 34
- 21
- 47
- 117
MW (kDa)
Palbociclib-48h
Control 0.625 1.25 2.5 5 10 uM
CDK6
P-Rb
Vinculin
- 36
- 110
- 117
MW (kDa)
Control 0.63 µM 1.25 µM 2.5 µM 5 µM 10 µM
HKP adjusted intesities
0.0049
0.0042
0.0070
0.0190
0.0012
0.0037
0.0045
0.0467
0.0437
0.0285
0.0176
pRb
p21
E2F-1
CDK4
CDK6

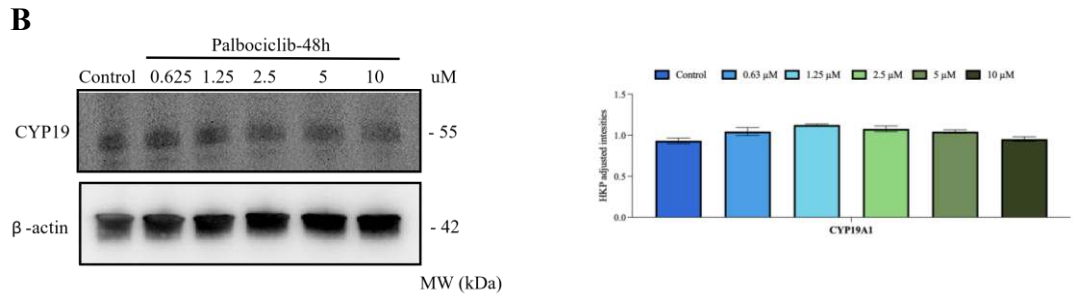
B
Palbociclib-48h
Control 0.625 1.25 2.5 5 10 uM
CYP19
β -actin
- 55
- 42
MW (kDa)
Control 0.63 µM 1.25 µM 2.5 µM 5 µM 10 µM
HKP adjusted intesities
CYP19A1

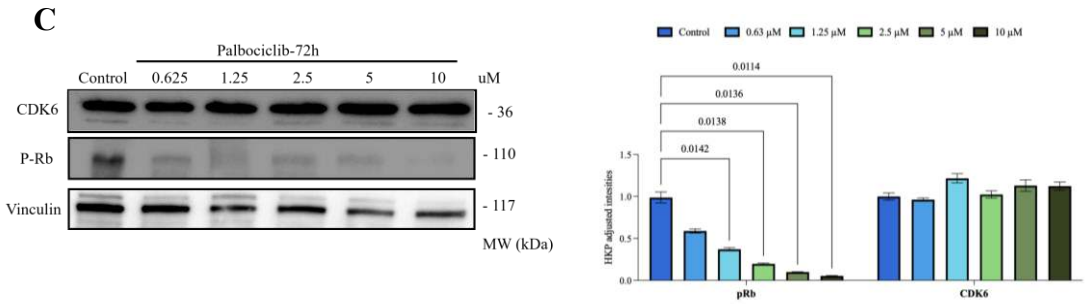
C
Palbociclib-72h
Control 0.625 1.25 2.5 5 10 uM
CDK6
P-Rb
Vinculin
- 36
- 110
- 117
MW (kDa)
Control 0.63 µM 1.25 µM 2.5 µM 5 µM 10 µM
0.0114
0.0136
0.0138
0.0142
HKP adjusted intesities
pRb
CDK6

Figure 20: Modulation of Rb pathway proteins and steroidogenic enzymes following palbociclib treatment for 48–72 h. (A) Western blot analysis and quantification at 48 h showing a dose-dependent decrease in phosphorylated Rb (pRb), induction of p21, and high-dose suppression of E2F1, while total Rb, CDK4, and CDK6 remained unchanged. (B) CYP19A1 protein levels at 48 h did not show significant variation across concentrations. (C) At 72 h, palbociclib further reduced pRb levels in a dose-dependent manner, whereas CDK6 remained stable. Band intensities were normalized to HKP (housekeeping protein; β-actin or vinculin).

3.3.2 Immunofluorescence Evaluation of CDK4/6 Inhibitor Effects in HGrC1 Cells

Immunofluorescence staining of HGrC1 cells treated with CDK4/6 inhibitors for 24 h demonstrated consistent alterations in Rb and phosphorylated Rb (pRb) expression. Following palbociclib treatment, quantitative analysis revealed a significant, dose-dependent reduction in pRb intensity compared to control ($p < 0.001$), whereas total Rb levels remained relatively stable across concentrations with only minor variation (Figure 20A). In the same experimental setting, CYP19A1 staining displayed a tendency to decrease at higher concentrations, while PARP expression did not show statistically significant differences compared to untreated controls (Figure 21).

Ribociclib exposure for 24 h produced a comparable staining pattern, with a significant reduction in pRb signal and largely unchanged Rb levels (Figure 22).

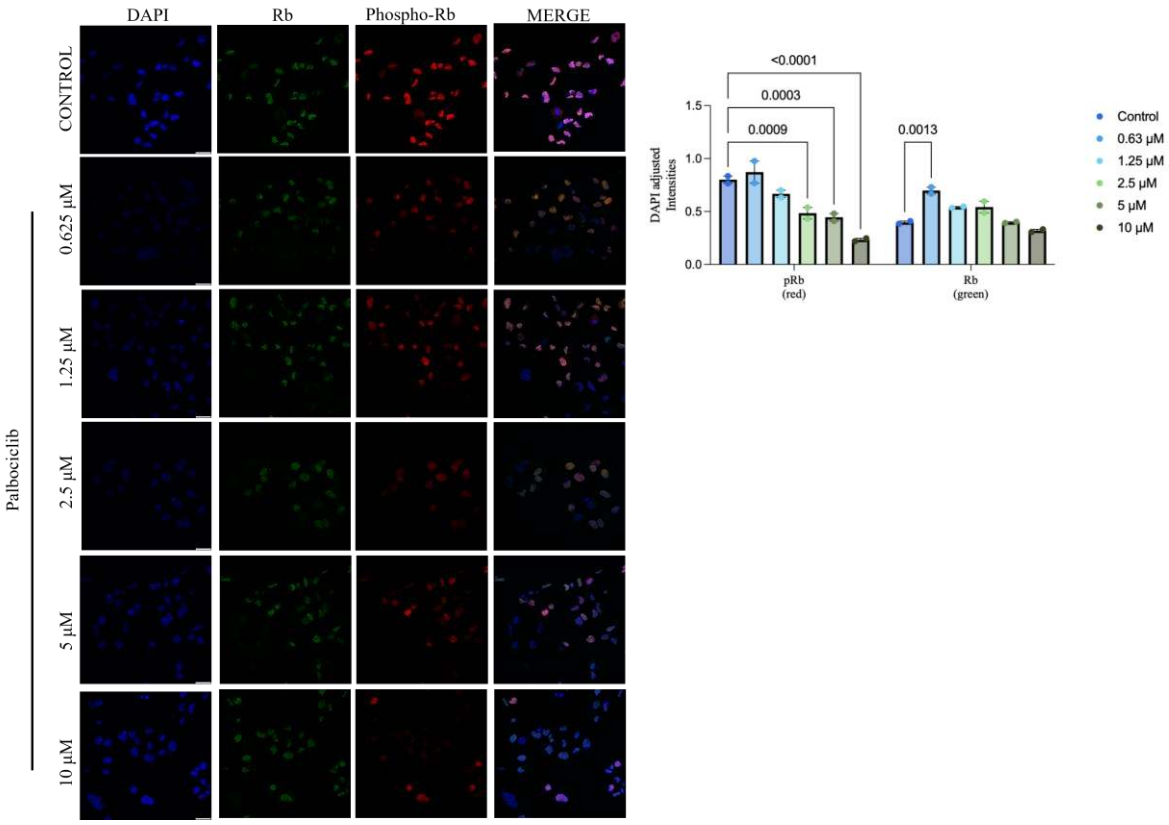

Figure 21: Immunofluorescence and quantitative analysis of Rb and phosphorylated Rb and pRb expression in HGrC1 cells treated with palbociclib (24 h). Immunofluorescence images showing total Rb (green), phosphorylated Rb (red), and nuclei (blue). pRb intensity decreased dose-dependently, while total Rb remained stable. Scale bars: 20 µm. Quantitative analysis confirmed significant reductions in pRb ($p < 0.001$), with no major changes in total Rb.

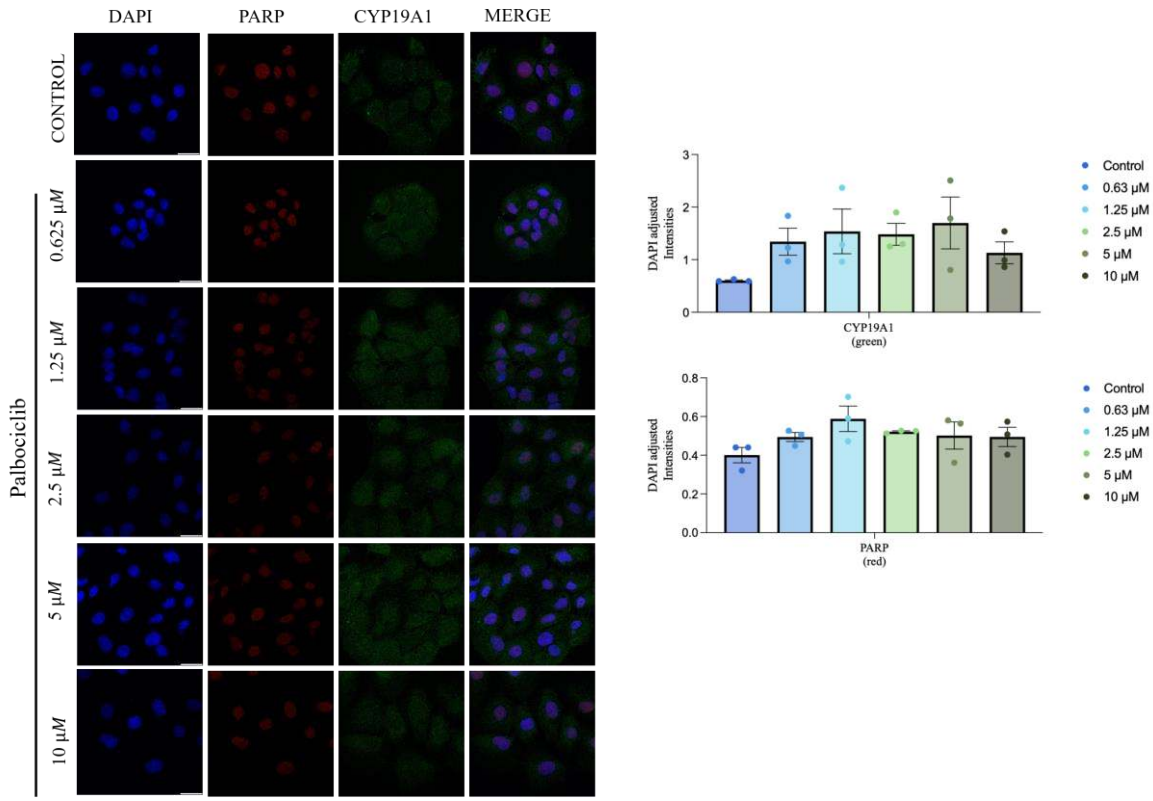

Figure 22: Immunofluorescence assessment of CYP19A1 and PARP expression in HGrC1 cells after 24 h palbociclib treatment. Representative immunofluorescence images of HGrC1 cells treated with palbociclib (0.625–10 µM, 24 h) showing CYP19A1 (green), PARP (red), and nuclei (DAPI, blue). Scale bars: 20 µm. Quantitative analysis of DAPI-normalized fluorescence intensities. CYP19A1 expression displayed a tendency to decrease at higher concentrations, whereas PARP expression did not differ significantly compared to control.

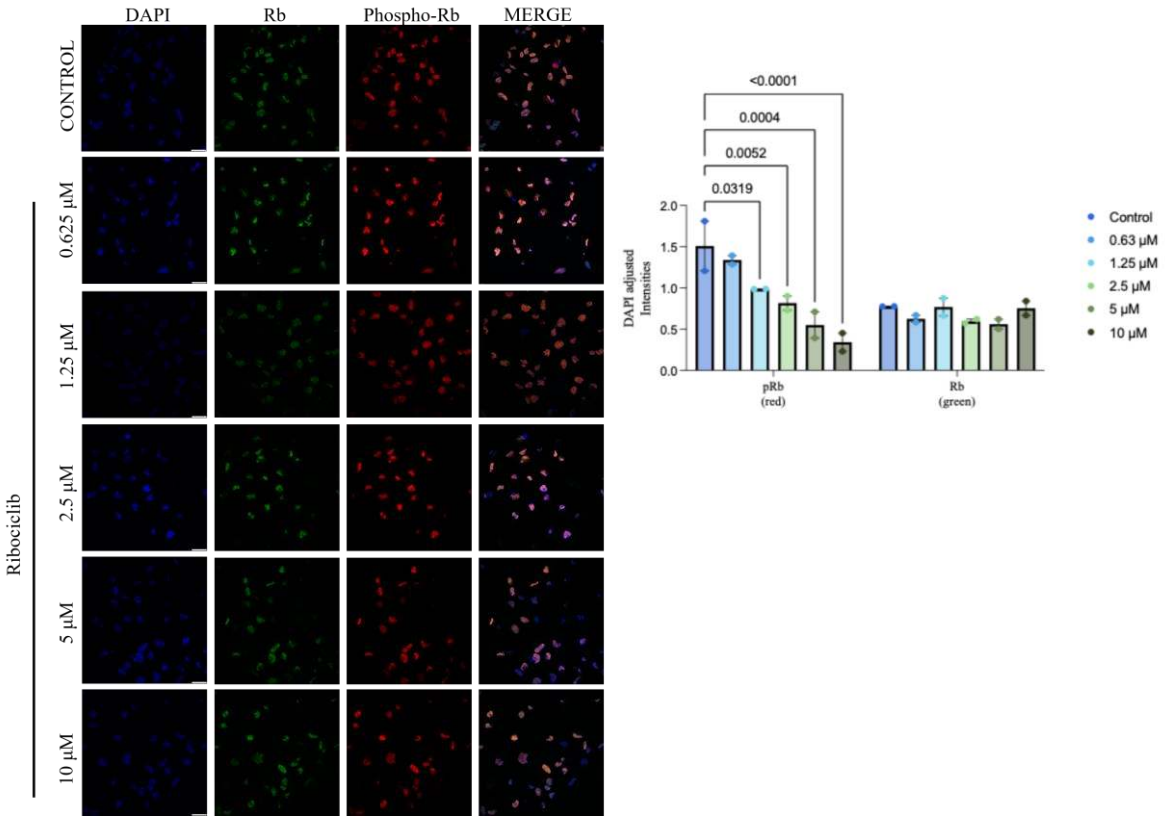

Figure 23: Immunofluorescence analysis of Rb and phosphorylated Rb (pRb) in HGrC1 cells after 24 hours of ribociclib treatment. Representative images of HGrC1 cells exposed to ribociclib (0.625–10 µM, 24 h) showing Rb (green), pRb (red), and nuclei (DAPI, blue). Scale bars: 20 µm. Quantitative analysis of DAPI-normalized intensities demonstrated a significant dose-dependent decrease in pRb expression, while total Rb levels remained largely unchanged. Data are presented as mean ± SEM.

3.3.3 Estradiol (E2) Secretion in HGrC1 Cells After CDK4/6 Inhibitor Treatment

Estradiol concentrations in culture supernatants of HGrC1 cells were measured following treatment with Ribociclib and Palbociclib at different doses and time points. In Ribociclib-treated cells, E2 levels remained comparable to those of the control at 24 hours, with no significant differences detected across the tested concentrations. At 48 and 72 hours, a slight reduction in E2 secretion was observed in both the control and treated groups, yet no dose-dependent changes were apparent.

Similarly, treatment with palbociclib for 24, 48 hours and 72 hours did not produce significant alterations in E2 levels compared with untreated controls. Across all tested concentrations, estradiol secretion showed only minor variations without a consistent dose-response pattern (Figure 23).

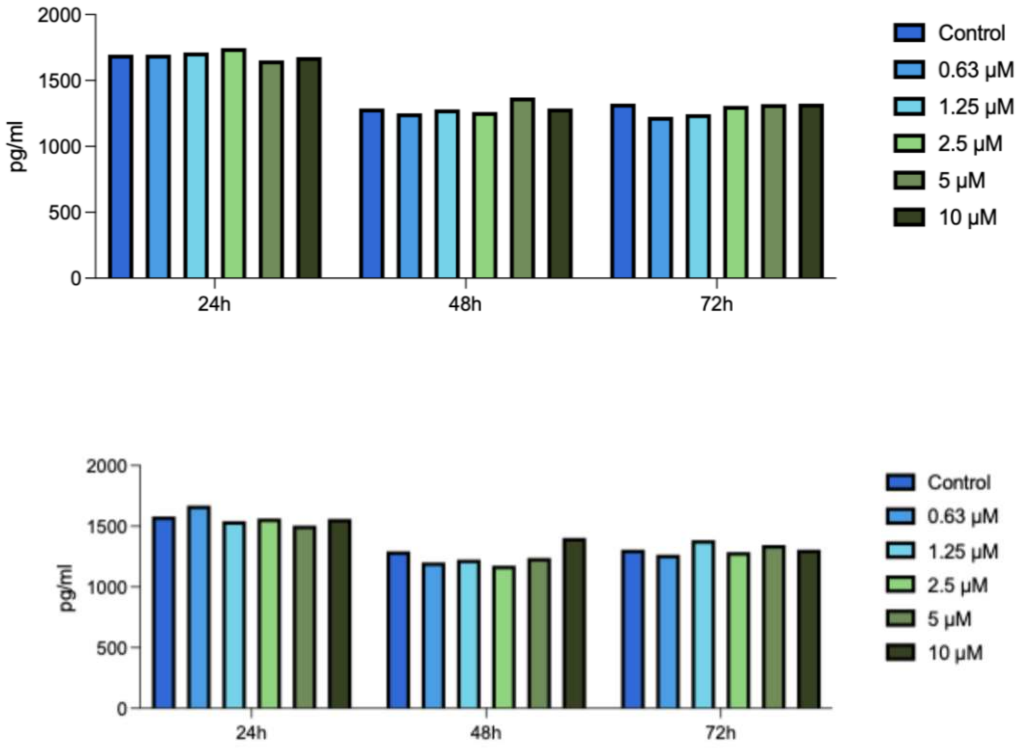

Figure 24: Estradiol (E2) levels in HGrC1 cells treated with CDK4/6 inhibitors. (A) Ribociclib and (B) palbociclib treatments (0.625–10 µM, 24–72 h) did not induce significant changes in E2 secretion compared with controls.

3.4 Palbociclib Suppresses pRb without Affecting Total Rb, CYP19A1, or Estradiol Secretion in COV434 Cells

To extend the results obtained in HGrC1 cells, we next examined the effects of CDK4/6 inhibition in the COV434 cell line. In immunoblot analysis, a dose-dependent reduction in phosphorylated Rb (pRb) was observed after palbociclib treatment at 24 h and 48 h, while total Rb expression remained stable. CYP19A1 protein levels did not show significant variation at either time point, indicating that short-term CDK4/6 inhibition does not substantially alter aromatase expression. Quantitative analysis confirmed significant decreases in pRb ($p < 0.01$), whereas total Rb and CYP19A1 remained unaffected (Figure 24A and 24B). In parallel, immunofluorescence staining

at 24 h demonstrated stable CYP19A1 expression, consistent with the immunoblot results, and no marked differences in PARP intensity compared with controls (Figure 25). Finally, estradiol (E2) secretion, measured at 24, 48, and 72 hours, showed no significant changes in hormone production following either ribociclib or palbociclib treatment (Figure 26).

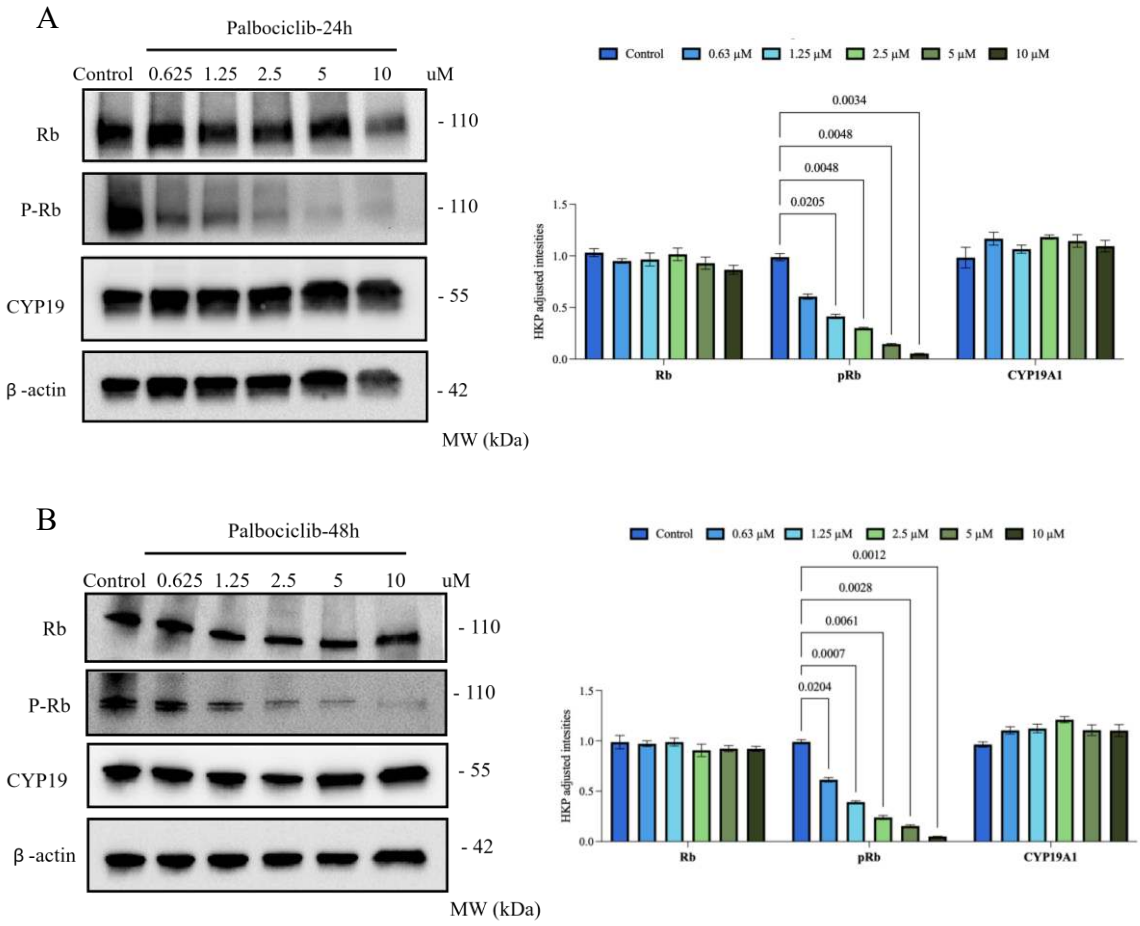

Figure 25: Palbociclib reduces phosphorylated Rb (pRb) while total Rb and CYP19A1 remain unchanged in COV434 cells. (A) Western blot and quantification at 24 h showing a dose-dependent decrease in pRb, while total Rb and CYP19A1 levels were not significantly altered. (B) At 48 h, palbociclib treatment continued to suppress pRb without affecting total Rb or CYP19A1 expression. Band intensities were normalized to HKP (housekeeping protein; β-actin).

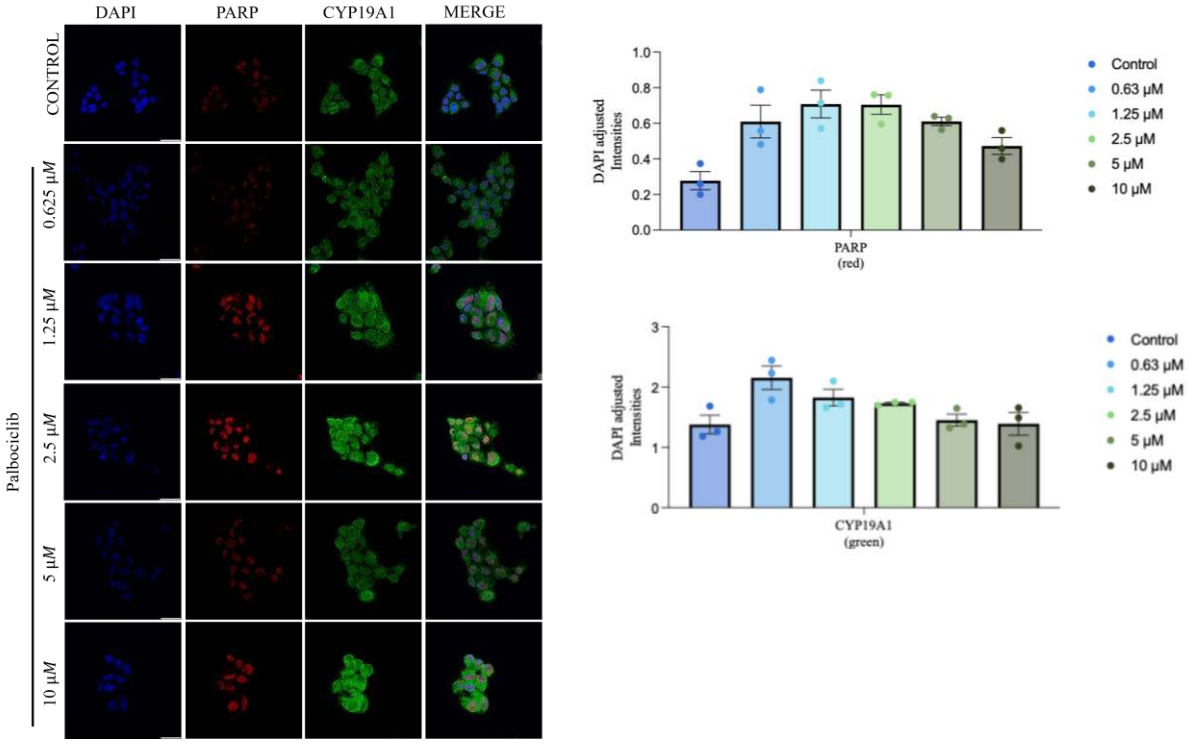

Figure 26: Palbociclib does not alter CYP19A1 or PARP expression in COV434 cells after 24 h. Representative images show PARP (red), CYP19A1 (green), and nuclei (DAPI, blue). Quantification revealed no significant changes in PARP intensity, and CYP19A1 expression remained stable across concentrations. Scale bars represent 20 µm.

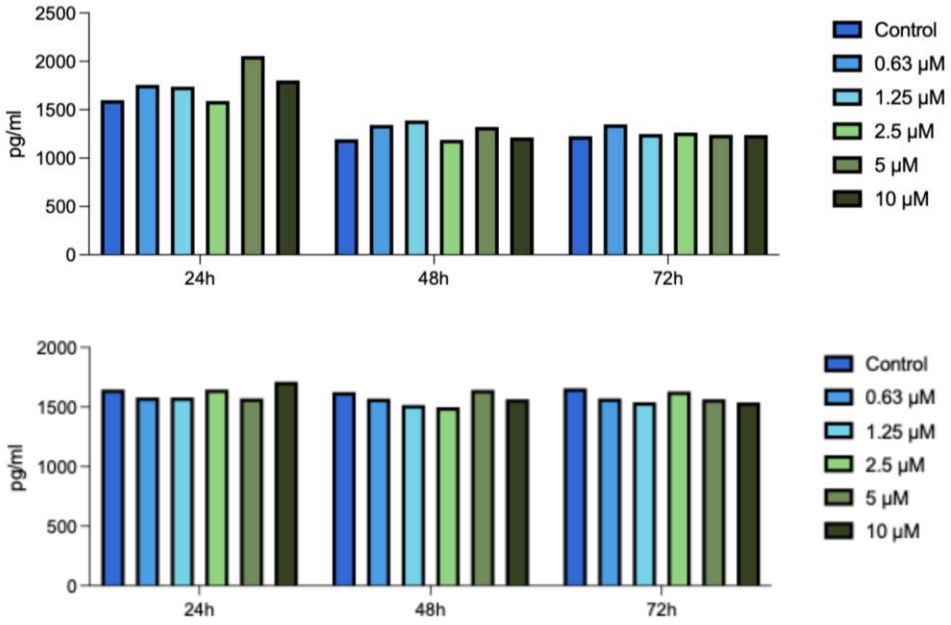

Figure 27: CDK4/6 inhibition with ribociclib or palbociclib did not alter estradiol secretion in COV434 cells. The upper panel shows E2 concentrations after ribociclib treatment at 24, 48, and 72 hours, and the lower panel illustrates results following palbociclib exposure at the same time points. Quantification revealed no significant alterations in hormone levels compared with untreated controls, indicating that short-term CDK4/6 inhibition does not impair estradiol production.

3.5 Effects of CDK4/6 Inhibition on the Steroidogenic Function of Human Luteinized Granulosa Cells

To extend our findings from non-luteinized granulosa HGrC1 and granulosa cell tumour-derived COV434 cell lines to a more physiologically relevant context, we next investigated the effects of CDK4/6 inhibition in primary human luteinized granulosa cells. After luteinization, these cells lose their ability to undergo mitosis. They represent a differentiated state with active steroidogenic function, thereby providing additional insight into the impact of Palbociclib and Ribociclib on both cell-cycle regulation and steroidogenesis.

After 24 h of palbociclib exposure, a clear dose-dependent reduction in phosphorylated Rb (pRb) levels was observed ($p < 0.05$), while total Rb expression remained largely unchanged. CDK6 protein levels also showed no significant variation across concentrations. In parallel, analysis of the steroidogenic markers 3β-HSD and StAR showed stable expression without significant alterations (Figure 27A and 27B).

At 48 h of palbociclib exposure, phosphorylated Rb (pRb) levels showed a dose-dependent decline, with significant reductions at 2.5 μM and 10 μM ($p < 0.05$), while total Rb expression remained stable. CDK6 protein levels did not display notable variation across treatments. Among steroidogenic markers, 3β-HSD expression was decreased at the highest dose of 10 μM ($p < 0.05$), whereas StAR levels showed no significant alteration. CYP19A1 protein also exhibited a modest but significant reduction at elevated concentrations ($p < 0.05$) (Figure 28A-28B).

At 72 h, palbociclib treatment continued to suppress pRb, with strong reductions observed at 2.5 μM and 10 μM ($p < 0.01$). In contrast, CDK6 expression remained unchanged compared with controls. No additional alterations in steroidogenic proteins

were detected at this later time point, and the predominant effect was the sustained inhibition of Rb phosphorylation (Figure 28C).

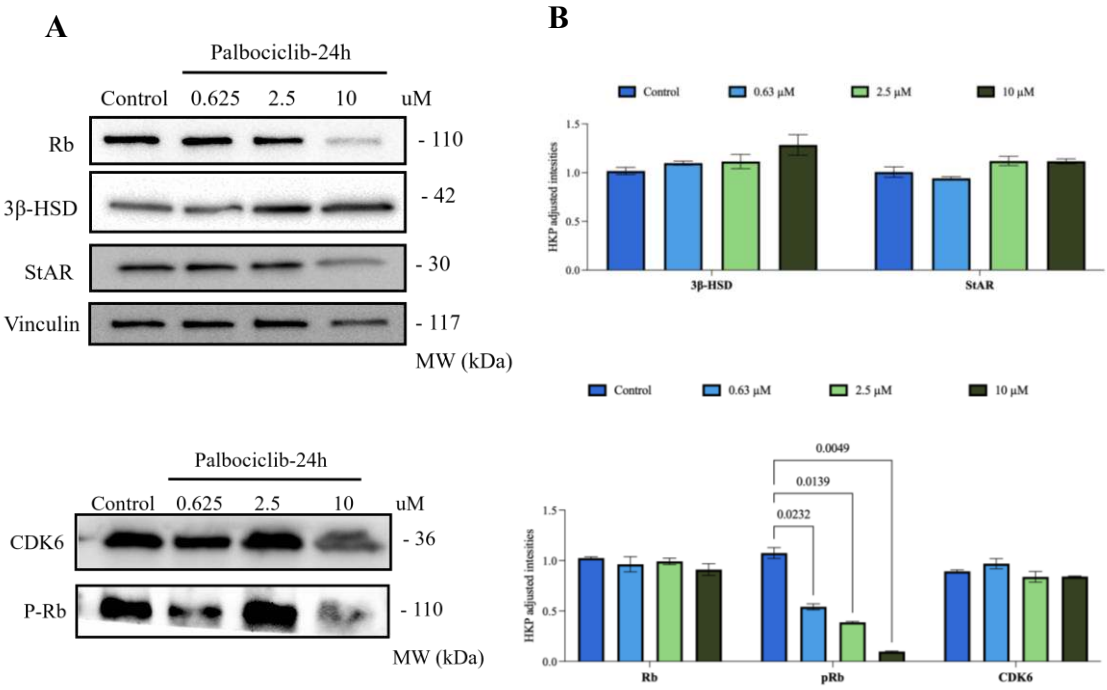

Figure 28: Impact of palbociclib on phosphorylated Rb and steroidogenic enzymes in luteal granulosa cells (24 h). (A) Protein expression analysis by Western blot demonstrating a dose-dependent decrease in phosphorylated Rb (pRb), while total Rb and CDK6 levels remained unchanged. Steroidogenic markers 3β-HSD and StAR also displayed stable expression across concentrations. (B) Quantification of band intensities normalized to HKP (housekeeping protein; vinculin) confirmed the significant reduction in pRb, whereas Rb, CDK6, 3β-HSD, and StAR did not show significant alterations.

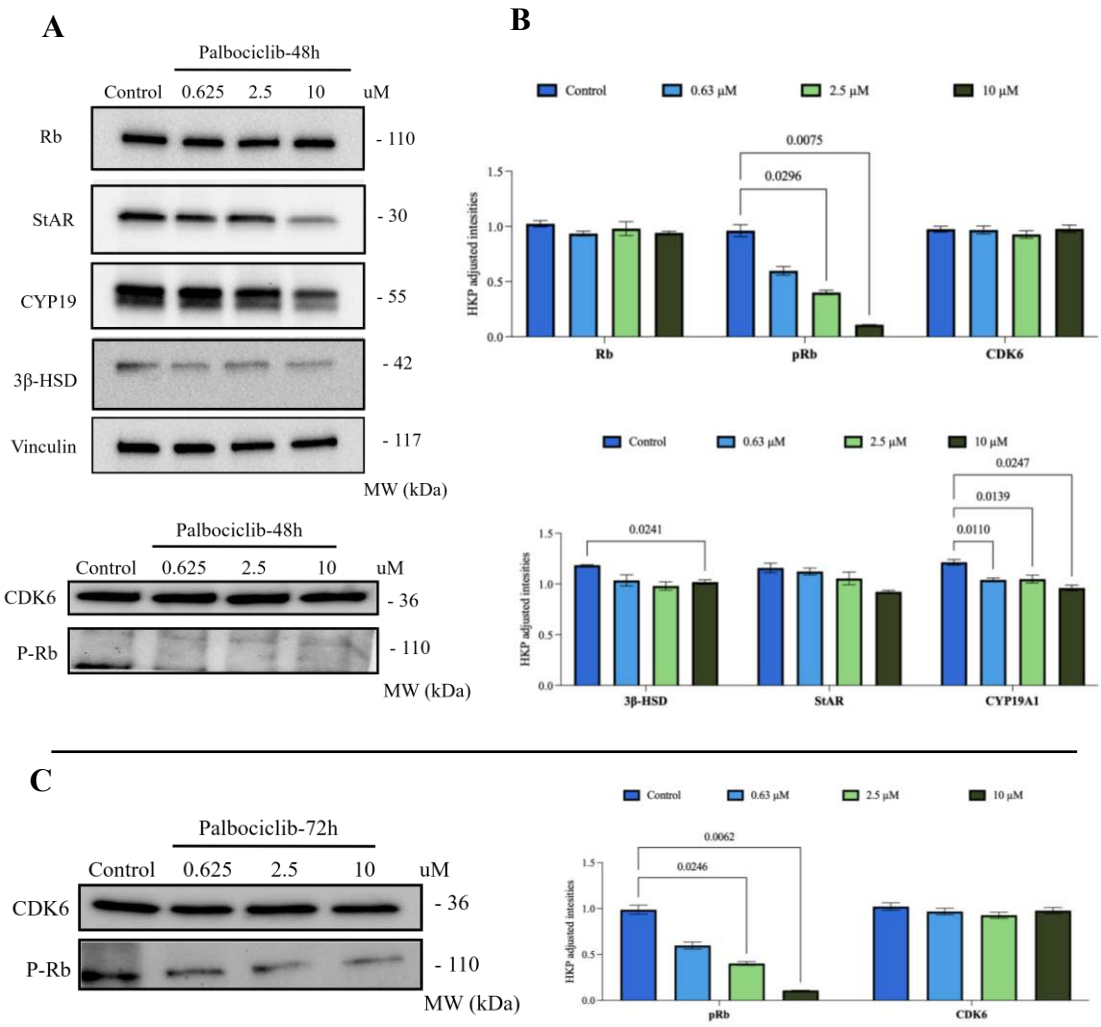

Figure 29: Dose-dependent inhibition of pRb and modulation of steroidogenic proteins by palbociclib in luteal granulosa cells. (A) Western blot analysis at 48 hours showed a dose-dependent reduction in phosphorylated Rb (pRb), with significant decreases observed at 2.5 µM and 10 µM, while total Rb and CDK6 remained unchanged. Steroidogenic markers revealed a decrease in 3β-HSD at 10 µM and a modest reduction in CYP19A1 at higher concentrations, whereas StAR expression was stable. (B) Quantification of band intensities normalized to HKP (housekeeping protein; vinculin). (C) At 72 h, palbociclib sustained its inhibitory effect on pRb, with strong suppression at 2.5 µM and 10 µM, while CDK6 expression was unaffected.

To assess whether the effects observed with palbociclib were conserved across CDK4/6 inhibitors, we next evaluated ribociclib in luteinized granulosa cells. After 24 h of treatment, phosphorylated Rb (pRb) levels were significantly reduced in a dose-dependent manner ($p < 0.01$), while total Rb and CDK6 expression remained stable. In the same setting, 3β-HSD, StAR, and CYP19A1 showed no significant changes, indicating that steroidogenic enzyme expression was preserved at this early time point (Figure 29A–29B).

With extended ribociclib exposure up to 48 h, its suppressive effect on pRb was maintained, again reaching significance at higher concentrations ($p < 0.05$). At this time point, 3β-HSD displayed a reduction at 10 µM ($p < 0.05$), and CYP19A1 showed a modest but significant decrease at elevated doses, whereas StAR remained unaffected (Figure 30A-30B). By 72 h, strong suppression of pRb was evident at 2.5 µM and 10 µM ($p < 0.01$), while total Rb and CDK6 remained unchanged (Figure 30C).

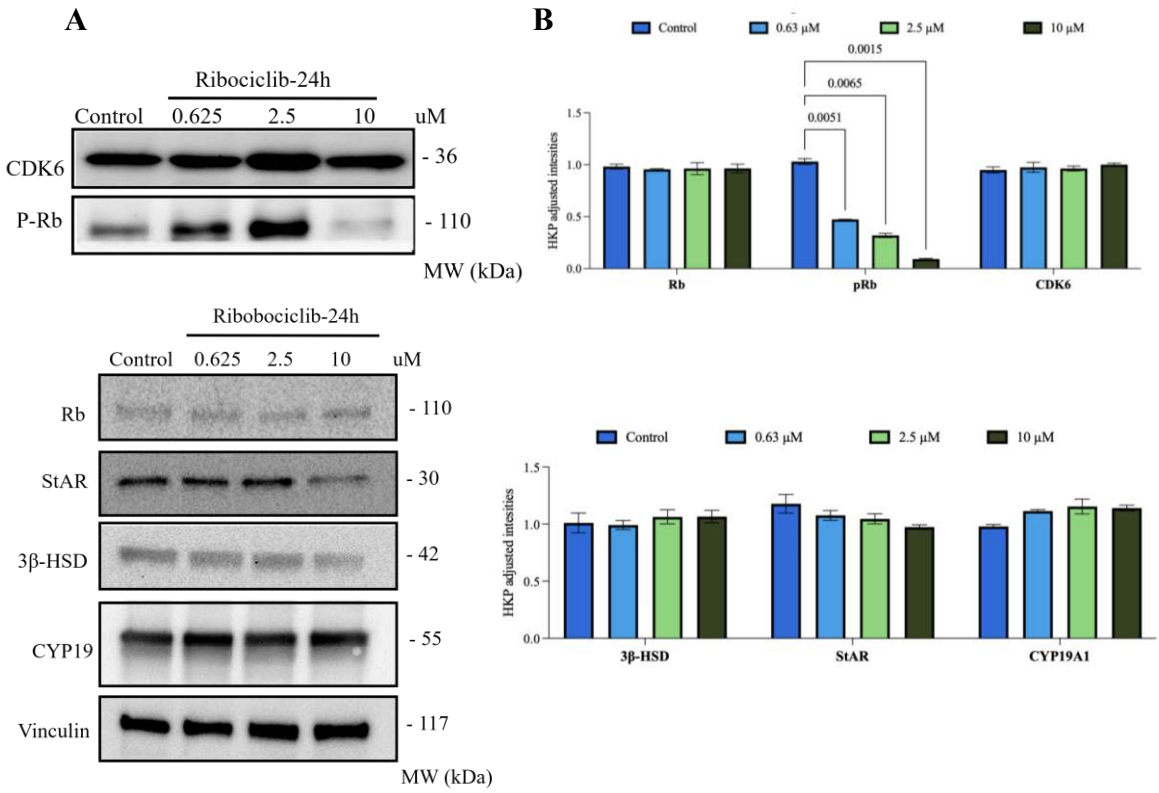

Figure 30: Expression of Rb, CDK6, and steroidogenic markers in luteal granulosa cells treated with ribociclib for 24 h. (A) Immunoblot analysis showing a dose-dependent reduction of phosphorylated Rb (pRb), with total Rb and CDK6 remaining

stable. Steroidogenic markers 3β-HSD, StAR, and CYP19A1 did not display significant changes across concentrations. (B) Quantification of band intensities normalized to housekeeping protein (HKP; vinculin) confirms the significant reduction in pRb ($p < 0.01$), while Rb, CDK6, 3β-HSD, StAR, and CYP19A1 remained unchanged.

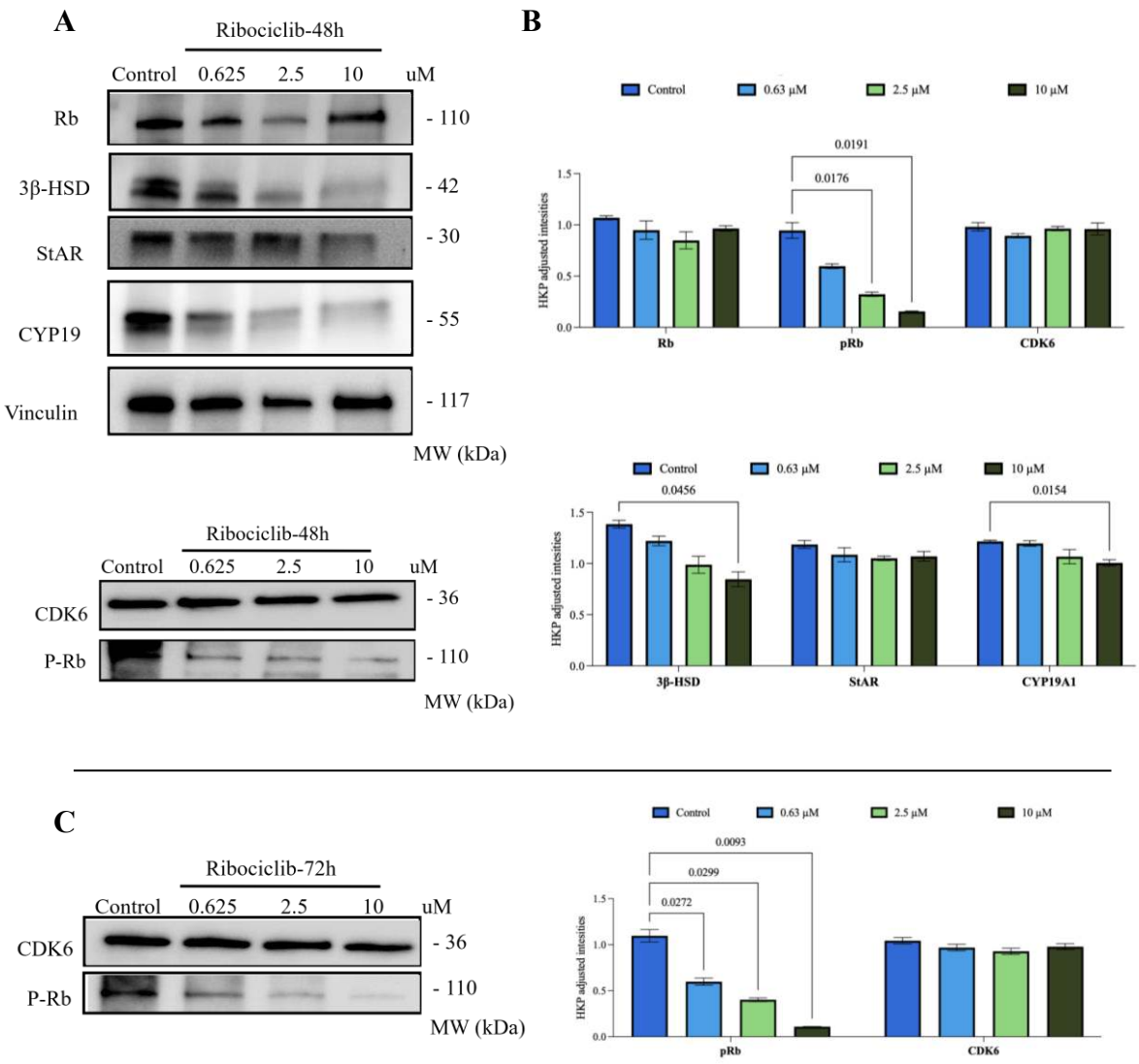

Figure 31: Ribociclib-mediated inhibition of pRb and dose-dependent modulation of steroidogenic proteins over 48–72 h in luteal granulosa cells. (A–B) At 48 h, ribociclib treatment induced a marked reduction in phosphorylated Rb (pRb) levels at 2.5 µM and 10 µM, while total Rb and CDK6 remained unchanged. Among the steroidogenic proteins, 3β-HSD and CYP19A1 showed significant decreases at higher doses ($p < 0.05$), whereas StAR expression remained stable. Band intensities were quantified relative to HKP (housekeeping protein; vinculin). (C) At 72 h, ribociclib exposure

sustained the inhibitory effect on pRb, with strong suppression at 2.5 µM and 10 µM ($p < 0.01$), while total Rb and CDK6 expression remained unchanged. Band intensities were quantified relative to HKP (housekeeping protein; vinculin).

To further validate the impact of CDK4/6 inhibition on luteal granulosa cells, we performed immunofluorescence staining after 24 hours of exposure to palbociclib and ribociclib, focusing on PARP as a DNA repair–associated protein responsive to DNA damage and 3β-HSD as a key steroidogenic enzyme. In palbociclib-treated cells, 3β-HSD immunoreactivity remained comparable to controls at all concentrations, consistent with the western blot results. PARP staining also showed no significant alterations, indicating that short-term palbociclib exposure does not trigger detectable DNA damage–associated stress responses in this context. By contrast, ribociclib treatment yielded a distinct pattern. A marked reduction in 3β-HSD signal was observed at 2.5 µM and 10 µM ($p < 0.001$), in agreement with the modest decreases detected by immunoblot analysis. PARP intensity similarly declined in a dose-dependent manner, reaching significance at higher concentrations ($p < 0.01$). Quantitative analysis confirmed these changes, demonstrating pronounced reductions in both markers with ribociclib, whereas palbociclib treatment preserved stable expression levels (Figure 31A-31B).

A

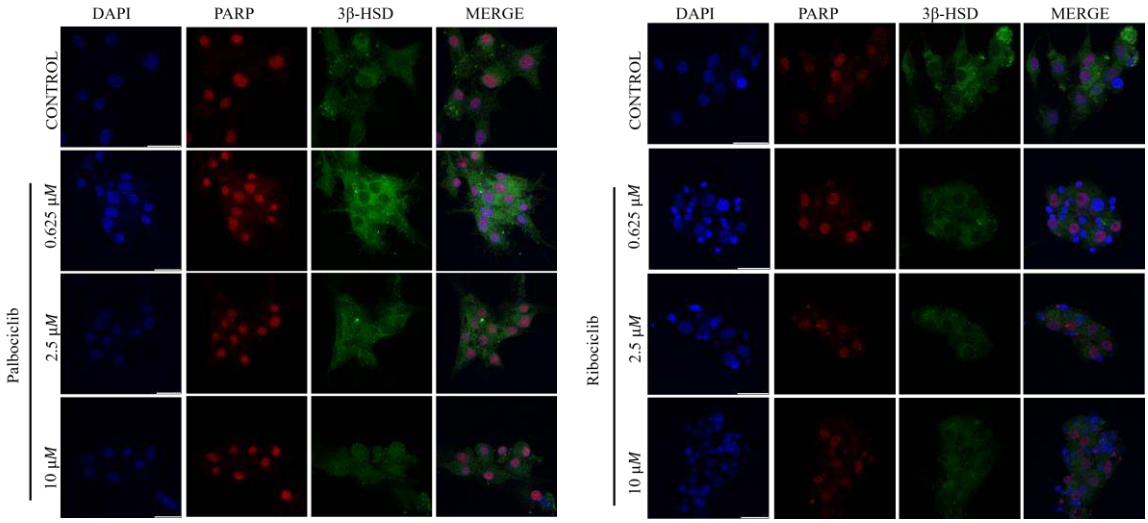

B

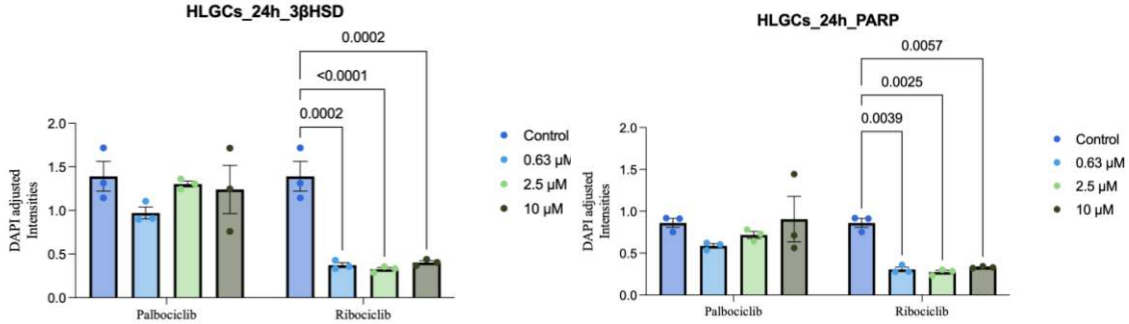

Figure 32: Immunofluorescence analysis of PARP and 3β-HSD expression in luteal granulosa cells after 24 h of CDK4/6 inhibitor treatment. (A) Representative images showing DAPI (blue), PARP (red), and 3β-HSD (green) staining in cells treated with palbociclib or ribociclib at the indicated concentrations. Scale bar = 20 μm. (B) Fluorescence intensity analysis revealed no significant changes in palbociclib-treated cells, whereas ribociclib induced a dose-dependent reduction in both 3β-HSD and PARP expression, reaching statistical significance at higher concentrations.

To evaluate whether CDK4/6 inhibition affects hormone secretion in luteinized granulosa cells, estradiol (E2) and progesterone (P4) concentrations were measured after 24, 48, and 72 h of treatment with palbociclib or ribociclib at 0.63, 2.5, and 10 μM.

Palbociclib exposure also did not alter E2 production, with hormone levels remaining consistent with those of the controls at 24, 48, and 72 h (Figure 32A). P4 secretion likewise did not show significant changes, with comparable levels observed in both control and treated groups throughout the experimental period (Figure 32B).

In ribociclib-treated cells, E2 levels remained stable across all time points and concentrations, with no significant aberrations from those of the controls (Figure 33A). Similarly, P4 secretion showed comparable profiles, and although higher values were detected at 72 hours, these changes were not treatment dependent (Figure 33B). Overall, these results indicate that up to 72 h of CDK4/6 inhibition with either palbociclib or ribociclib did not significantly alter estradiol or progesterone secretion in luteinized granulosa cells.

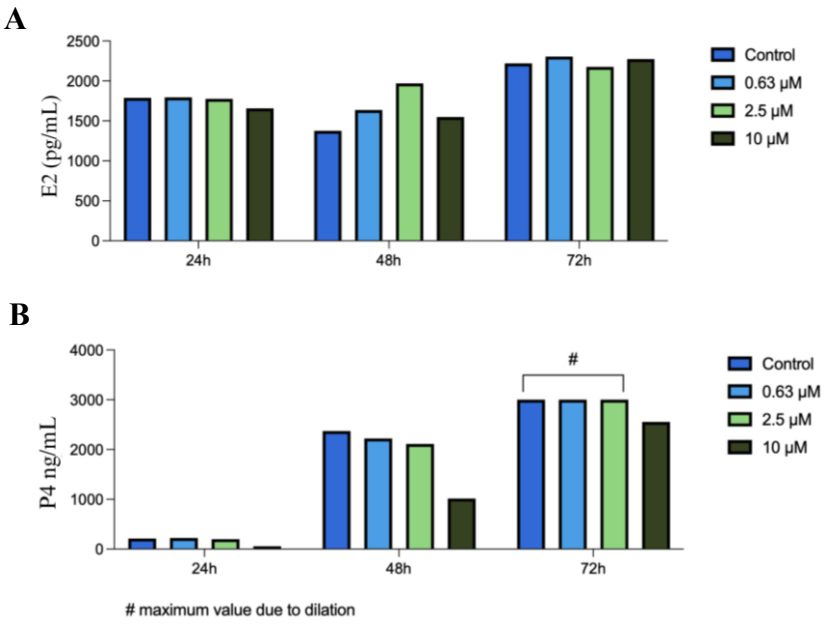

Figure 33: Palbociclib did not alter estradiol or progesterone secretion in luteal granulosa cells. (A) Estradiol (E2) concentrations measured in culture medium following 24, 48, and 72 h of palbociclib exposure (0.63, 2.5, and 10 µM) remained comparable to untreated controls at all time points. (B) Progesterone (P4) secretion under the same treatment conditions showed no treatment-related differences. # indicates maximum values reached due to sample dilution.

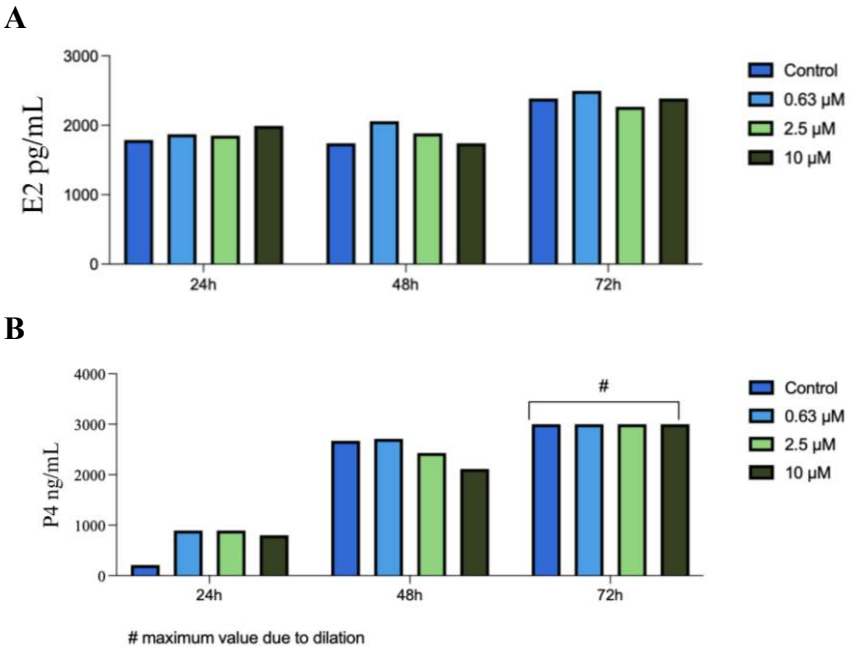

Figure 34: Ribociclib exposure maintains stable estradiol and progesterone levels in luteal granulosa cells. (A) Estradiol (E2) concentrations were measured after 24, 48, and 72 h of ribociclib treatment at 0.63, 2.5, and 10 μM. E2 levels remained comparable to untreated controls across all time points. (B) Progesterone (P4) secretion assessed under the same conditions. While an overall increase was noted at later time points (48 and 72 h; # indicates maximum values due to dilution), this pattern was consistent between control and treated groups, indicating that ribociclib did not alter P4 secretion.

3.6 CDK4/6 inhibition did not alter protein expression or hormone secretion in human ovarian tissue

Following the findings obtained from granulosa cell lines (HGrC1 and COV434) and primary human luteal granulosa cells, the analysis was extended to whole ovarian tissue explants to provide a more integrated perspective. After 24 h exposure to palbociclib and ribociclib at 0.625 and 10 μM, western blot analysis demonstrated that the expression of Rb, CYP19A1, and StAR remained unchanged across treatment groups. Densitometric analysis confirmed the absence of significant differences compared with untreated controls, indicating that short-term CDK4/6 inhibition did not alter these proteins at the ovarian tissue level (Figure 34 and Figure 35).

In addition, hormone levels were measured to assess estradiol production and follicular reserve markers. Estradiol (E2) (Figure 36A) and anti-Müllerian hormone (AMH) (Figure 37A) remained stable at 24 h and were maintained over 48–72 h in both palbociclib and ribociclib-treated samples (Figure 36B and 37B), even at the highest tested concentration of 10 μM. Collectively, these results indicate that ovarian tissue exposed to CDK4/6 inhibitors did not significantly alter estradiol output or follicular reserve markers.

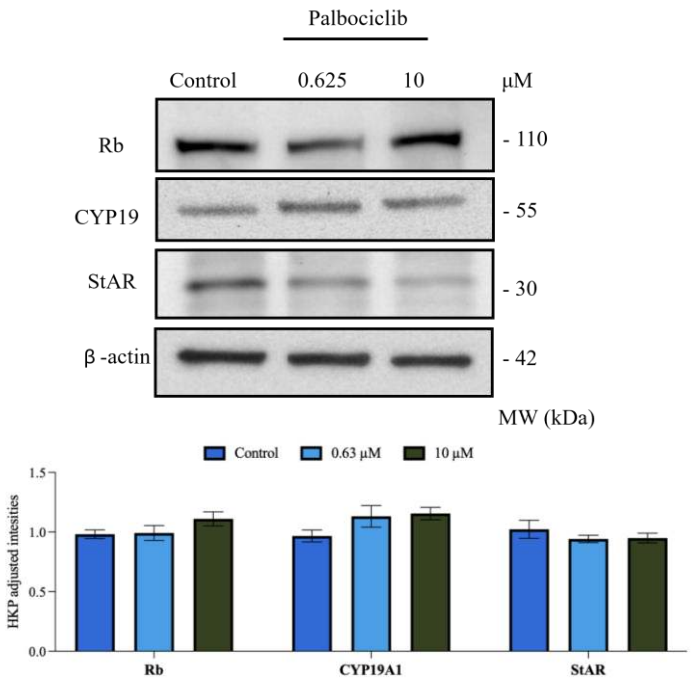

Figure 35: Palbociclib exposure did not alter Rb, CYP19A1, or StAR protein expression in human ovarian tissue. Western blot analysis of ovarian explants treated with palbociclib (0.63 and 10 µM) for 24 h. Expression of Rb, CYP19A1, and StAR remained comparable across treatment groups. β-actin was used as a housekeeping protein (HKP). Quantification of band intensities showed no significant differences relative to control samples.

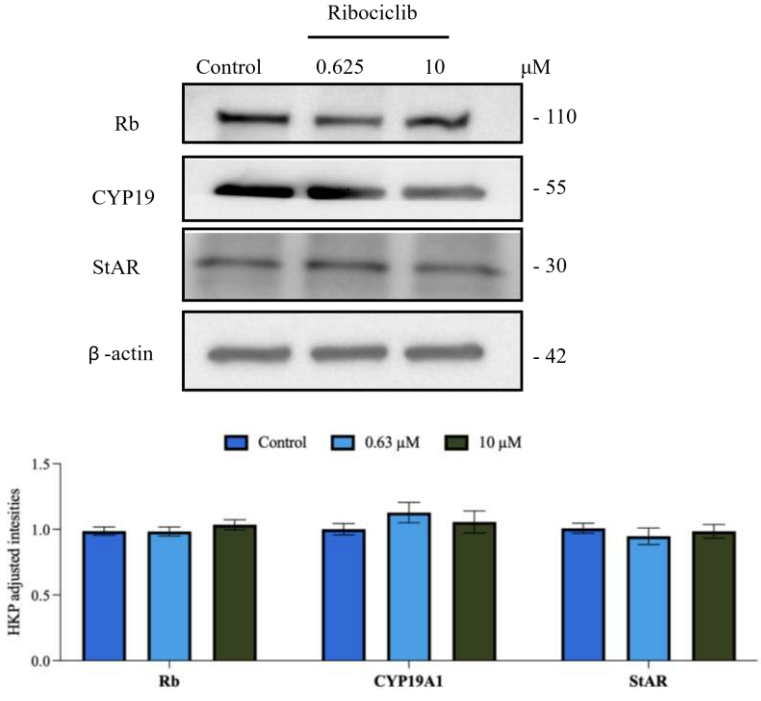

Figure 36: Ribociclib exposure did not alter Rb, CYP19A1, or StAR protein expression in human ovarian tissue. Western blot analysis of ovarian explants treated with ribociclib (0.63 and 10 μM) for 24 h. Expression levels of Rb, CYP19A1, and StAR were maintained at similar levels to those of untreated controls. β-actin served as a housekeeping protein (HKP). Densitometric analysis confirmed stable expression across groups.

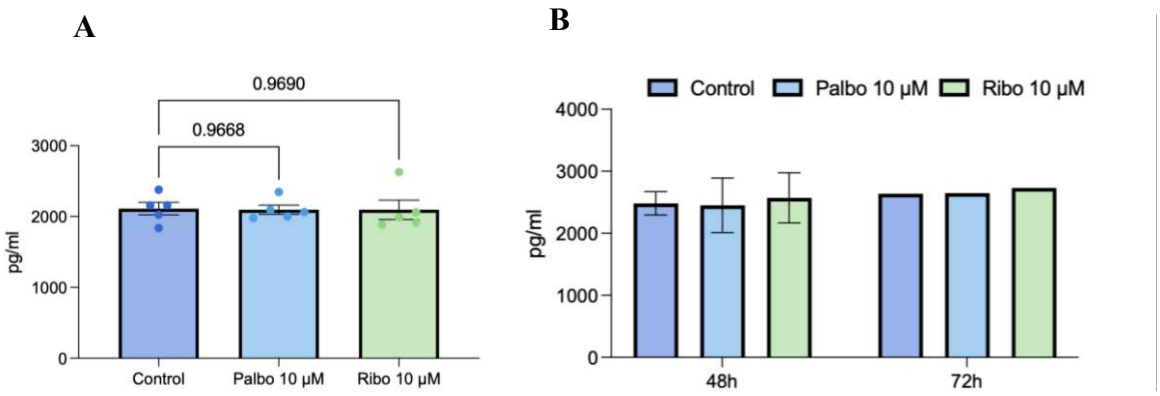

Figure 37: Estradiol (E2) secretion in human ovarian tissue exposed to CDK4/6 inhibitors. (A) E2 levels measured in culture medium after 24 h exposure to palbociclib (10 μM) and ribociclib (10 μM) compared with untreated controls. No significant differences were detected across groups. (B) Time-dependent E2 measurements after 48 h and 72 h exposure under the same treatment conditions. Estradiol levels remained stable throughout the treatment period, indicating that short-term CDK4/6 inhibition did not alter estrogen production in ovarian tissue.

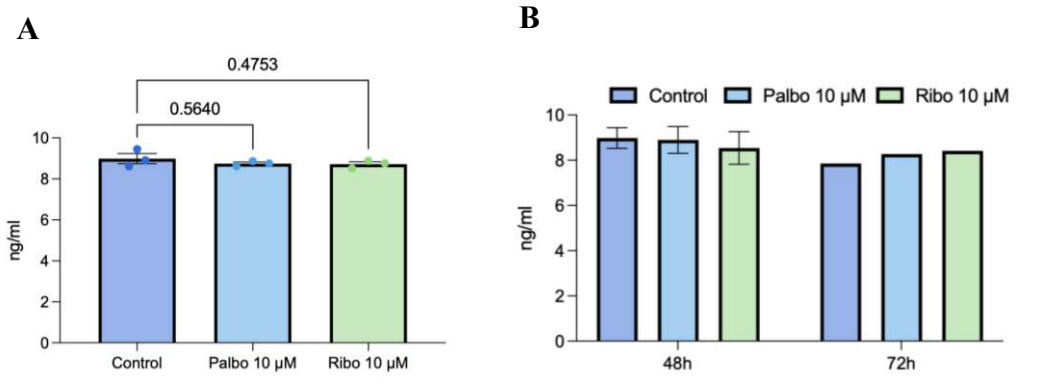

Figure 38: AMH levels remain unaffected by short-term CDK4/6 inhibition in ovarian tissue. (A) AMH levels measured after 24 h exposure to palbociclib (10 μM) or ribociclib (10 μM) compared with untreated controls. No significant differences were detected between treatment and control groups. (B) Time-course measurements at 48 h and 72h under the same treatment conditions showed that AMH concentrations remained stable

CHAPTER 4

DISCUSSION

Cyclin-dependent kinases (CDKs) are crucial for regulating the cell cycle, coordinating mitogenic signals with internal checkpoints that control DNA replication and cell division (73,80). Specifically, CDK4 and CDK6 are key in managing the transition from the G1 phase to the S phase, forming active complexes with D-type cyclins to phosphorylate the retinoblastoma protein (Rb). This phosphorylation releases E2F transcription factors, which then activate genes required for DNA synthesis (40). Dysregulation of this pathway is a key feature of many types of cancer, making CDK4/6 a promising target for treatment (80,83). Selective inhibitors (palbociclib, ribociclib, abemaciclib) bind the CDK4/6 ATP pocket, block Rb phosphorylation, induce G1 arrest, and have improved outcomes in HR+ breast cancer trials (114). These agents are generally better tolerated than earlier pan-CDK inhibitors and are used with endocrine therapy as standard of care (73,114). Although they have demonstrated clinical success, concerns exist about potential off-target or tissue-specific effects, particularly in younger patients and reproductive tissues. Ovarian function relies on the coordinated growth and development of granulosa and theca cells, as well as steroid production, all of which involve CDK4/6 activity (40). Pivotal oncology trials largely enrolled postmenopausal patients and did not assess fertility endpoints, leaving a gap in understanding reproductive risks for premenopausal women (40,83). Therefore, systematic preclinical and translational studies assessing viability, cell cycle distribution, steroidogenic enzyme expression, and hormone secretion at clinically relevant exposures are needed to determine reversibility and the impact on ovarian reserve (40,83). Notably, clinical trials in oncology that confirmed the safety of CDK4/6 inhibitors didn't focus on fertility outcomes. Since most patients were postmenopausal, there's a substantial gap in our understanding of reproductive risks for premenopausal women (40,83). Current

evidence, therefore, highlights a need for a thorough evaluation of whether CDK4/6 inhibitors have gonadotoxic or cytostatic effects on ovarian tissue. Using preclinical models can help bridge this gap by allowing us to assess cell viability, cell-cycle arrest, steroidogenic enzyme expression, and hormone secretion. By combining these results, we can gain a better understanding of whether the observed effects are temporary and reversible or may have lasting consequences for ovarian health.

Overall, CDK4/6 inhibitors have become key players in cancer treatment; however, their effects on ovarian function remain unclear. This knowledge gap drives the current study, which examines how CDK4/6 inhibition affects multiple types of granulosa cells and human ovarian tissue. This study investigates the impact of CDK4/6 inhibition on multiple granulosa cell types and human ovarian tissue by combining cell cycle analysis, steroidogenic enzyme assessment, and hormone production measurements.

The present study examined the effects of CDK4/6 inhibition across proliferative granulosa cell lines, primary human luteinized granulosa cells, and intact ovarian tissue, thereby providing a multilayered framework for interpreting potential gonadotoxic impacts on human ovary. A consistent finding in proliferative granulosa cells (HGrC1 and COV434) was the suppression of phosphorylated Rb (pRb) following treatment with palbociclib and ribociclib, confirming that these agents enforce a G1 arrest via the inhibition of Rb phosphorylation rather than the depletion of total Rb protein. This mechanism aligns with the canonical pRb–E2F pathway described in cancer biology, where CDK4/6 inhibition restricts E2F-driven entry into S phase (94,140). Flow cytometry supported this effect, demonstrating dose-dependent accumulation in G0/G1 with reduced S-phase fractions at 24 h, while G2/M proportions remained stable. Importantly, dead-cell percentages consistently remained very low, underscoring a cytostatic rather than cytotoxic action. Mechanistically, the increased p21 expression and reduced E2F1 in HGrC1 cells further demonstrated that CDK4/6 inhibition operates through the canonical pRb–E2F1–p21 cascade. These results align with those of (140), who emphasized that CDK4/6 inhibitors induce reversible G1 arrest without inducing apoptosis in short-term models.

Steroidogenic function was largely preserved in proliferative systems. In HGrC1 cells, StAR and CYP19A1 expression remained unchanged, and estradiol secretion was stable across all treatment conditions. In COV434, a granulosa tumour–derived line, CYP19A1 expression and estradiol production were also unaffected by

palbociclib. This is consistent with prior analyses of ovarian tumour cell lines, where CDK4/6 inhibition predominantly enforced G0/G1 arrest without inducing apoptosis or metabolic collapse (149). Our data extend this framework by showing that proliferative arrest can occur alongside preserved endocrine output, underlining a distinction between cell-cycle control and steroidogenic capacity in granulosa models.

In primary human luteinized granulosa cells (HLGCs), which are non-mitotic luteinized, responses were distinct. Viability assays showed no decline at any concentration, consistent with their post-mitotic status and lack of CDK4/6 dependency for short-term survival, as reported by Moons et al., 2002, who demonstrated that luteinized cells are BrdU-negative and express p27, confirming their cell-cycle exit. Our study extends these insights by directly testing steroidogenic enzyme expression in primary human luteal cells, an aspect not addressed in earlier reports. At 48 h, palbociclib reduced CYP19A1 expression at all doses and decreased 3β-HSD only at the highest concentration, whereas ribociclib produced more modest effects, with both CYP19A1 and 3β-HSD reduced only at 10 μM. StAR expression remained stable up to 48 hours in both palbociclib- and ribociclib-treated groups, and neither estradiol nor progesterone secretion was altered across 24–72 hours, indicating preserved endocrine output despite enzyme modulation. For 3β-HSD, immunofluorescence suggested broader reductions at 24 h than western blot, a discrepancy that may reflect methodological sensitivity rather than true biological divergence. However, it is important to note that their study also demonstrated that Cdk4 knockout in mice resulted in defective luteinization process characterized by a rapid decline in progesterone secretion that was reversible with exogenous progesterone and linked to reduced prolactin support. It should be emphasized, however, that the luteal phenotype reported by Moons et al., 2002 reflects chronic, systemic genetic loss of Cdk4 in vivo, which does not directly model the acute, short-term pharmacologic inhibition tested here. This highlights that while short-term pharmacologic CDK4/6 inhibition in vitro does not compromise luteal viability or acute steroidogenesis, chronic or systemic modulation of the Cdk4 axis could still impair luteal endocrine function in vivo.

In primary human luteinized granulosa cells (HLGCs), 24h treatment with palbociclib did not alter total PARP levels, whereas ribociclib caused a consistent decrease across all tested concentrations. Similarly, PARP remained unchanged in HGrC1 and COV434 cells after 24 hours of palbociclib treatment. These findings

suggest that palbociclib does not activate apoptosis in the short term, while ribociclib may exert a compound-specific effect. This is in line with (139), who showed that palbociclib reduced chemerin-induced apoptosis in immortalized, mitotically active granulosa-lutein cells, but our study differs in using primary, non-mitotic HLGCs. It should also be noted that only total PARP was assessed, not cleaved PARP, and measurements were limited to a single 24-h time point. Therefore, our results are best interpreted as indicating no overt apoptotic activation with palbociclib and a ribociclib-related reduction in PARP, which may reflect either on-target or off-target effects and requires further investigation.

In whole ovarian tissue explants, CDK4/6 inhibition did not alter Rb, StAR, or CYP19A1 expression after 24 h, and both estradiol and AMH levels remained stable up to 72 h. These results indicate that, at least in the short term, neither endocrine output nor reserve-related markers are compromised. To our knowledge, no prior study has directly tested the pharmacologic inhibition of CDK4/6 in human ovarian explants, underscoring the novelty of this dataset. The absence of immediate changes contrasts with genetic mouse models (93), where germline Cdk4 loss impaired luteal maintenance and rapidly lowered progesterone differences, likely reflecting chronic, systemic gene loss in vivo versus acute, short-term pharmacologic inhibition ex vivo. Nevertheless, while stable AMH levels are reassuring as a biochemical marker of ovarian reserve, they may not capture subtle changes in follicular dynamics. Additional histological analyses, such as follicle counting in treated ovarian sections, will therefore be essential to validate whether CDK4/6 inhibitors exert any long-term or cumulative effects on ovarian reserve.

Overall, this study suggests that CDK4/6 inhibitors consistently cytostatic in proliferative granulosa cells by targeting the pRb–E2F1–p21 pathway. Meanwhile, the expression of steroidogenic enzymes and hormone production is generally maintained across granulosa models and ovarian tissue. The key nuance is that in HLGCs, palbociclib shows broader suppression of CYP19A1 than ribociclib, though without translating into hormonal deficits in the short term. These findings suggest that ovarian steroidogenesis is resilient to acute CDK4/6 inhibition, but dose- and compound-specific vulnerabilities exist at the enzyme level that warrant further mechanistic and long-term investigation.

CONCLUSION

This study shows that CDK4/6 inhibitors consistently act as cytostatic agents in human granulosa cells by preventing Rb phosphorylation and thereby restraining the downstream pRb–E2F1–p21 signalling cascade. Across proliferative granulosa cell lines, human primary luteinized granulosa cells, and ovarian tissue explants, short-term steroidogenic function and reserve markers were largely preserved. In luteal cells, modest dose and compound-specific reductions in CYP19A1 and 3β-HSD were observed, but these did not translate into hormonal alterations within the studied timeframe. Importantly, ovarian tissue explants confirmed that estradiol and AMH secretion remained stable, supporting that overall endocrine function and reserve markers are not acutely compromised. Taken together, these findings suggest that ovarian steroidogenesis may be resilient to acute inhibition of CDK4/6. Nevertheless, establishing the long-term and in vivo consequences remains essential to fully clarify the implications for ovarian function and reproductive safety. By combining proliferative granulosa models, primary luteinized cells, and ovarian explants, this study provides the first integrated human preclinical evidence on how CDK4/6 inhibition impacts both steroidogenesis and markers of ovarian reserve, thereby addressing the gap in understanding their effects on dormant follicles and ovarian function.

Limitations

The present study is limited by its reliance on short-term in vitro models, with most analyses performed within 24–72 hours. While this time frame allowed us to establish acute cytostatic effects and preserved steroidogenesis, it does not capture potential cumulative or delayed responses. Moreover, total PARP, rather than cleaved PARP, was assessed, which limits the interpretation of apoptotic signalling. In luteal cells, method-related differences between western blot and immunofluorescence for 3β-HSD further emphasize that readouts may be technique-sensitive. Finally, although ovarian explants provided a more integrated model, histological analyses such as follicle counting could not be completed due to time constraints, and their inclusion would be essential to fully evaluate the potential effects of CDK inhibitors on ovarian function. The impact of CDK inhibitors on the dormant primordial follicle pool and growing follicle fraction could not be assessed due to relatively low number of ovarian cortex available for these experiments.

Future Directions

This study provides the first preclinical evidence that CDK4/6 inhibitors act as cytostatic agents in primary human granulosa cells while largely preserving short-term steroidogenic function and reserve markers. However, the reductions in CYP19A1 and 3β-HSD observed in luteal cells raise the possibility of steroidogenic level vulnerabilities with prolonged exposure. Future studies should therefore extend beyond short-term in vitro models to long-term and in vivo settings, incorporating systemic endocrine regulation and histological assessments such as follicle counts. Moreover, the compound-specific differences between palbociclib and ribociclib highlight the need to clarify whether distinct inhibitors exert differential ovarian effects. Ultimately, integrating fertility endpoints into translational and clinical studies will be essential to determine reproductive safety in women of reproductive age.

BIBLIOGRAPHY

1. Schütz LF, Batalha IM. Granulosa Cells: Central Regulators of Female Fertility. Endocrines. 2024;5(4):547–65.
2. Bachelot A, Rouxel A, Massin N, Dulon J, Courtillot C, Matuchansky C, et al. Phenotyping and genetic studies of 357 consecutive patients presenting with premature ovarian failure. Eur J Endocrinol. 2009;161(1):179–87.
3. Shelling AN. Premature ovarian failure. Reproduction. 2010;140(5):633–41.
4. Kallen A, Polotsky AJ, Johnson J. Untapped Reserves: Controlling Primordial Follicle Growth Activation. Trends Mol Med [Internet]. 2018;24(3):319–31. Available from: http://dx.doi.org/10.1016/j.molmed.2018.01.008
5. Motta PM, Makabe S, Nottola SA. The ultrastructure of human reproduction. 1. The natural history of the female germ cell: Origin, migration and differentiation inside the developing ovary. Hum Reprod Update. 1997;3(3):281–95.
6. Wu R, Van der Hoek KH, Ryan NK, Norman RJ, Robker RL. Macrophage contributions to ovarian function. Hum Reprod Update. 2004;10(2):119–33.
7. Oktem O, Urman B. Understanding follicle growth in vivo. Hum Reprod. 2010;25(12):2944–54.
8. Zhang H, Liu K. Cellular and molecular regulation of the activation of mammalian primordial follicles: Somatic cells initiate follicle activation in adulthood. Hum Reprod Update. 2015;21(6):779–86.
9. McGee EA, Hsueh AJW. Initial and cyclic recruitment of ovarian follicles. Endocr Rev. 2000;21(2):200–14.
10. Zhang T, He M, Zhang J, Tong Y, Chen T, Wang C, et al. Mechanisms of primordial follicle activation and new pregnancy opportunity for premature ovarian failure patients. Front Physiol. 2023;14(February):1–12.
11. Picton HM. Activation of follicle development: The primordial follicle. Theriogenology. 2001;55(6):1193–210.

12. Skinner MK. Regulation of primordial follicle assembly and development. Hum Reprod Update. 2005;11(5):461–71.
13. Matsuda F, Inoue N, Manabe N, Ohkura S. Follicular growth and atresia in mammalian ovaries: Regulation by survival and death of granulosa cells. J Reprod Dev. 2012;58(1):44–50.
14. Gougeon A. Dynamics of follicular growth in the human: A model from preliminary results. Hum Reprod. 1986;1(2):81–7.
15. Hirshfield AN. Relationship between the supply of primordial follicles and the onset of follicular growth in rats. Biol Reprod. 1994;50(2):421–8.
16. Young JM, McNeilly AS. Theca: The forgotten cell of the ovarian follicle. Reproduction. 2010;140(4):489–504.
17. Richards JAS, Ren YA, Candelaria N, Adams JE, Rajkovic A. Ovarian follicular theca cell recruitment, differentiation, and impact on fertility: 2017 update. Endocr Rev. 2018;39(1):1–20.
18. Campbell BK, Baird DT, Webb R. Effects of dose of LH on androgen production and luteinization of ovine theca cells cultured in a serum-free system. J Reprod Fertil. 1998;112(1):69–77.
19. Hartanti MD, Hummitzsch K, Bonner WM, Bastian NA, Irving-Rodgers HF, Rodgers RJ. Formation of the Bovine Ovarian Surface Epithelium during Fetal Development. J Histochem Cytochem. 2020;68(2):113–26.
20. Bukovsky A, Gupta SK, Virant-Klun I, Upadhyaya NB, Copas P, Van Meter SE, et al. Study origin of germ cells and formation of new primary follicles in adult human and rat ovaries. Methods Mol Biol. 2008;450:233–65.
21. Berkholtz CB, Shea LD, Woodruff TK. Extracellular matrix functions in follicle maturation. Semin Reprod Med. 2006;24(4):262–9.
22. McArthur ME, Irving-Rodgers HF, Byers S, Rodgers RJ. Identification and immunolocalization of decorin, versican, perlecan, nidogen, and chondroitin sulfate proteoglycans in bovine small-antral ovarian follicles. Biol Reprod. 2000;63(3):913–24.
23. Reddy P, Liu L, Adhikari D, Jagarlamudi K, Rajareddy S, Shen Y, et al. Oocyte-specific deletion of pten causes premature activation of the primordial follicle pool. Science (80-). 2008;319(5863):611–3.
24. John GB, Gallardo TD, Shirley LJ, Castrillon DH. Foxo3 is a PI3K-dependent molecular switch controlling the initiation of oocyte growth. Dev Biol.

2008;321(1):197–204.

25. Shah JS, Sabouni R, Cayton Vaught KC, Owen CM, Albertini DF, Segars JH. Biomechanics and mechanical signaling in the ovary: a systematic review. J Assist Reprod Genet. 2018;35(7):1135–48.
26. Li-Ping Z, Da-Lei Z, Jian H, Liang-Quan X, Ai-Xia X, Xiao-Yu D, et al. Proto-oncogene c-erbB2 initiates rat primordial follicle growth via PKC and MAPK pathways. Reprod Biol Endocrinol. 2010;8:1–9.
27. Webber L, Franks S. Premature Ovarian Insufficiency. Encycl Reprod Vol 1-6, Second Ed. 2018;4:82–6.
28. Zhao Y, Feng H, Zhang Y, Zhang J V., Wang X, Liu D, et al. Current understandings of core pathways for the activation of mammalian primordial follicles. Cells. 2021;10(6).
29. Lew R. Natural history of ovarian function including assessment of ovarian reserve and premature ovarian failure. Best Pract Res Clin Obstet Gynaecol [Internet]. 2019;55:2–13. Available from: https://doi.org/10.1016/j.bpobgyn.2018.05.005
30. Liu K, Zhang H, Risal S, Gorre N, Busayavalasa K, Li X, et al. Somatic cells initiate primordial follicle activation and govern the development of dormant oocytes in mice. Curr Biol. 2014;24(21):2501–8.
31. Ford EA, Beckett EL, Roman SD, McLaughlin EA, Sutherland JM. Advances in human primordial follicle activation and premature ovarian insufficiency. Vol. 159, Reproduction. BioScientifica Ltd.; 2020. p. R15–29.
32. Zheng W, Nagaraju G, Liu Z, Liu K. Functional roles of the phosphatidylinositol 3-kinases (PI3Ks) signaling in the mammalian ovary. Mol Cell Endocrinol [Internet]. 2012;356(1–2):24–30. Available from: http://dx.doi.org/10.1016/j.mce.2011.05.027
33. Chen Y, Yang W, Shi X, Zhang C, Song G, Huang D. The Factors and Pathways Regulating the Activation of Mammalian Primordial Follicles in vivo. Front Cell Dev Biol. 2020;8(September):1–11.
34. Maidarti M, Clarkson YL, Mclaughlin M, Anderson RA, Telfer EE. Inhibition of PTEN activates bovine non-growing follicles in vitro but increases DNA damage and reduces DNA repair response. Hum Reprod. 2019;34(2):297–307.
35. McLaughlin M, Innell HL, Anderson RA, Telfer EE. Inhibition of phosphatase and tensin homologue (PTEN) in human ovary in vitro results in increased activation of primordial follicles but compromises development of growing follicles. Mol Hum Reprod. 2014;20(8):736–44.

36. Laplante M, Sabatini DM. MTOR signaling in growth control and disease. Cell [Internet]. 2012;149(2):274–93. Available from: http://dx.doi.org/10.1016/j.cell.2012.03.017
37. Adhikari D, Zheng W, Shen Y, Gorre N, Hämäläinen T, Cooney AJ, et al. Tsc/mTORC1 signaling in oocytes governs the quiescence and activation of primordial follicles. Hum Mol Genet. 2009;19(3):397–410.
38. Hirashima Y, Moniruzzaman M, Miyano T. P27KIP1 negatively regulates the activation of murine primordial oocytes. J Reprod Dev. 2011;57(2):217–22.
39. Rajareddy S, Reddy P, Du C, Liu L, Jagarlamudi K, Tang W, et al. p27kip1 (cyclin-dependent kinase inhibitor 1B) controls ovarian development by suppressing follicle endowment and activation and promoting follicle atresia in mice. Mol Endocrinol. 2007;21(9):2189–202.
40. Scavone G, Ottonello S, Blondeaux E, Arecco L, Scaruffi P, Stigliani S, et al. The Role of Cyclin-Dependent Kinases (CDK) 4/6 in the Ovarian Tissue and the Possible Effects of Their Exogenous Inhibition. Cancers (Basel). 2023;15(20).
41. Ernst EH, Grøndahl ML, Grund S, Hardy K, Heuck A, Sunde L, et al. Dormancy and activation of human oocytes from primordial and primary follicles: Molecular clues to oocyte regulation. Hum Reprod. 2017;32(8):1684–700.
42. Ataei-Nazari S, Amoushahi M, Madsen JF, Jensen J, Heuck A, Mohammadi-Sangcheshmeh A, et al. Cyclin-dependent kinase 6 (CDK6) as a potent regulator of the ovarian primordial-to-primary follicle transition. Front Cell Dev Biol. 2022;10(December):1–15.
43. Zhang L, Zhang L, Guo F. MiRNA-494-3p Regulates Bupivacaine-Induced Neurotoxicity by the CDK6-PI3K/AKT Signaling. Neurotox Res [Internet]. 2021;39(6):2007–17. Available from: https://doi.org/10.1007/s12640-021-00427-w
44. Visser JA, Themmen APN. Anti-Müllerian hormone and folliculogenesis. Mol Cell Endocrinol. 2005;234(1–2):81–6.
45. Wang ZP, Mu XY, Guo M, Wang YJ, Teng Z, Mao GP, et al. Transforming growth factor-β signaling participates in the maintenance of the primordial follicle pool in the mouse ovary. J Biol Chem [Internet]. 2014;289(12):8299–311. Available from: http://dx.doi.org/10.1074/jbc.M113.532952
46. Benayoun BA, Georges AB, L'Hôtel D, Andersson N, Dipietromaria A, Todeschini AL, et al. Transcription factor FOXl2 protects granulosa cells from stress and delays cell cycle: Role of its regulation by the SIRT1 deacetylase. Hum Mol Genet.

2011;20(9):1673–86.
47. Pangas SA, Choi Y, Ballow DJ, Zhao Y, Westphal H, Matzuk MM, et al. Oogenesis requires germ cell-specific transcriptional regulators Sohlh1 and Lhx8. Proc Natl Acad Sci U S A. 2006;103(21):8090–5.
48. Kaldis P. Another Piece of the p27Kip1 Puzzle. Cell. 2007;128(2):241–4.
49. Zhang T, He M, Zhao L, Qin S, Zhu Z, Du X, et al. HDAC6 regulates primordial follicle activation through mTOR signaling pathway. Cell Death Dis [Internet]. 2021;12(6):1–12. Available from: http://dx.doi.org/10.1038/s41419-021-03842-1
50. Tatone C, di Emidio G, Barbonetti A, Carta G, Luciano AM, Falone S, et al. Sirtuins in gamete biology and reproductive physiology: Emerging roles and therapeutic potential in female and male infertility. Hum Reprod Update. 2018;24(3):267–89.
51. Miller WL, Auchus RJ. The molecular biology, biochemistry, and physiology of human steroidogenesis and its disorders. Endocr Rev. 2011;32(1):81–151.
52. Sullivan MW, Stewart-Akers A, Krasnow JS, Berga SL, Zeleznik AJ. Ovarian responses in women to recombinant follicle-stimulating hormone and luteinizing hormone (LH): A role for LH in the final stages of follicular maturation. J Clin Endocrinol Metab. 1999;84(1):228–32.
53. Jeppesen JV, Kristensen SG, Nielsen ME, Humaidan P, Dal Canto M, Fadini R, et al. LH-receptor gene expression in human granulosa and cumulus cells from antral and preovulatory follicles. J Clin Endocrinol Metab. 2012;97(8):1524–31.
54. Wickenheisser JK, Nelson-DeGrave VL, McAllister JM. Human ovarian theca cells in culture. Trends Endocrinol Metab. 2006;17(2):65–71.
55. Andersen CY, Ezcurra D. Human steroidogenesis: Implications for controlled ovarian stimulation with exogenous gonadotropins. Reprod Biol Endocrinol. 2014;12(1):1–11.
56. Zheng M, Andersen CY, Rasmussen FR, Cadenas J, Christensen ST, Mamsen LS. Expression of genes and enzymes involved in ovarian steroidogenesis in relation to human follicular development. Front Endocrinol (Lausanne). 2023;14(October):1–17.
57. Kristensen SG, Mamsen LS, Jeppesen J V., Bøtkjær JA, Pors SE, Borgbo T, et al. Hallmarks of human small antral follicle development: Implications for regulation of ovarian steroidogenesis and selection of the dominant follicle. Front Endocrinol (Lausanne). 2018;8(JAN):1–10.
58. Smyth CD, Mir F, Howles CM, Hillier SG. Ovarian Thecal / Interstitial. 2015;133(4):1532–8.
59. Nahum R, Thong KJ, Hillier SG. Metabolic regulation of androgen production by

human thecal cells in vitro. Hum Reprod. 1995;10(1):75–81.
60. Jozkowiak M, Piotrowska-Kempisty H, Kobylarek D, Gorska N, Mozdziak P, Kempisty B, et al. Endocrine Disrupting Chemicals in Polycystic Ovary Syndrome: The Relevant Role of the Theca and Granulosa Cells in the Pathogenesis of the Ovarian Dysfunction. Cells. 2023;12(1).
61. Oktem O, Akin N, Bildik G, Yakin K, Alper E, Balaban B, et al. FSH Stimulation promotes progesterone synthesis and output from human granulosa cells without luteinization. Hum Reprod. 2017;32(3):643–52.
62. Pellarin I, Dall'Acqua A, Favero A, Segatto I, Rossi V, Crestan N, et al. Cyclin-dependent protein kinases and cell cycle regulation in biology and disease. Signal Transduct Target Ther [Internet]. 2025;10(1). Available from: http://dx.doi.org/10.1038/s41392-024-02080-z
63. Pluta AJ, Studniarek C, Murphy S, Norbury CJ. Cyclin-dependent kinases: Masters of the eukaryotic universe. Wiley Interdiscip Rev RNA. 2024;15(1):1–49.
64. Malumbres M. Cyclin-dependent kinases. Genome Biol. 2014;15(6):1–10.
65. Vermeulen K, Van Bockstaele DR, Berneman ZN. The cell cycle: A review of regulation, deregulation and therapeutic targets in cancer. Cell Prolif. 2003;36(3):131–49.
66. Ohtsubo M, Theodoras AM, Schumacher J, Roberts JM, Pagano M. Human Cyclin E, a Nuclear Protein Essential for the G 1 -to-S Phase Transition . Mol Cell Biol. 1995;15(5):2612–24.
67. Petersen BO, Lukas J, Sørensen CS, Bartek J, Helin K. Phosphorylation of mammalian CDC6 by cyclin A/CDK2 regulates its subcellular localization. EMBO J. 1999;18(2):396–410.
68. Kaldis P. The cdk-activating kinase (CAK): From yeast to mammals. Cell Mol Life Sci. 1999;55(2):284–96.
69. Bury M, Le Calvé B, Ferbeyre G, Blank V, Lessard F. New Insights into CDK Regulators: Novel Opportunities for Cancer Therapy. Trends Cell Biol [Internet]. 2021;31(5):331–44. Available from: https://doi.org/10.1016/j.tcb.2021.01.010
70. Asghar U, Witkiewicz AK, Turner NC, Knudsen ES. The history and future of targeting cyclin-dependent kinases in cancer therapy. Nat Rev Drug Discov. 2015;14(2):130–46.
71. Bharadwaj R, Yu H. The spindle checkpoint, aneuploidy, and cancer. Oncogene. 2004;23(11 REV. ISS. 1):2016–27.

72. Rampioni Vinciguerra GL, Sonego M, Segatto I, Dall'Acqua A, Vecchione A, Baldassarre G, et al. CDK4/6 Inhibitors in Combination Therapies: Better in Company Than Alone: A Mini Review. Front Oncol. 2022;12(May):1–14.
73. Ettl T, Schulz D, Bauer RJ. The Renaissance of Cyclin Dependent Kinase Inhibitors. Cancers (Basel). 2022;14(2).
74. Romero-Pozuelo J, Figlia G, Kaya O, Martin-Villalba A, Teleman AA. Cdk4 and Cdk6 Couple the Cell-Cycle Machinery to Cell Growth via mTORC1. Cell Rep. 2020;31(2).
75. Wu Y, Zhang Y, Pi H, Sheng Y. Current therapeutic progress of CDK4/6 inhibitors in breast cancer. Cancer Manag Res. 2020;12:3477–87.
76. Mende N, Kuchen EE, Lesche M, Grinenko T, Kokkaliaris KD, Hanenberg H, et al. CCND1-CDK4-mediated cell cycle progression provides a competitive advantage for human hematopoietic stem cells in vivo. J Exp Med. 2015;212(8):1171–83.
77. O'Leary B, Finn RS, Turner NC. Treating cancer with selective CDK4/6 inhibitors. Nat Rev Clin Oncol. 2016;13(7):417–30.
78. Joan Massagué. A G1 engine of cyclins and kinases. Nature [Internet]. 2004;432(November). Available from: www.nature.com/nature
79. Topacio BR, Zatulovskiy E, Cristea S, Xie S, Tambo CS, Rubin SM, et al. Cyclin D-Cdk4,6 Drives Cell-Cycle Progression via the Retinoblastoma Protein's C-Terminal Helix. Mol Cell. 2019;74(4):758-770.e4.
80. Łukasik P, Baranowska-bosiacka I, Kulczycka K, Gutowska I. Inhibitors of cyclin-dependent kinases: Types and their mechanism of action. Int J Mol Sci. 2021;22(6):1–23.
81. Malumbres M, Barbacid M. Mammalian cyclin-dependent kinases. Trends Biochem Sci. 2005;30(11):630–41.
82. Nurse P. A long twentieth century of the cell cycle and beyond. Cell. 2000;100(1):71–8.
83. Dall'acqua A, Bartoletti M, Masoudi-Khoram N, Sorio R, Puglisi F, Belletti B, et al. Inhibition of cdk4/6 as therapeutic approach for ovarian cancer patients: Current evidences and future perspectives. Cancers (Basel). 2021;13(12):1–20.
84. Kozar K, Sicinski P. Cell cycle progression without cyclin D-CDK4 and cyclin D-CDK6 complexes. Cell Cycle. 2005;4(3):388–91.
85. Lin ZP, Zhu YL, Ratner ES. Targeting cyclin-dependent kinases for treatment of gynecologic cancers. Front Oncol. 2018;8(AUG).
86. Yang P, Roy SK. Follicle Stimulating Hormone-Induced DNA Synthesis in the

Granulosa Cells of Hamster Preantral Follicles Involves Activation of Cyclin-Dependent Kinase-4 Rather Than Cyclin D2 Synthesis. Biol Reprod. 2004;70(2):509–17.

87. Carthon BC, Neumann CA, Das M, Pawlyk B, Li T, Geng Y, et al. Genetic Replacement of Cyclin D1 Function in Mouse Development by Cyclin D2. Mol Cell Biol. 2005;25(3):1081–8.
88. Kayampilly PP, Menon KMJ. Dihydrotestosterone inhibits insulin-stimulated cyclin D2 messenger ribonucleic acid expression in rat ovarian granulosa cells by reducing the phosphorylation of insulin receptor substrate-1. Endocrinology. 2006;147(1):464–71.
89. Granados-Aparici S, Hardy K, Franks S, Sharum IB, Waite SL, Fenwick MA. SMAD3 directly regulates cell cycle genes to maintain arrest in granulosa cells of mouse primordial follicles. Sci Rep. 2019;9(1):1–12.
90. Isao Matsuura, Natalia G. Denissova, Guannan Wang, Dongming He, Jianyin Long, Fang Liu. Cyclin-dependent kinases regulate the antiproliferative function of Smads. Nature. 2004;430(6996):226–31.
91. Rubin SM, Sage J, Skotheim JM. Integrating Old and New Paradigms of G1/S Control. Mol Cell [Internet]. 2020;80(2):183–92. Available from: https://doi.org/10.1016/j.molcel.2020.08.020
92. Harbour JW, Luo RX, Dei Santi A, Postigo AA, Dean DC. Cdk phosphorylation triggers sequential intramolecular interactions that progressively block Rb functions as cells move through G1. Cell. 1999;98(6):859–69.
93. Moons DS, Jirawatnotai S, Tsutsui T, Franks R, Parlow AF, Hales DB, et al. Intact follicular maturation and defective luteal function in mice deficient for cyclin-dependent kinase-4. Endocrinology. 2002;143(2):647–54.
94. Malumbres M, Sotillo R, Santamaría D, Galán J, Cerezo A, Ortega S, et al. Mammalian cells cycle without the D-type cyclin-dependent kinases Cdk4 and Cdk6. Cell. 2004;118(4):493–504.
95. Ernst EH, Franks S, Hardy K, Villesen P, Lykke-Hartmann K. Granulosa cells from human primordial and primary follicles show differential global gene expression profiles. Hum Reprod. 2018;33(4):666–79.
96. Adhikari D, Zheng W, Shen Y, Gorre N, Ning Y, Halet G, et al. Cdk1, but not Cdk2, is the sole Cdk that is essential and sufficient to drive resumption of meiosis in mouse oocytes. Hum Mol Genet. 2012;21(11):2476–84.

97. Barbieri F, Cagnoli M, Ragni N, Foglia G, Bruzzo C, Pedullà F, et al. Increased cyclin D1 expression is associated with features of malignancy and disease recurrence in ovarian tumors. Clin Cancer Res. 1999;5(7):1837–42.
98. Larochelle S, Merrick KA, Terret ME, Wohlbold L, Barboza NM, Zhang C, et al. Requirements for Cdk7 in the Assembly of Cdk1/Cyclin B and Activation of Cdk2 Revealed by Chemical Genetics in Human Cells. Mol Cell. 2007;25(6):839–50.
99. Olson CM, Liang Y, Leggett A, Park WD, Li L, Mills CE, et al. Development of a Selective CDK7 Covalent Inhibitor Reveals Predominant Cell-Cycle Phenotype. Cell Chem Biol. 2019;26(6):792-803.e10.
100. Donner AJ, Szostek S, Hoover JM, Espinosa JM. CDK8 Is a Stimulus-Specific Positive Coregulator of p53 Target Genes. Mol Cell. 2007;27(1):121–33.
101. Luke JJ, D'Adamo DR, Dickson MA, Keohan ML, Carvajal RD, Maki RG, et al. The cyclin-dependent kinase inhibitor flavopiridol potentiates doxorubicin efficacy in advanced sarcomas: Preclinical investigations and results of a phase I dose-escalation clinical trial. Clin Cancer Res. 2012;18(9):2638–47.
102. Marra A, Curigliano G. Are all cyclin-dependent kinases 4/6 inhibitors created equal? npj Breast Cancer [Internet]. 2019;5(1):1–9. Available from: http://dx.doi.org/10.1038/s41523-019-0121-y
103. Schettini F, De Santo I, Rea CG, De Placido P, Formisano L, Giuliano M, et al. CDK 4/6 inhibitors as single agent in advanced solid tumors. Front Oncol. 2018;8(December):1–12.
104. Knudsen ES, Hutcheson J, Vail P, Witkiewicz AK. Biological specificity of CDK4/6 inhibitors: Dose response relationship, in vivo signaling, and composite response signaturez. Oncotarget. 2017;8(27):43678–91.
105. Dhillon S. Trilaciclib: First Approval. Drugs [Internet]. 2021;81(7):867–74. Available from: https://doi.org/10.1007/s40265-021-01508-y
106. Coll-Martínez B, Delgado A, Crosas B. The Potential of Proteolytic Chimeras as Pharmacological Tools and Therapeutic Agents. Molecules. 2020;25(24).
107. Naito M, Ohoka N, Shibata N, Tsukumo Y. Targeted Protein Degradation by Chimeric Small Molecules, PROTACs and SNIPERs. Front Chem. 2019;7(December):1–5.
108. Hamilton E, Infante JR. Targeting CDK4/6 in patients with cancer. Cancer Treat Rev [Internet]. 2016;45:129–38. Available from: http://dx.doi.org/10.1016/j.ctrv.2016.03.002
109. Jhaveri K, Burris HA, Yap TA, Hamilton E, Rugo HS, Goldman JW, et al. The

evolution of cyclin dependent kinase inhibitors in the treatment of cancer. Expert Rev Anticancer Ther [Internet]. 2021;21(10):1105–24. Available from: https://doi.org/10.1080/14737140.2021.1944109

110. Tripathy D, Bardia A, Sellers WR. Ribociclib (LEE011): Mechanism of Action and Clinical Impact of This Selective Cyclin-Dependent Kinase 4/6 Inhibitor in Various Solid Tumors. Clin Cancer Res. 2017;23(13):3251–62.
111. Liu M, Liu H, Chen J. Mechanisms of the CDK4/6 inhibitor palbociclib (PD 0332991) and its future application in cancer treatment (Review). Oncol Rep. 2018;39(3):901–11.
112. Fry DW, Harvey PJ, Keller PR, Elliott WL, Meade MA, Trachet E, et al. Specific inhibition of cyclin-dependent kinase 4/6 by PD 0332991 and associated antitumor activity in human tumor xenografts. Mol Cancer Ther. 2004;3(11):1427–37.
113. Toogood PL. Cyclin-Dependent Kinase Inhibitors forTreating Cancer. 21(6):487–98.
114. Xu H, Yu S, Liu Q, Yuan X, Mani S, Pestell RG, et al. Recent advances of highly selective CDK4/6 inhibitors in breast cancer. J Hematol Oncol. 2017;10(1):1–12.
115. Yang C, Li Z, Bhatt T, Dickler M, Giri D, Scaltriti M, et al. Acquired CDK6 amplification promotes breast cancer resistance to CDK4/6 inhibitors and loss of ER signaling and dependence. Oncogene. 2017;36(16):2255–64.
116. Gong X, Litchfield LM, Webster Y, Chio LC, Wong SS, Stewart TR, et al. Genomic Aberrations that Activate D-type Cyclins Are Associated with Enhanced Sensitivity to the CDK4 and CDK6 Inhibitor Abemaciclib. Cancer Cell. 2017;32(6):761-776.e6.
117. Pack LR, Daigh LH, Chung M, Meyer T. Clinical CDK4/6 inhibitors induce selective and immediate dissociation of p21 from cyclin D-CDK4 to inhibit CDK2. Nat Commun [Internet]. 2021;12(1):1–12. Available from: http://dx.doi.org/10.1038/s41467-021-23612-z
118. Choi YJ, Li X, Hydbring P, Sanda T, Stefano J, Christie AL, et al. The Requirement for Cyclin D Function in Tumor Maintenance. Cancer Cell [Internet]. 2012;22(4):438–51. Available from: http://dx.doi.org/10.1016/j.ccr.2012.09.015
119. Park HJ, Carr JR, Wang Z, Nogueira V, Hay N, Tyner AL, et al. FoxM1, a critical regulator of oxidative stress during oncogenesis. EMBO J [Internet]. 2009;28(19):2908–18. Available from: http://dx.doi.org/10.1038/emboj.2009.239
120. Finn RS, Dering J, Conklin D, Kalous O, Cohen DJ, Desai AJ, et al. PD 0332991, a selective cyclin D kinase 4/6 inhibitor, preferentially inhibits proliferation of luminal estrogen receptor-positive human breast cancer cell lines in vitro. Breast Cancer Res.

2009;11(5):1–13.

121. Michaud K, Solomon DA, Oermann E, Kim JS, Zhong WZ, Prados MD, et al. Pharmacologic inhibition of cyclin-dependent kinases 4 and 6 arrests the growth of glioblastoma multiforme intracranial xenografts. Cancer Res. 2010;70(8):3228–38.
122. Comstock CES, Augello MA, Goodwin JF, De Leeuw R, Schiewer MJ, Ostrander WF, et al. Targeting cell cycle and hormone receptor pathways in cancer. Oncogene. 2013;32(48):5481–91.
123. Perez M, Muñoz-Galván S, Jiménez-García MP, Marín JJ, Carnero A. Efficacy of CDK4 inhibition against sarcomas depends on their levels of CDK4 and p16ink4 mRNA. Oncotarget. 2015;6(38):40557–74.
124. Liu F, Korc M. Cdk4/6 inhibition induces epithelial-mesenchymal transition and enhances invasiveness in pancreatic cancer cells. Mol Cancer Ther. 2012;11(10):2138–48.
125. Young RJ, Waldeck K, Martin C, Foo JH, Cameron DP, Kirby L, et al. Loss of CDKN2A expression is a frequent event in primary invasive melanoma and correlates with sensitivity to the CDK4/6 inhibitor PD0332991 in melanoma cell lines. Pigment Cell Melanoma Res. 2014;27(4):590–600.
126. Puyol M, Martín A, Dubus P, Mulero F, Pizcueta P, Khan G, et al. A Synthetic Lethal Interaction between K-Ras Oncogenes and Cdk4 Unveils a Therapeutic Strategy for Non-small Cell Lung Carcinoma. Cancer Cell. 2010;18(1):63–73.
127. Vaughn DJ, Hwang WT, Lal P, Rosen MA, Gallagher M, O'Dwyer PJ. Phase 2 trial of the cyclin-dependent kinase 4/6 inhibitor palbociclib in patients with retinoblastoma protein-expressing germ cell tumors. Cancer. 2015;121(9):1463–8.
128. Sumi NJ, Kuenzi BM, Knezevic CE, Remsing Rix LL, Rix U. Chemoproteomics Reveals Novel Protein and Lipid Kinase Targets of Clinical CDK4/6 Inhibitors in Lung Cancer. ACS Chem Biol. 2015;10(12):2680–6.
129. Chen P, Lee N V., Hu W, Xu M, Ferre RA, Lam H, et al. Spectrum and degree of CDK drug interactions predicts clinical performance. Mol Cancer Ther. 2016;15(10):2273–81.
130. Rader J, Russell MR, Hart LS, Nakazawa MS, Belcastro LT, Martinez D, et al. Dual CDK4/CDK6 inhibition induces cell-cycle arrest and senescence in neuroblastoma. Clin Cancer Res. 2013;19(22):6173–82.
131. Zhang YX, Sicinska E, Czaplinski JT, Remillard SP, Moss S, Wang Y, et al. Antiproliferative effects of CDK4/6 inhibition in CDK4-amplified human liposarcoma

in vitro and in vivo. Mol Cancer Ther. 2014;13(9):2184–93.
132. Du Q, Guo X, Wang M, Li Y, Sun X, Li Q. The application and prospect of CDK4/6 inhibitors in malignant solid tumors. J Hematol Oncol. 2020;13(1):1–12.
133. Oktem O, Oktay K. A novel ovarian xenografting model to characterize the impact of chemotherapy agents on human primordial follicle reserve. Cancer Res. 2007;67(21):10159–62.
134. Meirow D, Dor J, Kaufman B, Shrim A, Rabinovici J, Schiff E, et al. Cortical fibrosis and blood-vessels damage in human ovaries exposed to chemotherapy. Potential mechanisms of ovarian injury. Hum Reprod. 2007;22(6):1626–33.
135. Kalich-Philosoph L, Roness H, Carmely A, Fishel-Bartal M, Ligumsky H, Paglin S, et al. Cyclophosphamide triggers follicle activation and "burnout "; AS101 prevents follicle loss and preserves fertility. Sci Transl Med. 2013;5(185).
136. Gennari A, André F, Barrios CH, Cortés J, de Azambuja E, DeMichele A, et al. ESMO Clinical Practice Guideline for the diagnosis, staging and treatment of patients with metastatic breast cancer ☆. Ann Oncol. 2021;32(12):1475–95.
137. Paternot S, Colleoni B, Bisteau X, Roger PP. The CDK4/CDK6 inhibitor PD0332991 paradoxically stabilizes activated cyclin D3-CDK4/6 complexes. Cell Cycle. 2014;13(18):2879–88.
138. Yao J, Li Z, Fu Y, Wu R, Wang Y, Liu C, et al. Involvement of obesity-associated upregulation of chemerin/chemokine-like receptor 1 in oxidative stress and apoptosis in ovaries and granulosa cells. Biochem Biophys Res Commun [Internet]. 2019;510(3):449–55. Available from: https://doi.org/10.1016/j.bbrc.2019.01.125
139. Li Y, Zhang L, Shan Y, Jia C, Xu Y. CDK4/6 inhibitor protects chemerin-induced human granulosa-lutein cells from apoptosis by inhibiting the p53/p21 waf pathway. Mol Reprod Dev. 2019;86(11):1561–8.
140. Crozier L, Foy R, Mouery BL, Whitaker RH, Corno A, Spanos C, et al. CDK4/6 inhibitors induce replication stress to cause long-term cell cycle withdrawal. EMBO J. 2022;41(6):1–20.
141. Loibl S, Marmé F, Martin M, Untch M, Bonnefoi H, Kim SB, et al. Palbociclib for residual high-risk invasive HR-positive and HER2-negative early breast cancer-the penelope-B trial. J Clin Oncol. 2021;39(14):1518–30.
142. Furlanetto J, Marmé F, Thode C, Nekljudova V, Liu Y, Martin Jimenez M, et al. 60MO Ovarian function in young patients (pts) treated with postneoadjuvant

palbociclib (PAL) and endocrine therapy (ET) for hormone receptor (HR)-positive, HER2-negative early breast cancer (BC): Explorative analysis in Penelope-B. Ann Oncol [Internet]. 2022;33:S149–50. Available from: https://doi.org/10.1016/j.annonc.2022.03.076

143. Bildik G, Akin N, Senbabaoglu F, Sahin GN, Karahuseyinoglu S, Ince U, et al. GnRH agonist leuprolide acetate does not confer any protection against ovarian damage induced by chemotherapy and radiation in vitro. Hum Reprod. 2015;30(12):2912–25.
144. Bildik G, Akin N, Seyhan A, Esmaeilian Y, Yakin K, Keles I, et al. Luteal granulosa cells from natural cycles are more capable of maintaining their viability, steroidogenic activity and LH receptor expression than those of stimulated IVF cycles. Hum Reprod. 2019;34(2):345–55.
145. Zhang H, Vollmer M, De Geyter M, Litzistorf Y, Ladewig A, Dürrenberger M, et al. Characterization of an immortalized human granulosa cell line (COV434). Mol Hum Reprod. 2000;6(2):146–53.
146. Bayasula, Iwase A, Kiyono T, Takikawa S, Goto M, Nakamura T, et al. Establishment of a human nonluteinized granulosa cell line that transitions from the gonadotropin-independent to the gonadotropin-dependent status. Endocrinology. 2012;153(6):2851–60.
147. Riss TL, Moravec RA, Niles AL, Duellman S, Benink HA, Worzella TJ, et al. Cell Viability Assays. Assay Guid Man [Internet]. 2004;(Md):1–25. Available from: http://www.ncbi.nlm.nih.gov/pubmed/23805433
148. Bird C, Kirstein S. Real-time, label-free monitoring of cellular invasion and migration with the xCELLigence system. Nat Methods [Internet]. 2009;6(8):v–vi. Available from: http://dx.doi.org/
149. Konecny GE, Winterhoff B, Kolarova T, Qi J, Manivong K, Dering J, et al. Expression of p16 and retinoblastoma determines response to CDK4/6 inhibition in ovarian cancer. Clin Cancer Res. 2011;17(6):1591–602.

Appendix A

Appendix goes here.